

**Quest for Green Energetic Materials, Green Rocket Fuels and
Polyiodo Biocides**

A Dissertation

Presented in Partial Fulfillment of the Requirements for the

Degree of Doctor of Philosophy

with a

Major in Chemistry

in the

College of Graduate Studies

University of Idaho

by

Deepak Chand

May 2016

Major Professor: Jean'ne M. Shreeve, Ph.D.

Committee Members: Chien Wai, Ph.D., Richard Williams, Ph.D.,
Daniel Bukvich, M. M.

Department Administrator: Ray von Wandndruszka, Ph. D.

Authorization to Submit Dissertation

This dissertation of Deepak Chand, submitted for the degree of Doctor of Philosophy with a major in Chemistry and titled “Quest for Green Energetic Materials, Green Rocket Fuels and Polyiodo Biocides,” has been reviewed in final form. Permission as indicated by the signatures and dates below is now granted to submit final copies to the College of Graduate Studies for approval.

Major Professor: _____ Date: _____
Jean’ne M. Shreeve, Ph.D.

Committee
Members: _____ Date: _____
Chien Wai, Ph.D.

_____ Date: _____
Richard Williams, Ph.D.

_____ Date: _____
Daniel Bukvich, M. M.

Department
Administrator: _____ Date: _____
Ray von Wandruszka, Ph.D.

Abstract

The design of more powerful and greener explosives is an ongoing major concern in the energetic materials community. After examining azoles from pyrazole to pentazole as a basis for new energetic materials, the tetrazole ring seems to be a good compromise between high performance and low sensitivity. Keeping this in mind, we synthesized a family of new nitrogen-rich energetic tetrazoles, di(1*H*-tetrazol-5-yl)methanoneoxime and 5,5'- (hydrazonomethylene)bis(1*H*-tetrazole), in very good yields from inexpensive starting materials. By taking advantage of the acidity of these compounds, syntheses of nitrogen-rich energetic salts was possible.

Hypergolic ionic liquids tend to have low volatilities and high thermal and chemical stabilities, and often exhibit wide liquid ranges which could allow the use of these substances as bipropellant fuels under a variety of conditions. Borohydride ionic liquids are known for their short ignition delay times and wide liquid ranges; however, previously they were often synthesized by using toxic and expensive liquid ammonia and additionally, they are also sensitive to moisture. Now, we synthesized eight tetrahydroborate compounds using an efficient synthetic method which does not require liquid ammonia and which leads to improved hydrolytic stability of the borohydride compounds by an imaginative construction of the imidazolium cation.

Current methods for the iodination of pyrazoles suffer from a variety of difficulties such as requiring use of large quantities of reactants yielding mixtures of compounds in low yields. Because of the lack of good synthetic routes, the chemistry and properties of polyiodopyrazoles have not been studied widely. Now we report an efficient synthetic route to polyiodopyrazoles employing trifluoroperacetic acid. A variety of polyiodo compounds including 3,4,5-triiodopyrazole were synthesized in good yields. The decomposition products of these materials were determined by employing Cheetah 6 calculations. Trifluoroperacetic acid-mediated electrophilic iodination was also utilized with benzimidazoles. The new polyiodo benzimidazoles proved to be very good starting materials in the preparation of novel energetic materials.

Among the two triazole isomers, i.e., 1,2,3-triazole and 1,2,4-triazole, the former has favorable energy content for construction of energetic molecules. Therefore, we explored mono and diiodo 1,2,3-triazoles for their biocidal promise.

Acknowledgments

I would like to express my deep gratitude to my advisor, mentor, guardian and rescuer, Dr. Jean'ne M. Shreeve. Professor Shreeve has really helped me grow and find my own path during graduate school. I can't express how much I appreciate the freedom she gave me to explore and grow as a chemist. Thank you Dr. Shreeve for teaching me the value of hard work and honesty.

To my family:

I am very thankful to my parents for bringing me into this world and for their unconditional support and blessings. My dear wife Shailu, my clever son Saharsh, and my darling daughter Syra; thank you very much for making my life so colorful.

To my labmates:

I thank them for all their help and encouragement throughout my graduate work. I am grateful to Dr. Haixiang Gao, and Dr. Chunlin He for taking time to mentor me.

To the faculty and staff of the Chemistry Department at U of I:

I am thankful to the wonderful group of people that make up this department. I appreciate each and every person with whom I have had the opportunity to interact. I would like to especially thank the office staff (Cindy, and Deb) for all their help and keeping me on track. I am grateful to Dr. Richard Williams for his support and guidance.

Table of Contents

Authorization to Submit Dissertation	ii
Abstract.....	iii
Acknowledgments	iv
List of Figures.....	viii
List of Tables	x
List of Schemes	xi
Chapter 1	1
1.1 Introduction.....	1
1.2 References:	4
Chapter 2	6
Abstract.....	6
2.1 Introduction.....	6
2.2 Results and Discussion	8
2.3 Synthesis	8
2.4 Properties of the compounds.....	9
2.5 X-ray crystallography	12
2.6 Conclusion	15
2.7 Experimental part.....	16
2.8 General Methods.....	16
2.9 X-ray Crystallography.	16
General procedure for the preparation of salts (3–13):.....	18
2.10 References:	20
Chapter 3	23
Abstract.....	23
3.1 Introduction.....	24
3.2 Results and discussion	25
3.3 Computational Methods.....	29
3.4 Conclusions.....	30
3.5 Experimental section	31
3.6 References.....	34
Chapter 4	36

Abstract:.....	36
4.1 Introduction:	36
4.2 Results and Discussion	38
4.3 X-ray crystallography:	41
4.4 Conclusions.....	44
4.5 Experimental.....	44
4.6 General methods	44
4.7 X-ray crystallography	44
4.8 References.....	47
Chapter 5	50
Abstract.....	50
5.1 Introduction.....	50
5.2 Results and Discussion	51
5.3 Synthesis	51
5.4 Properties of compounds	54
5.5 Single-crystal X-ray structure analysis	56
5.6 Conclusions.....	59
5.7 Experimental Section.....	60
5.8 General Methods:.....	60
5.9 X-ray crystal analysis:	60
5.10 References.....	67
5.11 Supporting Information (SI)	69
5.12 Gaussian Calculations.....	69
5.13 GAMESS Calculations	70
5.14 References.....	70
Chapter 6	72
Abstract:.....	72
6.1 Introduction.....	72
6.2 Results and discussion	74
6.3 Synthesis	74
6.4 Properties of compounds	75
6.5 X-ray Crystallography	78
6.6 Conclusions.....	80

6.7 Experimental Section.....	80
6.8 General Methods.....	80
6.9 X-ray crystallography	81
6.10 References:	84
6.11 Supporting Information	86
Appendix 1: Proof of Approval.....	88

List of Figures

Figure 2.1 (I) 5-aminotetrazole; (II) 5-azidotetrazole; (III) 1,5-diamino-1 <i>H</i> -tetrazole; (IV) 5,5'-bistetrazole; (V) 5,5'-azobis-1 <i>H</i> -tetrazole.....	7
Figure 2.2 (a) Thermal ellipsoid plot (50%) and labelling scheme for di(1 <i>H</i> -tetrazol-5-yl)methanoneoxime 1 . Hydrogen atoms are included but are unlabeled for clarity. (b) Ball and stick packing diagram of 1 viewed down a axis. Dashed line indicates strong hydrogen bonding.....	12
Figure 2.3 (a) Thermal ellipsoid plot (50%) and labelling scheme for 5,5'-(hydrazonomethylene)bis(1 <i>H</i> -tetrazole) 2 . Hydrogen atoms are included but are unlabeled for clarity. (b) Ball and stick packing diagram of 2 viewed down a -axis. Dashed lines indicate strong hydrogen bonding	14
Figure 2.4 (a) Thermal ellipsoid plot (50%) of 12 . Hydrogen atoms are included but are unlabeled for clarity. (b) Ball and stick packing diagram of 12 viewed down the a-axis. Dashed lines indicate strong hydrogen bonding	14
Figure 3.1 The ID test recorded using a high-speed camera photos (1000 frames/sec) of ionic liquids 5 [AAIm]BH ₄] (top) and 1 [ABIm(BH ₄)] (bottom) with WFNNA	29
Figure 4.1 Possible ADWs - (a) Tetraiodofuran (TIF); (b) 2,3,4,5-Tetraiodo-1 <i>H</i> -pyrrole; (c) 3,4,5-Triiodo-1 <i>H</i> -pyrazole; (d) Ethane-1,2-diammonium-bis(triiodide).....	37
Figure 4.2 The sum of iodine-containing species in the detonation products of compounds 1 , 2 , 3 , 4 and 5 (weight percent).....	41
Figure 4.3 (a) Thermal ellipsoid plot (50%) of 5 . Hydrogen atoms are included but are unlabeled for clarity. (b) Ball and stick packing diagram of 5 viewed down the a-axis.....	42
Figure 5.1 Thermal ellipsoid plot (50%) and labelling scheme for 5 . (b) Packing diagram of 5 along a-axis	58
Figure 5.2 Thermal ellipsoid plot (50%) and labeling scheme for 10 . (b) Packing diagram of 10 along a-axis	58
Figure 5.3 (a) Thermal ellipsoid plot (50%) and labelling scheme for 14 . (b) Packing diagram of 14 along a-axis	59
Figure 5.4 Thermal ellipsoid plot (50%) and labeling scheme for 9	59
Figure 6.1 The iodine-containing species in the decomposition products of compounds 2 , 3 , 4 , 6 , 8 and 11 (weight percent).....	76

Figure 6.2 (a) Thermal ellipsoid plot (50%) and labeling scheme for 5 . (b) Packing diagram of 5 along a axis	78
Figure 6.3 Thermal ellipsoid plot (50%) and labeling scheme for 6 . (b) Packing diagram of 6 along a axis.....	79
Figure 6.4 Thermal ellipsoid plot (50%) and labeling scheme for 8 . (b) Packing diagram of 8 along a axis.....	79
Figure 6.5 Thermal ellipsoid plot (50%) and labeling scheme for 10 . (b) Packing diagram of 10 along a- axis	80

List of Tables

Table 2.1 Properties of 1–13 compared with TNT, TATB and RDX	10
Table 2.2 Crystallographic properties of 1 , 2 and 12	12
Table 3.1: Physicochemical properties of borohydride ionic liquids	26
Table 4.1 Physical properties of compounds 1–5	40
Table 4.2 Major detonation products shown by Cheetah 6.0 calculations [wt. % kg kg ⁻¹].....	42
Table 4.3 Crystallographic data for compound 5	43
Table 5.1: Properties of polyiodo compounds	54
Table 5.2 Properties of compounds 11 , 12 and 14	57
Table 5.3 Crystallographic data for 5 , 10 and 14	59
Table S1 Calculated (MP2/6-311++G**//B3LYP/6-31+G**) total energy (E_0), corrected MP2 total energy (E_{corr}), zero-point energy (ZPE), thermal correction to enthalpy (H_T), heat of reaction for the isodesmic reaction (ΔH_R) and gas phase heats of formation ($\Delta_f H_m^\circ$) from Gaussian 03.....	69
Table S2 Calculation of heat of formation of 14	70
Table 6.1 Properties of compounds 2 – 11	75
Table 6.2 Major decomposition products - Cheetah 7.0 calculations [wt. % kg kg ⁻¹]	76
Table 6.3 Crystallographic data for compounds 5 , 6 , 8 and 10	77

List of Schemes

Scheme 2.1 Synthesis of di(1 <i>H</i> -tetrazol-5-yl)methanone oxime 1 and 5,5' (hydrazonomethylene) bis(1 <i>H</i> -tetrazole) 2	8
Scheme 2.2 Syntheses of salts 3–13	9
Scheme 2.3 Born-Haber cycle for the formation of energetic salts.....	11
Scheme 3.1 Synthesis of borohydride ionic liquids.....	25
Scheme 3.2 Born–Haber cycle for the formation of ILs	30
Scheme 4.1 Synthesis of 1-5	38
Scheme 4.2 Delocalization of electrons in 4	39
Scheme 5.1 Synthesis of compounds 1 – 7	52
Scheme 5.2 Synthesis of 8 and 9	53
Scheme 5.3 Synthesis of compounds 10 – 14	53
Scheme S1: Isodesmic reactions for compounds 12 and 14	69
Scheme S2: Isodesmic reaction for 14	70
Scheme 6.1 Synthesis of Compounds 1 – 11	74

Chapter 1

1.1 Introduction

Research in the field of energetic materials has come a long way since Alfred Nobel introduced nitroglycerine as an explosive in the form of dynamite in 1866.¹ Development of new energetic materials has become a very versatile and competitive field. Looking at currently used explosives such as TNT and RDX, the combination of fuel and oxidizer in the same molecule is necessary to achieve high performance. The explosives that derive most of their energy from oxidation of their carbon backbones, i.e., conventional C/H/N/O explosives based on nitrocarbons, seem to have reached their limits and have become obsolete.² Moreover, the high toxicity of the fuel/oxidizer nitramine-derived cyclo trimethylenetrinitramine (RDX) drives its replacement.³

Nitrogen-rich materials with high heats of formation have been shown to possess some of the most promising characteristics.⁴ These compounds tend to liberate thermodynamically stable nitrogen gas which contributes to their energy content. For energetic materials based on this strategy, a strong correlation between increasing the heat of formation, increasing explosive performance, and, unfortunately, increasing sensitivity towards thermal and mechanical stimuli, can be observed. For example, when five-membered nitrogen heterocycles are compared, from pyrazole to pentazole, pyrazoles have low energy content and pentazoles are not stable enough for use in energetic materials.⁵ Of these heterocycles, the tetrazole ring has been found to occupy the ideal middle ground on the stability versus performance continuum for the preparation of new primary and secondary energetic materials. In addition the carbon atom at position 5 of the tetrazole ring offers possibilities for the introduction of oxygen-rich substituents, such as nitro or nitramine groups, to compensate for the low oxygen balance.

Of the energetic materials based on the tetrazole ring, a recurring theme is their preparation from 5-aminotetrazole; thus, this compound can act as a precursor for introducing the tetrazole ring synthon into a wide range of energetic materials.⁶ However, recently, a useful strategy for tailoring tetrazole-based energetic materials has involved the oxidation of the tetrazole rings into their corresponding tetrazole-N-oxides. N-oxides show increased performance, increased thermal stability, and decreased mechanical sensitivity.⁷

The tetrazole with the highest nitrogen content is 5-azido-1*H*-tetrazole, which was first described in patents in 1939 and is extremely sensitive.⁸ 5-N-substituted tetrazoles, e.g., 5-aminotetrazole, 5,5'-azotetrazolate, bis(1*H*-tetrazolyl)amine, and 5,5'-bis(1*H*-tetrazolyl)hydrazine show a nitrogen content above 82%.

Sharpless et al. reported a safer and exceptionally efficient process for transforming nitriles into tetrazoles in water; the only other reagents are sodium azide and a zinc salt as catalyst.⁹ By using this methodology we synthesized a new family of high nitrogen tetrazoles. The second chapter of this dissertation contains the synthesis and characterization of these tetrazoles, their energetic salts and their corresponding properties.

Ionic liquids are organic salts that melt at or below 100 °C and are normally composed of a large asymmetric organic cation and an inorganic or organic anion.¹⁰ Ionic liquids have unique properties such as low vapor pressure, a wide liquid range, high thermal stability, ionic conductivity, structural designability, the ability to dissolve a wide range of chemical species, and low vapor pressure.¹¹ Some ionic liquids are known to have hypergolic properties which is a spontaneous reaction of one chemical (fuel) when contacted with another (oxidizer). Rocket propellant systems can utilize energy derived from hypergolic burning.

In liquid bipropellants, fuels of choice are hydrazine, monomethylhydrazine (MMH), and unsymmetrical N,N-dimethylhydrazine (UDMH) with oxidizing agents such as white fuming nitric acid (WFNA), red-fuming nitric acid (RFNA), or nitrogen tetroxide (N₂O₄).¹² Hydrazine and its derivatives are a class of toxic and carcinogenic substances. They have high vapor pressures so that costly safety precautions and handling procedures are required. Therefore, there is an urgent need for alternative nontoxic liquid hypergolic fuels that exhibit low vapor pressure. Considering that energetic ionic liquids have many unique properties, for example, extremely low vapor pressure, high thermal and chemical stability, and tunable physicochemical characteristics, it is likely that they could have potential as liquid hypergolic fuels.

Our group has been involved extensively in hypergolic ionic liquid research; particularly boron-containing ionic liquids have shown very good promise. The dicyanoborate-based ionic liquids possess superior properties such as lower viscosities. Additionally, these ionic liquids are stable in aqueous solution and are, in fact, synthesized in water as the solvent of choice. With melting points and viscosities as low as -80 °C and 12.4

mPa s, and ignition delay times as short as 4 ms, the dicyanoborate-based compounds are the brightest hope to date to be the next class of hypergolic materials to replace hydrazine and its derivatives in hypergolic propellant systems.¹³

The cyanoborohydride, borohydride and borane solubilized ionic liquids also exhibit some appealing properties.¹⁴ Sodium borohydride, starting material used to prepare tetrahydroborate compounds, is the least expensive among hydrides of boron. Unfortunately borohydride ionic liquids are sensitive to moisture and are often synthesized by using toxic and expensive liquid ammonia. Chapter 3 of this dissertation describes our efforts directed towards improving the hydrolytic stability of borohydride compounds. This chapter also outlines the synthetic methodology that we explored for the synthesis of borohydride ionic liquids as well as their properties relevant to hypergolic performance.

With growing terrorist activities around the world, threat of terrorist attacks that involve weaponized biological agents, such as *Bacillus anthracis*, pose considerable potential public threat.¹⁵ As a result interest in developing Agent Defeat Weapons (ADWs) has grown remarkably during the last few years. ADWs are airborne warheads which contain anti bioagent materials such as iodine-rich compounds that form large amounts of elemental iodine as detonation or decomposition products.

A stable and non sublimable source of iodine is needed for ADWs. Polyiodopyrazoles are promising candidates to be explored for this purpose. Current methods for the iodination of pyrazoles suffer from a variety of difficulties. Pyrazoles with electron-donating substituents have been iodinated using iodine-iodide (I_2 -KI) or iodine monochloride (ICI); both routes often use large quantities of reactants.¹⁶ An iodine-aqueous ammonia combination gives a mixture of 3,4-diiodo- and 3,4,5-triiodopyrazoles in very low yields.¹⁷ Only diiodo derivatives were obtained when an oxidative iodination methodology – I_2 -HIO₃ – was attempted. Likely because of the lack of good synthetic routes, the chemistry and properties of polyiodopyrazoles have not been widely studied.

We explored electrophilic iodination of pyrazoles using trifluoroacetic acid. Chapter 4 contains a detailed description of the method which we used for iodination of pyrazoles. We also assessed biocidal properties of these polyiodopyrazole using theoretical investigations. Chapter 5 of this dissertation contains further elaboration of trifluoroacetic acid mediated iodination. Various polyiodopyrazole and polyiodobenzimidazoles were

synthesized and fully characterized. The trifluoroacetic acid-mediated electrophilic iodination was also utilized with benzimidazoles. The new polyiodopyrazoles were found to be good starting materials for the synthesis of energetic materials.

The syntheses of mono and diiodo-1,2,3-triazoles, and calculation of their releasable biocide content are presented in Chapter 6. An efficient synthesis of mono and diiodo-1,2,3-triazoles by using inexpensive and readily available aqueous ammonia was established.

1.2 References:

- (1) a) Agrawal, J. P.; Hodgson, R. D. *Organic Chemistry of Explosives*; John Wiley & Sons, Ltd.: Chichester, **2007**; p 243. b) Krause, H. H. In *Energetic Materials*; Teipel, U., Ed.; VCH: Weinheim, **2005**; pp 1–25.
- (2) a) T. M. Klapötke, *Chemistry of High-Energy Materials*, 2nd ed., de Gruyter, Berlin, **2011**. b) D. Fischer, T. M. Klapötke, D. G. Piercey, J. Stierstorfer, *Chem. Eur. J.* **2013**, 19, 4602 – 4613.
- (3) a) P. Y. Robidoux, J. Hawari, G. Bardai, L. Paquet, G. Ampleman, S. Thiboutot, G. I. Sunahara, *Arch. Environ. Contam. Toxicol.* **2002**, 43, 379 –388.
- (4) a) M. H. V. Huynh, M. A. Hiskey, D. E. Chavez, D. L. Naud, R. D. Gilardi, *J. Am. Chem. Soc.* **2005**, 127, 12537 – 12543. b) D. E. Chavez, M. A. Hiskey, R. D. Gilardi, *Org. Lett.* **2004**, 6, 2889 – 2891.
- (5) P. Carlquist, H. Ostmark, T. Brinck, *J. Phys. Chem. A*, **2004**, 108, 7463 – 7467.
- (6) a) Y-H. Joo, B. Twamley, S. Garg, J. M. Shreeve, *Angew. Chem. Int. Ed.* **2008**, 47, 6236 –6239. b) Y-H. Joo, J. M. Shreeve, *Angew. Chem. Int. Ed.* **2010**, 49, 7320 – 7323. c) Y-H. Joo, J. M. Shreeve, *Eur. J. Org. Chem.* **2009**, 3573–3578. d) H. Gao, J. M. Shreeve, *Chem. Rev.*, **2011**, 111, 7377–7436.
- (7) a) N. Fischer, D. Fischer, T. M. Klapötke, D. G. Piercey, J. Stierstorfer, *J. Mater. Chem.* **2012**, 22, 20418–20422. b) A. J. Liepa, D. A. Jones, T. D. McCarthy, R. H. Nearn, *Aust. J. Chem.* 2000, 53, 619-622.

- (8) a) W. Friedrich, K. Flick, **1942**, DE 719135. b) W. Friedrich, **1940**, GB 519069 19400315. c) W. Friedrich, K. Flick, **1939**, US 2179783 19391114.
- (9) Z. P. Demko, K. B. Sharpless, *J. Org. Chem.* **2001**, 66, 7945-7950.
- (10) a) P. Wasserscheid, T. Welton, *Ionic Liquids in Synthesis*, WileyVCH: New York, **2003**. b) R. D. Rogers, K. R. Seddon, S. Volkov, *Green Industrial Applications of Ionic Liquids*; Springer: New York, **2003**.
- (11) Q. Zhang, J. M. Shreeve, *Chem. Rev.* **2014**, 114, 10527–10574
- (12) a) A. Osmont, L. Catoire, T. M. Klapötke, G. L. Vaghjiani, M. T. Swihart, *Propellants Explos. Pyrotech.* **2008**, 33, 209 – 212. b) G. P. Sutton, *J. Propul. Power* **2003**, 19, 978 – 1007. c) L. Catoire, N. Chaumeix, C. Paillard, *J. Propul. Power* **2004**, 20, 87 – 92. d) I. Frank, A. Hammerl, T. M. Klapötke, C. Nonnenberg, H. Zewen, *Propellants Explos. Pyrotech.* 2005, 30, 44 – 52. d) C. Nonnenberg, I. Frank, T. M. Klapötke, *Angew. Chem.* **2004**, 116, 4686 – 4689.
- (13) Y. Zhang, J. M. Shreeve, *Angew. Chem. Int. Ed.* **2011**, 50, 935 –937.
- (14) a) S. Li, H. Gao, J. M. Shreeve, *Angew. Chem. Int. Ed.* **2014**, 53, 2969 –2972. b) Q. Zhang, P. Yin, J. Zhang, J. M. Shreeve, *Chem. Eur. J.* **2014**, 20, 6909 – 6914. c) P. V. Ramachandran, A. S. Kulkarni, M. A. Pfeil, J. D. Dennis, J. D. Willits, S. D. Heister, S. F. Son, T. L. Pourpoint, *Chem. Eur. J.* **2014**, 20, 16869 – 16872. d) T. Liu, X. Qi, S. Huang, L. Jiang, J. Li, C. Tang, Q. Zhang, *Chem. Commun.*, **2016**, 52, 2031–2034. e) K. Wang, Y. Zhang, D. Chand, J. M. Shreeve, *Chem. Eur. J.*, **2012**, 18, 16931–16937.
- (15) a) B. R. Clark, M. L. Pantoya, *Phys. Chem. Chem. Phys.* **2010**, 12, 12653–12657. b) H. Wang, G. Jian, W. Zhou, J. B. DeLisio, V. T. Lee, M. R. Z. Zachariah, *ACS Appl. Mater. Interfaces.* **2015**, 7, 17363–17370.
- (16) a) R. Hüttel, O. Schäfer and P. Jochum, *Liebigs Ann. Chem.* **1955**, 593, 200–207. b) J. F. Hansen, Y. I. Kim, L. J. Griswold, G. W. Hoelle, D. L. Taylor and D. E. Vietti, *J. Org. Chem.* **1980**, 45, 76–80. (c) W. Holzer and H. Gruber, *J. Heterocycl. Chem.* **1995**, 32, 1351–1354.
- (17) a) D. Giles, E. W. Parnell and J. D. Renwick, *J. Chem. Soc. C* **1966**, 1179–1184. b) M. M. Kim, R. T. Ruck, D. Zhao, M. A. Huffman, *Tetrahedron Lett.* **2008**, 4026–4028.

Chapter 2

Di(1*H*-tetrazol-5-yl)methanone oxime and 5,5' (hydrazonomethylene)bis(1*H*-tetrazole) and their salts: a family of highly useful new tetrazoles and energetic materials

by

Deepak Chand, Damon A. Parrish, and Jean'ne M. Shreeve

published in

Journal of Materials Chemistry A

(D. Chand, D. A. Parrish, J. M. Shreeve, *J. Mater. Chem. A*, **2013**, 1, 15383–15389.

Copyright ©The Royal Society of Chemistry **2013**)

Abstract

A family of new nitrogen-rich energetic tetrazoles, di(1*H*-tetrazol-5-yl)methanone oxime and 5,5'-(hydrazonomethylene)bis(1*H*-tetrazole), was synthesized in very good yields from inexpensive starting materials. These tetrazoles have excellent thermal stabilities and very high nitrogen content as well as very acceptable impact and friction sensitivities and were employed as precursors to nitrogen rich energetic salts. The hydrazinium and hydroxyl ammonium salts of 5,5'-(hydrazonomethylene)- bis(1*H*-tetrazole) exhibit excellent detonation velocities (9050 m s⁻¹ and 8839 m s⁻¹, respectively) as well as very good detonation pressures and thermal stabilities. The new compounds may have the potential to replace current nitrogen-rich energetic materials.

2.1 Introduction

Much research is focused currently on the development of nitrogen-rich compounds which are very important to the field of energetic materials research. Fundamental properties such as high heat of formation, high nitrogen content, low sensitivity, and ring or cage strain, must be considered during the development of these energetic ingredients.¹ The tetrazole moiety has inherently favorable properties including a large number of N–N bonds, and good stability because of the aromaticity associated with the ring. Higher nitrogen content leads to a higher heat of formation and a more enthusiastic performance. Unfortunately most energetic

materials with high performance characteristics tend concomitantly toward greater sensitivity.¹ When the nitrogen content increases from pyrazole to pentazole, the performance increases while destabilization occurs with pentazole which is not stable even in its neutral form. In this regard, tetrazoles are significant because they have reasonable stability as well as good performance associated with high nitrogen content and ring strain. A few of the most familiar high nitrogen-containing tetrazoles currently known are (Fig. 2.1).²

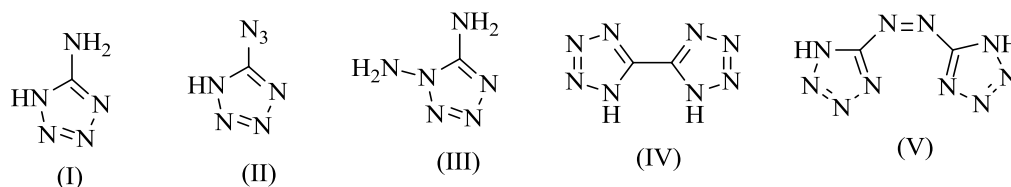
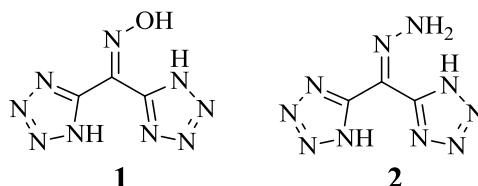


Figure 2.1 (I) 5-aminotetrazole; (II) 5-azidotetrazole; (III) 1,5-diamino-1H-tetrazole; (IV) 5,5'-bistetrazole; (V) 5,5'-azobis-1H-tetrazole

Some of these tetrazoles tend to be sensitive to impact and friction and their syntheses are not straightforward which often precludes practical applications.² It is well known that increasing the nitrogen content by introducing an azide or diazo group has an adverse effect on the sensitivity of the compound while concomitantly enhancing the performance significantly.² For a nitrogen rich material to find practical use as a high explosive, high thermal and mechanical stabilities are required.

Herein we report facile and inexpensive syntheses of **1** [di(1H-tetrazol-5-yl)methanone oxime] and **2** [5,5'-(hydrazonomethylene)bis(1H-tetrazole)] – precursors to a family of new nitrogen-rich energetic tetrazoles. Despite being nitrogen-rich, they have outstanding thermal stability and insensitivity. Also reported are energetic salts derived from these tetrazoles, some of which show excellent performance and stability.



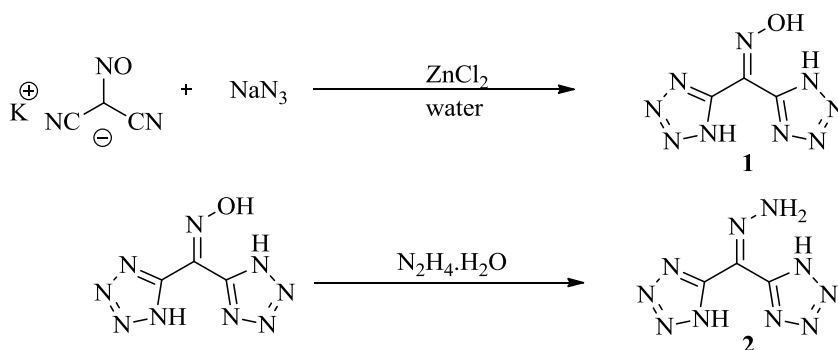
Oximes are employed to generate many heterocyclic frameworks.³ Here the oxime is simply employed to increase the nitrogen content of the molecule in a reasonably straightforward manner. Many of the salts of these tetrazoles exhibit high heats of formation

and competitive detonation properties. These materials are environmentally benign, high-energy-density materials with lower vapor pressures, and enhanced thermal stabilities compared with their atomically similar nonionic analogues. There appears to be a good balance between the stability and performance of these new energetic materials which may hold some promise for application as solid propellants and explosives.

2.2 Results and Discussion

2.3 Synthesis

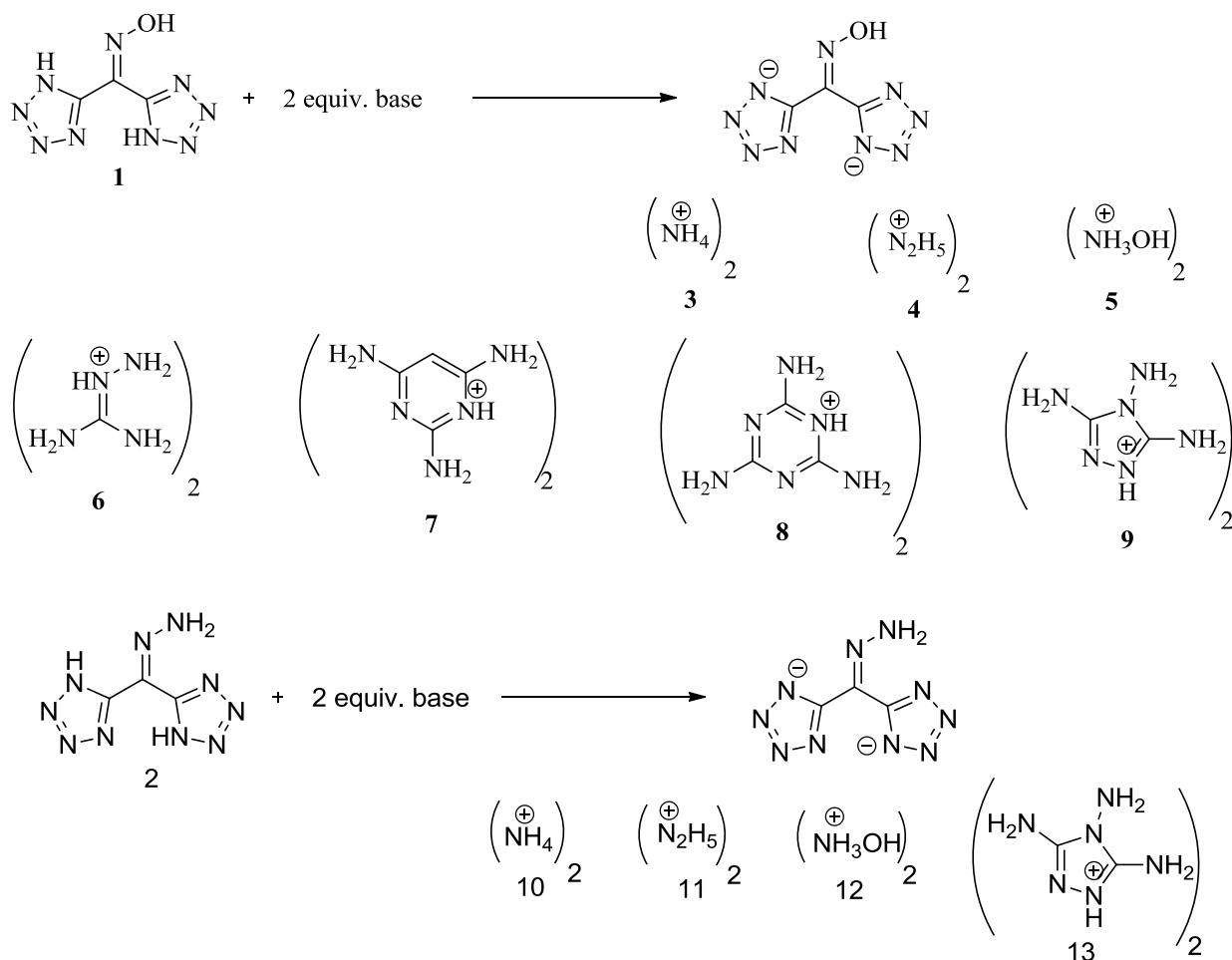
The starting material, potassium dicyanonitrosomethanide was synthesized according to the literature,^{4a-b} and was used subsequently in reaction with sodium azide in the presence of zinc chloride in aqueous solution to prepare di(1H-tetrazol-5-yl)methanone oxime (**1**) in essentially quantitative yield.^{4c-d} The resulting oxime when treated with four equivalents of hydrazine hydrate gave 5,5'-(hydrazonomethylene)bis(1H-tetrazole) (**2**) (Scheme 2.1).



Scheme 2.1 Synthesis of di(1H-tetrazol-5-yl)methanone oxime (**1**) and 5,5'-(hydrazonomethylene) bis(1H-tetrazole) (**2**).

Salts of **1** and **2** were synthesized by treating them with various bases (Scheme 2.2). The structures of **1–13** are supported by IR, and ¹H and ¹³C NMR spectral data as well as elemental analyses. Compounds **1** and **2** exhibit three carbon resonance bands in the ¹³C NMR spectra because restricted rotation around the carbon-nitrogen double bond gives a fixed geometry and three nonequivalent carbon atoms. The imine carbon of **1**, which appears at 132.1 ppm in the ¹³C NMR, is shifted up field significantly to 109.2 ppm in **2** because of

the electron releasing effect of the amino group. The NH₂ proton, in **2** resonates at 10.2 ppm in proton NMR.



Scheme 2.2 Syntheses of salts **3–13**.

2.4 Properties of the compounds

Thermal stability is one of the most important properties of energetic materials; all of the new energetic compounds were examined using differential scanning calorimetry (DSC). Compound **1** melts at 143.9 °C and decomposes (onset temperature) at 288 °C, while **2** decomposes (onset temperature) without melting at 247.6 °C; higher than that of RDX ($T_{\text{dec}} = 230$ °C). Salts **3–13** also show very good thermal stabilities (Table 1). Density is another important physical property of energetic materials. Densities of **1** and **2** are 1.74 and 1.71 g/cm³, respectively, which are lower than that of RDX (1.82 g/cm³). The salts **3–13** exhibit densities ranging between 1.45 and 1.66 g/cm³.

Table 2.1 Properties of **1–13** compared with TNT, TATB and RDX

Compd	T_m^a [°C]	T_d^b [°C]	ρ^c [g cm ⁻³]	ΔH_f^d (cation) [kJmol ⁻¹]	ΔH_f^d (salt) [kJ mol ⁻¹]/[kJ g ⁻¹]	P^e [Gpa]	vD^f [ms ⁻¹]	IS^g [J]
1	143.9	288.7	1.74	-	590.5/ 2.9 ^h	27.4	8226	> 40
2	-	247.6	1.71	-	646.5/3.5 ^h	25.3	8307	25
3	-	262.9	1.56	626.4	860.8/4.0	21.8	7894	35
4	178.9	211.5	1.62	770.0	632.2/2.5	26.7	8292	40
5	133.5	260.4	1.60	669.5	534.3/2.2	26.6	8318	40
6	187.7	197.7	1.48	684.4	591.4/1.8	17.9	7248	> 40
7	-	278.7	1.58	654.3	582.8/1.4	15.8	6859	> 40
8	-	325.1	1.63	651.0	576.9/1.3	17.5	7028	> 40
9	193.3	249.0	1.66	877.6	798.2/2.0	19.8	7676	> 40
10	176.0	239.9	1.45	626.4	860.8/4.0	21.8	7894	> 40
11	-	212.1	1.68	770.0	1002.4/4.1	31.6	8996	35
12	188.4	237.8	1.68	669.5	902.9/3.7	32.9	9044	20
13	-	191.0	1.66	877.6	1170.6/2.9	23.1	8215	>40
TNT	80.4	295	1.65	-	-	19.5	6881	15
TATB	-	318	1.94	-	-	31.2	8114	50
RDX	-	230	1.82	-	80/0.36 ^h	35.2	8977	7.4

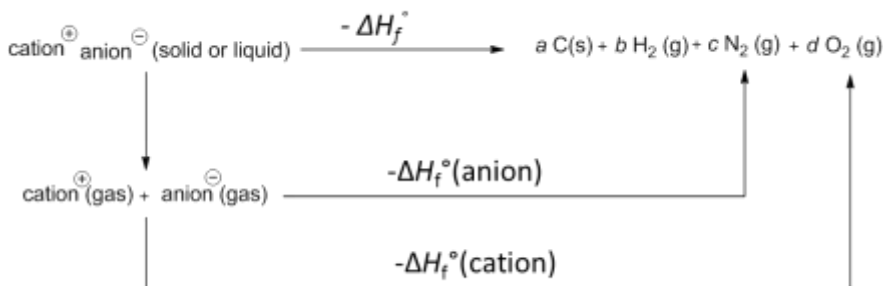
^a Melting temperature (DSC, 5 °C min⁻¹). ^b Decomposition temperature (DSC [(onset)]. ^c Density (25 °C). ^d Heat of formation. The calculated heats of formation for the anions **1**²⁻ and **2**²⁻ are 345.2 and 720.4 kJ mol⁻¹, respectively. ^e Detonation pressure. ^f Detonation velocity. ^g Impact sensitivity. ^h Values for the molecular compounds, **1**, **2** and RDX.

The heat of formation of an energetic molecule which is directly related to the number of nitrogen-nitrogen bonds in the molecule is also very important for evaluating the energetic performance of HEDMs (high energy density materials). All ab initio calculations were carried out by using the Gaussian 03 (Revision D.01) suite of programs. The geometric optimization of the structures and frequency analyses were accomplished by using the B3LYP with the 6-31+G** basis set,⁵ and single-point energies were calculated at the MP2/6-311++G** level. Atomization energies were calculated by the G2 method. All of the optimized structures were characterized to be true local energy minima on the potential-energy surface without imaginary frequencies. The remaining task is to determine the heats of formation of these new energetic compounds are computed by using the method of isodesmic reactions (Supporting information). Thus, the heat of formation of the species being investigated can be easily extracted. As seen in Table 2.1, the tetrazoles and their energetic

salts exhibit positive heats of formation. The heat of formation for **1** is 3.0 kJ/g and that of **2** is 3.6 kJ/g; both exceed the heats of formation of RDX (0.4 kJ/g) and HMX(0.4 kJ/g).

The Born-Haber cycle is given in Scheme 3 permits the calculation of the heat of formation of salt as given by equation (1) in which ΔH_L is the lattice energy of the salts,

$$\Delta H_f^\circ(\text{salt}, 298\text{ K}) = \Delta H_f^\circ(\text{cation}, 298\text{K}) + \Delta H_f^\circ(\text{anion}, 298\text{K}) - \Delta H_L \quad (1)$$



Scheme 2.3 Born-Haber cycle for the formation of energetic salts.

which could be predicted by using the formula suggested by Jenkins, et al. [Eq. 2]:⁶

$$\Delta H_L = U_{\text{pot}} + [p(n_M/2 - 2) + q(n_X/2 - 2)]RT \quad (2)$$

in which n_M and n_X depend on the nature of the ions Mp^+ and Xq^- , respectively, and are equal to three for monoatomic ions, five for linear polyatomic ions, and six for nonlinear polyatomic ions. The equation for lattice potential energy U_{pot} [Eq. (3)] has the form:

$$U_{\text{POT}} [\text{kJ mol}^{-1}] = \gamma(\rho_m/M_m)^{1/3} + \delta \quad (3)$$

in which ρ_m [gcm^{-3}] is the density, M_m is the chemical formula mass of the ionic material, and values for γ and the coefficients γ ($\text{kJmol}^{-1} \text{ cm}$) and δ (kJmol^{-1}) are taken from the literature.⁶

The enthalpy of the reaction (ΔH_{f298°) is obtained by combining the MP2/6-311++G** energy difference for the reaction, the scaled zero point energies, and other thermal factors. Thus, the heats of formation of the species being investigated can be readily extracted. With values of the heats of formation and densities, the detonation pressures (P) and velocities (v_D) were calculated using EXPLO 5.05.⁷ The detonation velocities (v_D) of **1** and **2** are 8226 m/s and 8307 m/s, respectively, which exceed the detonation velocity of TATB (8114 m/s). The detonation pressures (P) of **1** and **2** are 27.4 and 25.3 Gpa, respectively. Among the salts **3–13**, salts **11** and **12** have remarkable detonation properties; salt **11** has a v_D of 8996 m/s and **12** has 9044 m/s, both \geq RDX (8977 m/s). Detonation pressures of salts **11** and **12** are 31.6 and 32.9 Gpa, respectively, and both exceed the detonation pressure of TATB (31.2 Gpa).

Impact sensitivity is another very important parameter on which to judge an energetic material. These measurements were made using standard BAM Fallhammer techniques.⁸ Most of the compounds synthesized are insensitive materials. Compounds **1** and **2** have impact sensitivities of 40 and 25 J, respectively. Especially as potential explosives, **11** and **12** display excellent integrated performance, i. e., v_D values comparable with those of RDX, and lower impact sensitivities than RDX and HMX. The impact sensitivity of **11** is 35 J while **12** is 20 J. At 25 J, a loud explosion occurs with **12**. With the exception of **2** at 80N, all compounds have friction sensitivities ≥ 360 N.

2.5 X-ray crystallography

Suitable crystals of **1**, **2** and **12** were obtained for X-ray crystal structuring. Compound **1** was crystallized by slow evaporation of a saturated solution in DMSO. It crystallizes with a molecule of DMSO. Crystals of **2** were obtained by cooling its saturated solution in boiling water, which resulted in having one molecule of water as a water of crystallization. Similarly crystals of **2** were obtained by slow evaporation of a saturated solution in water. Their structures are shown in Figures 2.2-2.4 and crystallographic data are summarized in Table 2.2. The three crystals are in three different space groups and their crystal systems also differ from one another. Crystals of **1**, **2** and **12** are triclinic, monoclinic, and orthorhombic, respectively; **1** falls into space group P-1, while **2** and **12** are in space groups $P2_1/c$ and $P2_12_12_1$, respectively.

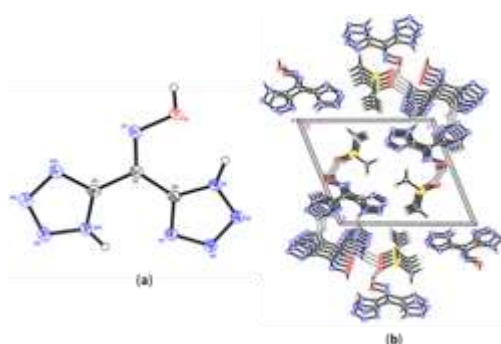


Figure 2.2 (a) Thermal ellipsoid plot (50%) and labelling scheme for di(1H-tetrazol-5-yl)methanoneoxime (**1**). Hydrogen atoms are included but are unlabeled for clarity. (b) Ball and stick packing diagram of **1** viewed down a axis. Dashed line indicate strong hydrogen bonding

Table 2.2 Crystallographic properties of **1**, **2**, and **12**

	1	2	12
Formula	C ₅ H ₉ N ₉ O ₂ S	C ₃ H ₆ N ₁₀ O ₁	C ₃ H ₁₀ N ₁₂ O ₂
CCDC number	953372	953373	953374
<i>M_f</i>	259.27	198.18	246.23
Crystal size [mm ³]	0.25 x 0.23 x 0.14	0.15 x 0.15 x 0.12	0.19 x 0.10 x 0.02
Crystal system	Triclinic	Monoclinic	Orthorhombic
Space group	P-1	P2 ₁ /c	P2 ₁ 2 ₁ 2 ₁
<i>a</i> [Å]	4.3993(9)	4.7217(4)	6.5633(11)
<i>b</i> [Å]	10.477(2)	16.4748(14)	7.6976(13)
<i>c</i> [Å]	12.184(3)	10.3658(9)	19.158(3)
<i>α</i> [°]	68.811(3)	90	90
<i>β</i> [°]	84.903(3)	101.975(2)	90
<i>γ</i> [°]	89.122(3)	90	90
<i>V</i> [Å ³]	521.49(19)	788.80(12)	967.9(3)
<i>Z</i>	2	4	4
<i>T</i> [K]	150(2)	150(2)	150(2)
<i>ρ</i> _{calcd} [Mg m ⁻³]	1.612	1.636	1.668
<i>μ</i> [mm ⁻¹]	0.321	0.135	0.141
<i>F</i> (000)	268	408	512
<i>θ</i> [°]	1.80 to 29.18	2.36 to 26.49	2.13 to 26.57
Index ranges	-6 ≤ <i>h</i> ≤ 6	-5 ≤ <i>h</i> ≤ 5	-8 ≤ <i>h</i> ≤ 8
	-14 ≤ <i>h</i> ≤ 14	-20 ≤ <i>h</i> ≤ 20	-9 ≤ <i>h</i> ≤ 9
	-16 ≤ <i>h</i> ≤ 16	-12 ≤ <i>h</i> ≤ 12	-23 ≤ <i>h</i> ≤ 23
Reflections collected	5676	7413	8823
Independent reflections (<i>R</i> _{int})	2709 [<i>R</i> _{int} =	1611 [<i>R</i> _{int} =	1993 [<i>R</i> _{int} =
Data/restraints/parameters	2709 / 0 / 157	1611 / 2 / 134	1993 / 0 / 174
GOF on <i>F</i> ²	1.036	1.062	1.086
<i>R</i> ₁ (<i>I</i> > 2 <i>σ</i> (<i>I</i>)) ^a	0.0381	0.0334	0.0384
<i>wR</i> ₂ (<i>I</i> > 2 <i>σ</i> (<i>I</i>)) ^b	0.0905	0.0871	0.0932
<i>R</i> ₁ (all data)	0.0514	0.0367	0.0437
<i>wR</i> ₂ (all data)	0.0975	0.0898	0.0964
Largest diff. peak and hole [e.	0.349 and -0.425	0.431 and -0.391	0.265 and -0.277

$$^a R_1 = \sum ||F_o| - |F_c| | / \sum |F_o|, \quad ^b R_2 = [\sum w(F_o^2 - F_c^2)^2 / \sum w(F_o^2)^2]^{1/2}$$

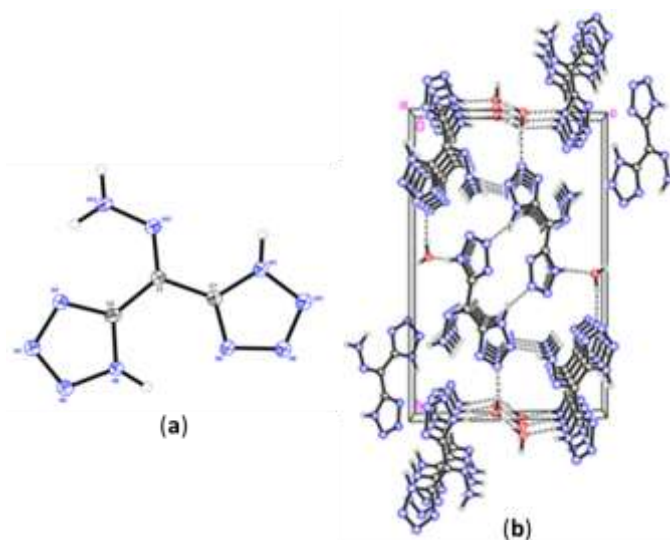


Figure 2.3 (a) Thermal ellipsoid plot (50%) and labeling scheme for 5,5'-(hydrazonomethylene)bis(1H-tetrazole) (**2**). Hydrogen atoms are included but are unlabeled for clarity. (b) Ball and stick packing diagram of **2** viewed down the *a*-axis. Dashed lines indicate strong hydrogen bonding.

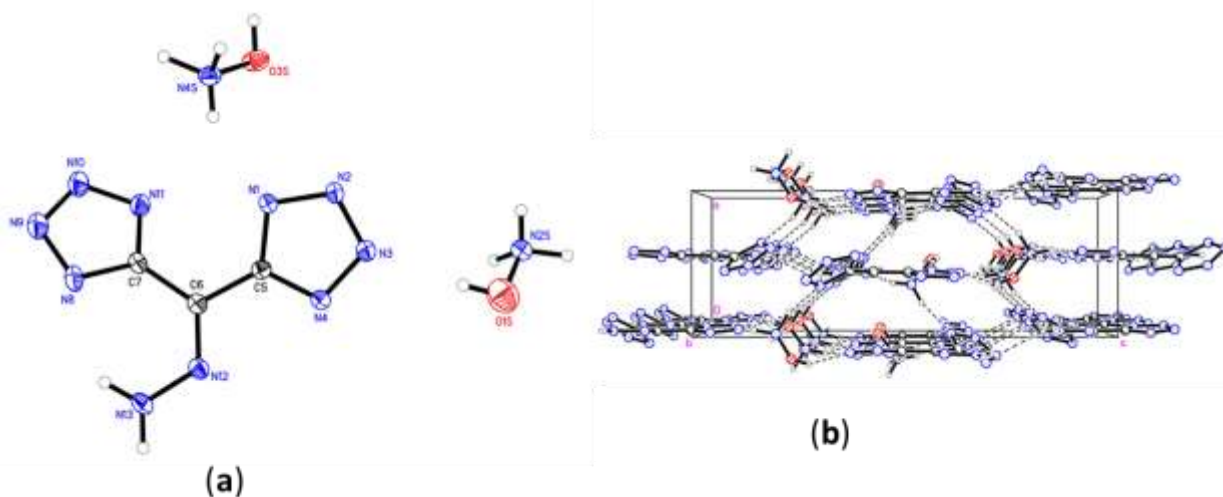


Figure 2.4 (a) thermal ellipsoid plot (50%) of **12**. Hydrogen atoms are included but are unlabeled for clarity. (b) Ball and stick packing diagram of **12** viewed down the *a*-axis. Dashed lines indicate strong hydrogen bonding.

For **1**, the bond lengths between the tetrazole ring atoms N1, N2, N3 and N4 as well as N10, N11, N12, N13 vary from 1.297 to 1.359 Å falling in the range between N-N single bonds (1.363(11)-1.366(12) Å) and N=N double bonds (1.290(12) Å). The C(6)-N(7) bond length 1.289 Å is in the range of a C=N double bond (1.279 Å). As seen in Fig. 1, the solvent

molecule is involved in hydrogen bonding with the hydrogen atom of the tetrazole ring and the hydrogen of the oxime. The bond C(6)-N(7)-O(8) is twisted with a bond angle of 113.25(14) Å in a fixed geometry; the twisting is towards the NH proton of the tetrazole ring.

Colorless prisms of **2** have 4 molecules in the unit cell. The C(1)-N(12) bond length is 1.3085(17) Å which is longer in comparison with C(6)-N(7) [1.289(2) Å] of **1**. Thus there is a lengthening of the C-N double bond on replacement of the electron withdrawing -OH group with the electron releasing NH₂ group. The bond angle C(1)-N(12)-N(13) is 121.16(11) Å which is larger than bond angle C(6)-N(7)-O(8) (113.25(14) Å) of **1**, i.e., there is less twisting in **2** in comparison to **1** and the twisting is away from NH proton of the tetrazole ring. Thus, the NH₂ group plays a significant role in the geometry of molecule. The N6-H6 and N11-H11 bond lengths are the same at 0.8800 Å as the N1-H1 and N10-H10 bond lengths of **1**. Thus there is no direct correlation of acidity with replacement of -OH by -NH₂ group. As seen in Fig. 2, there is strong hydrogen bonding between the -NH₂ proton and the N2 of the tetrazole ring. A water molecule is involved in intermolecular hydrogen bonding with N3 of the tetrazole ring and the NH.

There are four atoms in a unit cell of **12**. Two hydroxyl ammonium cations are situated away from the -NH₂ group. There is not significant change in the C-N double bond (1.300(3) Å) on the formation of a salt. Of the four N-H bonds of the hydroxyl ammonium cation only one differs from the other hydroxyl ammonium cations. As seen in Fig. 3, there is extensive hydrogen bonding in the molecule, which makes this compound a candidate for consideration as a good explosive. The hydroxyl ammonium cation is involved in hydrogen bonding with N1 of the tetrazole ring and the -NH₂ proton is also involved in hydrogen bonding with N1 of the tetrazole ring. Further details concerning the crystallographic data are provided in ESI.

2.6 Conclusion

A family of new high nitrogen-containing tetrazoles and their energetic salts was synthesized and fully characterized. The structures of **1**, **2** and **12** are confirmed by single crystal X-ray structuring. The tetrazoles are synthesized in high yield from inexpensive starting materials. All these energetic compounds exhibit good thermal stability, high density, and acceptable detonation properties, especially **11** and **12** with high heats of formation, and

competitive detonation pressures (31.6 Gpa and 32.9 Gpa) and velocities (8996 m/s and 9044 m/s). Particularly attractive are their impact sensitivities at 35 J and 20 J. These compounds have potential to compete with some existing explosives, viz., TNT and TATB, and based on impact sensitivity, RDX.

2.7 Experimental part

Caution! Although none of the compounds described herein has exploded or detonated in the course of this research, these materials should be handled with extreme care using the best safety practices.

2.8 General Methods.

^1H , and ^{13}C spectra were recorded on a 300 MHz (Bruker AVANCE 300) nuclear magnetic resonance spectrometer operating at 300.13, and 75.48 by using $[\text{D}_6]\text{DMSO}$ as solvent and locking solvent unless otherwise stated. Chemical shifts in ^1H , and ^{13}C NMR spectra are reported relative to Me_4Si . The decomposition temperatures (onset) were obtained using a differential scanning calorimeter (TA Instruments Q 10) at a scan rate of $5\text{ }^\circ\text{C min}^{-1}$ in closed aluminum containers with a small hole in the lids. IR spectra were recorded using KBr pellets for solids on a BIORAD model 3000 FTS spectrometer. Densities were determined at room temperature by employing a Micromeritics AccuPyc 1330 gas pycnometer. Elemental analyses were carried out using an Exeter CE-440 elemental analyzer.

2.9 X-ray Crystallography.

A colorless plate with dimensions $0.25 \times 0.23 \times 0.14\text{ mm}^3$ for **1** or a colorless prism of dimensions $0.15 \times 0.15 \times 0.12\text{ mm}^3$ for **2** or a colorless plate crystal of dimensions $0.19 \times 0.10 \times 0.02\text{ mm}^3$ for **12** was mounted on a MiteGen MicroMesh using a small amount of Cargille immersion oil. Data were collected on a Bruker three-circle platform diffractometer equipped with a SMART APEX II CCD detector. The crystals were irradiated using graphite monochromated MoK_α radiation ($\lambda = 0.71073$). An Oxford Cobra low temperature device was used to keep the crystals at a constant 150(2) K during data collection.

Data collection was performed and the unit cell was initially refined using *APEX2* [v2010.3-0].⁹ Data reduction was performed using *SAINT* [v7.68A]¹⁰ and *XPREP* [v2008/2].¹¹

Corrections were applied for Lorentz, polarization, and absorption effects using *SADABS* [v2008/1].¹² The structure was solved and refined with the aid of the programs in the *SHELXTL-plus* [v2008/4] system of programs.¹³ The full-matrix least-squares refinement on F2 included atomic coordinates and anisotropic thermal parameters for all non-H atoms. The H atoms were included using a riding model.

Di(1*H*-tetrazol-5-yl)methanone oxime (1)

Potassium dicyanonitrosomethanide^{4a-b} (2.79 g, 21 mmol), sodium azide (2.66g, 42 mmol) and zinc chloride (7g, 51 mmol) were suspended in ~200 mL water and refluxed for 6 h. A yellow precipitate, which turned brown over time, formed immediately. The reaction mixture was cooled to room temperature and was acidified with 2N HCl. The brown precipitate dissolved, and a new precipitate formed on stirring. The precipitate was filtered and washed with water and dried under vacuum to give a white solid, 81.5 % yield. This reaction can be scaled up to larger amounts.

$T_m = 143.9\text{ }^\circ\text{C}$ $T_{\text{dec}}(\text{onset}) = 288.7\text{ }^\circ\text{C}$, IR (KBr) ν 3552, 3407, 2966, 2879, 1831, 1627, 1572, 1523, 1476, 1418, 1328, 1242, 1134, 1077, 945, 761, 474 cm^{-1} ; ^{13}C NMR δ 151.1, 145.5, 132.1; elemental analysis (%) calcd for $\text{C}_3\text{H}_3\text{N}_9\text{O} \cdot \text{H}_2\text{O}$ (199.13): C, 18.09; H, 2.53; N, 63.31; found C, 18.08; H, 2.21; N, 63.20.

5,5'-(Hydrazonomethylene)bis(1*H*-tetrazole) (2):

One equivalent of di(1*H*-tetrazol-5-yl)methanone oxime was suspended in water and four equivalents of hydrazine hydrate were added slowly with constant stirring, and the resulting solution was heated at reflux overnight. It was cooled to room temperature and acidified with concentrated HCl to form a white precipitate which was filtered, and washed with water. The filtrate was checked for complete precipitation. The combined precipitate was dried under vacuum. The yield was nearly quantitative.

$T_{\text{dec}}(\text{onset}) = 247.6\text{ }^\circ\text{C}$, IR (KBr) ν 3400, 3362, 3164, 1641, 1617, 1581, 1551, 1415, 1327, 1247, 1197, 1136, 1069, 1040, 933, 873, 742, 582 cm^{-1} ; ^1H NMR δ 16.42 (s, 2H, NH), 10.24 (s, 2H, NH_2); ^{13}C NMR δ 152.83, 147.26, 109.26; elemental analysis (%) calcd for $\text{C}_3\text{H}_4\text{N}_{10}$ (181.13): C, 20.00; H, 2.24; N, 77.76; found C, 19.65; H, 2.22; N, 76.95.

General procedure for the preparation of salts (3–13):

Compound **1** has good solubility in ethanol and **2** is soluble in hot methanol but their salts are not soluble in either of the solvents and thus can be recovered as pure compounds from ethanol and/or methanol. In general, one millimole of **1** was dissolved in ethanol with the help of sonication followed by addition of two millimoles of either aqueous ammonia, hydrazine hydrate, 50% solution of hydroxylamine, triaminopyrimidine, triaminotriazole, melamine, and triaminotriazole and the solution stirred overnight. The precipitate was filtered and dried to give pure material. The aminoguanidine salt did not precipitate so the solvent was evaporated and the crude compound was recrystallized from methanol. Aminoguanidine bicarbonate was used as a precursor to the aminoguanidine salt.

Similarly, one millimole of **2** was dissolved in refluxing methanol and then cooled to room temperature; two mmol of aqueous ammonia, hydrazine hydrate, 50 % hydroxylamine, or triaminotriazole was added and stirred overnight. A precipitate was filtered and dried to give pure material.

3 off-white powder, T_{dec} (onset) = 262.9 °C; IR (KBr) ν 3436, 3274, 3188, 3013, 1630, 1452, 1014, 943 cm^{-1} ; ^1H NMR δ 7.5(br, NH_4^+); ^{13}C NMR δ 159.2, 155.1, 141.8; elemental analysis (%) calcd for $\text{C}_3\text{H}_9\text{N}_{11}\text{O}$ (215.18): C, 16.75; H, 4.22; N, 71.60; found C, 16.96; H, 4.33; N, 71.59.

4 off-white powder, T_{melt} = 178.9, T_{dec} (onset) = 211.5 °C, IR (KBr) ν 3443, 3064, 1229, 1076, 1018, 949, 458 cm^{-1} ; ^1H NMR δ 6.6 (broad, N_2H_5^+); ^{13}C NMR δ 157.1, 155.5, 140.8; elemental analysis (%) calcd for $\text{C}_3\text{H}_{11}\text{N}_{13}\text{O}$ (245.21): C, 14.69; H, 4.52; N, 74.26; found C, 14.56; H, 4.45; N, 73.57.

5 off-white powder, T_{melt} = 133.4; T_{dec} (onset) = 260.4 °C, IR (KBr) ν 3397, 3163, 1636, 1518, 1450, 1404, 1377, 1357, 1251, 1141, 1081, 1030, 954, 852, 606, 455 cm^{-1} ; ^1H NMR δ 7.1 (NH_3OH^+); ^{13}C NMR δ 155.1, 153.5, 138.8; elemental analysis (%) calcd for $\text{C}_3\text{H}_9\text{N}_{11}\text{O}_3$ (247.18): C, 14.58; H, 3.67; N, 62.33; found C, 14.54; H, 4.20; N, 61.82.

6 pale yellow solid, $T_{\text{melt}} = 187.7$; $T_{\text{dec}} (\text{onset}) = 197.7$ °C; IR (KBr) ν 3419, 3358, 3296, 3171, 3071, 2874, 1664, 1480, 1415, 1371, 1347, 1209, 1136, 1101, 1035, 1008, 941, 760, 610, 509 cm^{-1} ; ^1H NMR δ 7.58 (broad, NH_2), 4.7 (s, NH); ^{13}C NMR δ 158.9, 157.4, 155.6, 141.2; elemental analysis (%) calcd for $\text{C}_5\text{H}_{17}\text{N}_{17}\text{O}$ (329.29): C, 18.24; H, 4.59; N, 72.31; found C, 18.38; H, 4.70; N, 70.78.

7 off-white solid, $T_{\text{dec}} (\text{onset}) = 278.7$ °C, IR (KBr) ν 3431, 3336, 3207, 3105, 1680, 1639, 1547, 1464, 1426, 1375, 1257, 1179, 1133, 1098, 1022, 981, 945, 789, 631, 520, 464 cm^{-1} ; ^1H NMR δ 7.3 (broad, NH), 7.12 (s, NH_2), 5.08 (CH); ^{13}C NMR δ 161.5, 157.6, 156.3, 155.5, 141.2, 74.4; elemental analysis (%) calcd for $\text{C}_{11}\text{H}_{17}\text{N}_{19}\text{O}$ (431.38): C, 30.63; H, 3.97; N, 61.69; found C, 30.86; H, 4.09; N, 61.27.

8 off-white solid, $T_{\text{dec}} (\text{onset}) = 325.1$ °C; IR (KBr) ν 3340, 3126, 1668, 1522, 1514, 1473, 1371, 1195, 1137, 1016, 942, 782, 574, 466 cm^{-1} ; ^1H NMR δ 12.38 (broad, NH), 7.00 (s, NH_2); ^{13}C NMR δ 163.1, 153.8, 152.0, 137.2; elemental analysis (%) calcd for $\text{C}_9\text{H}_{15}\text{N}_{21}\text{O}$ (433.36): C, 24.94; H, 3.49; N, 67.88; found C, 24.94; H, 3.68; N, 66.58.

9 off-white solid, $T_{\text{dec}} (\text{onset}) = 249.0$ °C; IR (KBr) ν 3310, 3246, 3128, 2896, 2818, 2748, 1706, 1663, 1622, 1528, 1450, 1377, 1143, 1122, 1108, 947, 922, 800, 696, 605, 513, 481 cm^{-1} ; ^1H NMR δ 6.7 (s, 8H), 5.5 (s, 4H); ^{13}C NMR δ 156.4, 154.7, 150.1, 140.3; elemental analysis (%) calcd for $\text{C}_7\text{H}_{15}\text{N}_{21}\text{O}$ (409.33): C, 20.54; H, 3.69; N, 71.86; found C, 20.23; H, 3.68; N, 71.02.

10 off-white solid, $T_{\text{melt}} = 176.0$; $T_{\text{dec}} (\text{onset}) = 239.9$ °C; IR (KBr) ν 3369, 3182, 2866, 1629, 1541, 1466, 1401, 1174, 1133, 1043, 958, 460 cm^{-1} ; ^1H NMR δ 8.71 (s, NH_2), 7.3 (s, NH_4^+); ^{13}C NMR δ 158.4, 156.9, 124.4; elemental analysis (%) calcd for $\text{C}_3\text{H}_{10}\text{N}_{12}$ (214.19): C, 16.82; H, 4.71; N, 78.47; found C, 16.59; H, 4.92; N, 76.77.

11 off-white solid, $T_{\text{dec}} (\text{onset}) = 212.1$ °C; IR (KBr) ν 3334, 3268, 3167, 3016, 2647, 1638, 1614, 1562, 1377, 1170, 1130, 1092, 1041, 954, 708, 460 cm^{-1} ; ^1H NMR δ 8.85 (s, NH_2), 7.02

(s, N_2H_5^+) ; ^{13}C NMR δ 158.6, 156.8, 123.9; elemental analysis (%) calcd for $\text{C}_3\text{H}_{12}\text{N}_{14}$ (244.22): C, 14.75; H, 4.95; N, 80.29; found C, 14.48; H, 4.88; N, 79.27.

12 off-white solid, $T_{\text{melt}} = 183.4$; $T_{\text{dec}}(\text{onset}) = 237.8^\circ\text{C}$, IR (KBr) ν 3375, 3302, 3213, 2926, 2665, 2643, 1562, 1502, 1384, 1360, 1229, 1182, 1147, 1029, 987, 960, 464 cm^{-1} ; ^1H NMR δ 9.89; ^{13}C NMR δ 155.9, 155.8, 119.5; elemental analysis (%) calcd for $\text{C}_3\text{H}_{10}\text{N}_{12}\text{O}_2$ (244.22): C, 14.64; H, 4.09; N, 68.27; found C, 14.74; H, 4.05; N, 67.52.

13 off-white solid, $T_{\text{melt}} = 182.6$; $T_{\text{dec}}(\text{onset}) = 191.0^\circ\text{C}$, IR (KBr) ν 3419, 3321, 3127, 2974, 2723, 1697, 1659, 1552, 1520, 1473, 1398, 1303, 1165, 1132, 1037, 951, 787, 709, 459 cm^{-1} ; ^1H NMR δ 9.4 (br. NH_2); 6.1(8H); 5.4 (4H) ^{13}C NMR δ 156.0, 150.2, 118.2; elemental analysis (%) calcd for $\text{C}_7\text{H}_{16}\text{N}_{22}$ (408.35): C, 20.59; H, 3.95; N, 75.46; found C, 20.61; H, 3.98; N, 74.54.

Acknowledgements

The authors gratefully acknowledge the support of ONR (N00014-12-1-0536), and (N00014-11-AF-0-0002)

2.10 References:

- (1) a) V. Thottempudi, H. Gao, J. M. Shreeve, *J. Am. Chem. Soc.* **2011**, 133, 6464–6471.
- b) V. Thottempudi, J. M. Shreeve, *J. Am. Chem. Soc.* **2011**, 133, 19982–19992.
- c) N. Fisher, L. Gao, T. M. Klapötke, J. Stierstorfer, *Polyhedron* **2013**, 51, 201–210.
- d) D. Fisher, T. M. Klapötke, D. G. Piercey, J. Stierstorfer, *Chem. Eur. J.* **2013**, 19, 4602–4613.
- e) R. P. Singh, H. Gao, D. T. Meshri, J. M. Shreeve, in *High Energy Density Materials*, T. M. Klapötke, (Ed.), Springer, Berlin, Heidelberg, **2007**, pp. 35–83;
- f) T. M. Klapötke, J. Stierstorfer, *J. Am. Chem. Soc.* **2009**, 131, 1122–1134.
- g) Y.-H. Joo, B. Twamley, S. Garg, J. M. Shreeve, *Angew. Chem.* **2008**, 120, 6332–6335; *Angew. Chem. Int. Ed.* **2008**, 47, 6236–6239;
- h) Y.-H. Joo, J. M. Shreeve, *Org. Lett.* **2008**, 10, 4665–4667.

- (2) a) Y. Tang, H. Yang, B. Wu, X. Ju, C. Lu, G. Cheng, *Angew. Chem. Int. Ed.* **2013**, 52, 4875–4877. b) T. M. Klapötke, D. G. Piercey, J. Stierstorfer, *Dalton Trans.* **2012**, 41, 9451–9459. d) Y.-H. Joo, J. M. Shreeve, *J. Am. Chem. Soc.* **2010**, 132, 15081–15090.
- (3) a) N. Fischer, T. M. Klapötke, S. Rappenglück, J. Stierstorfer, *ChemPlusChem.* **2012**, 77, 877–888; b) A. A. Dippold, D. Izsak, T. M. Klapötke, *Chem. Eur. J.* **2013**, 19, 1204 – 12051. c) R. P. Singh, R. D. Verma, D. T. Meshri, J. M. Shreeve, *Angew. Chem.* **2006**, 118, 3664–3682. *Angew. Chem. Int. Ed.* **2006**, 45, 3584–3601. d) Y. Zhang, Y. Guo, D. A. Parrish, J. M. Shreeve, *Chem. Eur. J.* **2010**, 16, 10778–10784. e) Y.-H. Joo, B. Twamley, J. M. Shreeve, *Chem. Eur. J.* **2009**, 15, 9097–9104.
- (4) a) N. Arulsamy, D. S. Bohle, B. G. Doleskti, *Inorg. Chem.* **1999**, 38, 2709–2715. b) N. Arulsamy, *J. Org. Chem.* **2000**, 65, 1139–1143. c) Z. P. Demco, K. B. Sharpless, *J. Org. Chem.* **2001**, 66, 7945–7950. c) A. A. Dippold, T. M. Klapötke, *Chem. Asian. J.* **2013**, 8, 1463–1471. d) Y.-H. Joo, J. M. Shreeve, *J. Am. Chem. Soc.*, **2010**, 132, 15081–15090. d) R. P. Singh, R. D. Verma, D. T. Meshri, J. M. Shreeve, *Angew. Chem.* **2006**, 118, 3664–3682. *Angew. Chem. Int. Ed.* **2006**, 45, 3584–3601.
- (5) Gaussian 03, Revision D.01, M. J. Frisch, G. W. Trucks, H. B. Schlegel, G. E. Scuseria, M. A. Robb, J. R. Cheeseman, J. A. Montgomery, Jr., T. Vreven, K. N. Kudin, J. C. Burant, J. M. Millam, S. S. Iyengar, J. Tomasi, V. Barone, B. Mennucci, M. Cossi, G. Scalmani, N. Rega, G. A. Petersson, H. Nakatsuji, M. Hada, M. Ehara, K. Toyota, R. Fukuda, J. Hasegawa, M. Ishida, T. Nakajima, Y. Honda, O. Kitao, H. Nakai, M. Klene, X. Li, J. E. Knox, H.P. Hratchian, J. B. Cross, V. Bakken, C. Adamo, J. Jaramillo, R. Gomperts, R. E. Stratmann, O. Yazyev, A. J. Austin, R. Cammi, C. Pomelli, J. W. Ochterski, P. Y. Ayala, K. Morokuma, G. A. Voth, P. Salvador, J. J. Dannenberg, V. G. Zakrzewski, S. Dapprich, A. D. Daniels, M. C. Strain, O. Farkas, D. K. Malick, A. D. Rabuck, K. Raghavachari, J. B. Foresman, J. V. Ortiz, Q. Cui, A. G. Baboul, S. Clifford, J. Cioslowski, B. B. Stefanov, G. Liu, A. Liashenko, P. Piskorz, I. Komaromi, R. L. Martin, D. J. Fox, T. Keith, M. A. Al-Laham, C. Y. Peng, A. Nanayakkara, M. Challacombe, P. M. W. Gill, B. Johnson, W. Chen, M. W. Wong, C. Gonzalez, J. A. Pople, Gaussian, Inc., Wallingford, CT, **2004**.
- (6) H. D. B. Jenkins, D. Tudela, L. Glasser, *Inorg. Chem.*, **2002**, 41, 2364–2367.

- (7) a) M. Sucaska, *EXPLO5 v5.05 Program*, Zagreb, Croatia, **2011**. b) M. Sucéska, *Mater. Sci. Forum*, **2004**, 465–466, 325–330.
- (8) a) www.bam.de; b) a portion of 20 mg of energetic compound was subjected to a drop-hammer test using a 5 or 10 kg weight. The range in impact sensitivities according to the UN Recommendations is: insensitive > 40J; less sensitive \geq 35J; sensitive \geq 4 J; very sensitive \leq 3J.
- (9) Bruker (2010). *APEX2 v2010.3-0*. Bruker AXS Inc., Madison, Wisconsin, USA.
- (10) Bruker (2009). *SAINT v7.68A*. Bruker AXS Inc., Madison, Wisconsin, USA.
- (11) Bruker (2008). *XPREP v2008/2*. Bruker AXS Inc., Madison, Wisconsin, USA.
- (12) Bruker (2008). *SADABS v2008/1*, Bruker AXS Inc., Madison, Wisconsin, USA.
- (13) Bruker (2008). *SHELXTL v2008/4*. Bruker AXS Inc., Madison, Wisconsin, USA.

Chapter 3

Borohydride ionic liquids as hypergolic fuels: a quest for improved stability

by

Deepak Chand, Jiaheng Zhang, and Jean'ne M. Shreeve

published in

Chemistry – A European Journal

(D. Chand, J. Zhang, J. M. Shreeve, *Chem. Eur. J.* **2015**, 21, 13297–13301. Copyright ©

2015 Wiley-VCH Verlag GmbH & Co. KGaA, Weinheim)

Abstract

Hydrazine and its derivatives are used as fuels in rocket propellant systems; however, due to high vapor pressure, toxicity, and carcinogenicity, handling of such compounds is extremely hazardous. Hypergolic ionic liquids have shown great promise to become viable replacements for hydrazines as fuels. Borohydride-containing ionic liquids have now been synthesized using a more efficient synthetic pathway which does not require liquid ammonia and halide precursors. Among the eight new compounds, 1-allyl-3-n-butyl-imidazolium borohydride (**1**) and 1, 3-diallylimidazolium borohydride (**5**) exhibit very short ignition-delay times (ID) of 8 and 3 ms, respectively. The hydrolytic stability of borohydride compounds has been greatly improved by attaching long chain alkyl substituents to the imidazole ring. 1, 3-Di-(n-octyl)-imidazolium borohydride (**3**) is a water stable borohydride-containing ionic liquid. 1,3-Di-(n-butyl)-imidazolium borohydride (**2**) is a unique example of a borohydride liquid crystal. These ionic liquids have some unusual advantages including negligible vapor pressures, good ignition delay (ID) times, and reduced synthetic and storage costs, thereby showing great application potential as environmentally friendly fuels in bipropellant formulations. In addition, they have potential applications in the form of reducing agents and hydrogen storage materials.

3.1 Introduction

Despite acute toxicity and carcinogenicity associated with hydrazine and its derivatives, they continue to be the fuels of choice in rocket propellant systems. High specific impulse, excellent ignition with a low ignition-delay (ID) time, and superior thrust control are attractive features associated with hydrazine and its derivatives [(unsymmetrical dimethylhydrazine (UDMH)].¹ Fuels that are environmentally benign while exhibiting properties and performance comparable to hydrazine derivatives are a major focus of space propulsion research. Ionic liquids (IL) are a group of organic salts ($MP \leq 100$ °C) which are most often considered environmentally friendly green compounds with low vapor pressure and low toxicity. They have unusual chemical and physical properties, including being air and moisture stable, good solvents, and virtually no vapor pressure. Some ionic liquids ignite spontaneously upon contact with a suitable oxidizer displaying a hypergolic behavior which is one of the focal points of space propulsion research.

Since the first hypergolic ionic liquid was reported in 2008, major efforts have been directed toward the synthesis of target ionic liquids with low melting points, wide liquid ranges, high thermal stabilities, and short ignition-delay (ID) times.^{2,3} A short ignition delay time is one of the most important parameters since it is controlled by the ignition process. The ignition of ionic liquids with an oxidizer is a complicated process controlled by several factors such as density, viscosity, heat of formation etc. Given that ignition is a redox process, the presence of oxidizable hydrogen atoms in a fuel has been shown to be an important element in determining ID.³

Sodium and potassium borohydrides are hypergolic with white fuming nitric acid and recently we also demonstrated that borane-solubilized borohydride ionic liquids exhibit ultrafast ignition-delay times and low viscosities.³ Therefore, in continuation of our efforts we have explored further the synthesis of borohydride ionic liquids. The properties of the target ionic liquids including polarity, solubility, hydrophobicity, conductivity, viscosity, density, melting point, and stability can be tailored by a smart choice of cation/anion, functional group, and even the length of the alkyl chain.⁴

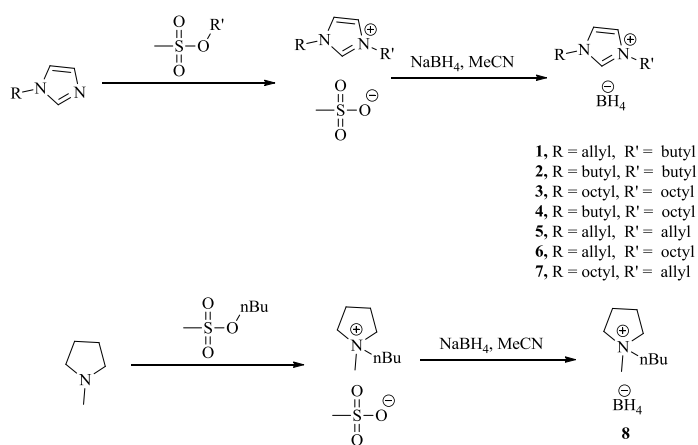
Asymmetric imidazolium cations are useful in obtaining organic salts that are liquid at room temperature, viz., ionic liquids. The C-2 proton of the imidazole ring is active and the hydrogen of the borohydride anion tends to react with it impacting the stability of the ionic

liquid as a whole.⁵ To improve the stability of imidazolium borohydride ionic liquids, it is imperative to decrease the acidity of the C-2 hydrogen. Borohydride ionic liquids have been synthesized using pressurized liquid ammonia as a solvent. The method uses halide precursors which often are solubilized by the ionic liquids and are difficult to remove.

Now we report a straightforward, ammonia and halide-free synthesis of borohydride ionic liquids. This method provides an opportunity to easily modify substituents on the imidazole ring, such as varying substituent alkyl chain lengths. It is important to note that alkyl chains with eight carbon atoms give compounds that are liquid at room temperature and overall stability is markedly improved owing to the electron-releasing nature of the long chain alkyl groups. Because of the latter effect, the presence of these substituents enhances the stability of borohydride ionic liquids. These alkyl chains are hydrophobic and as a result improve the hydrolytic stability of these ionic liquids by protecting the borohydride anion in a hydrophobic pocket of alkyl chains.

3.2 Results and discussion

Tetrahydroborate salts were synthesized with an efficient synthetic methodology. Methane sulfonate can be easily precipitated in the form of the sodium salt from methane sulfonate ionic liquids by treating them with sodium borohydride in dry acetonitrile. Previously liquid ammonia was used to realize such a transformation.^[3a, 6] In addition, there is no need to use halide precursors which almost always are solubilized in ionic liquids during their synthesis and are often difficult to remove.



Scheme 3.1 Synthesis of borohydride ionic liquids.

All the resulting tetrahydroborate compounds were fully characterized by ^1H , and ^{13}C NMR, and IR spectroscopy. Electrospray ionization mass spectrometry (ESI-MS) and elemental analysis (EA) were also used for characterization. These characterization data support the structures of the new ILs. The physicochemical properties of all the compounds (**1–8**) (Scheme 1), including their phase-transition temperatures (T_m or T_g), thermal decomposition temperatures (T_d , onset), viscosities (η), and densities (ρ), were determined by using a differential scanning calorimeter (DSC), micro VISC viscometer, and gas pycnometer, respectively. The heats of formation and heats of combustion of ILs were calculated by using the Gaussian 03 (Revision D.01) suite of programs and isodesmic reactions were employed (see Supporting Information). Their ID times were obtained by droplet tests using a high speed camera recording at 1000 frames/sec (Table 3.1).

Table 3.1: Physicochemical properties of borohydride ionic liquids

compound	T_m/T_g ^[a]	$T_d(\text{onset})$ ^[b]	ρ ^[c]	η ^[d]	ID ^[e]	ΔH_f ^[f]	ΔH_c ^[g]	I_{sp} ^[h]
1	<-80	110.3	0.92	670.2	8	174.3	-7766	198.3
2	129.9	-	0.92	nm ^[i]	40	25.4	-8585	185.9
3	13.7	115.7	0.85	nm ^[i]	222	-103.0	-13869	169.2
4	<-80	121.0	0.90	nm ^[i]	342	-89.0	-11195	171.7
5	<-80	120.8	0.93	175.1	3	314.2	-6921	212.7
6	<-80	118.2	0.88	892.0	62	117.1	-6089	185.0
7	<-80	105.4	0.88	678.2	46	116.6	-6089	184.9
8	161.0	187.8	0.85	-	68	-71.0	-7536	192.3

^[a] Melting point/glass transition temperature. ^[b] Decomposition temperature (DSC [onset]). ^[c] Density (25 °C). ^[d] Viscosity. ^[e] Ignition-delay time. ^[f] Heat of formation. ^[g] Heat of combustion. ^[h] Specific impulse (Explo5 v6.01). ^[i] Not measured.

Thermal properties of hypergolic ionic liquids are very important parameters; all compounds with the exception of **1**, **2** and **8** have very good liquid ranges starting from less than -80 °C. 1, 3-Di-n-butyl imidazolium borohydride, **2**, is liquid at room temperature but it melts at 129.9 °C which shows it is a liquid crystal.^[7] Among the liquids, **3** has the highest melting point at 13.7°C. Compound **8** melts at 161.0 °C which is too high to be classified as an ionic liquid. All of the new ionic liquids decompose above 100 °C. The length of the alkyl

chain substituents does not appear to have any significant influence on the thermal stabilities of the ionic liquids.

Density is a very important parameter – the higher the density the smaller the volume required for the fuel in the rocket fuel tank. The densities range from 0.85 g/cm³ to 0.93 g/cm³ which is higher than UDMH (0.793 g/cm³),⁷ thus the new ILs possess higher loading capacity than traditional hydrazine derivatives as propellant fuels.

Viscosity of fuels is a third property of considerable importance in bipropellant thrust engines. Lower viscosity facilitates easy mixing of the fuel with oxidizer and efficient burning can be attained. The borohydride ionic liquids are viscous compounds; compound **5** has the lowest viscosity at 175.1 mPa s. In this case, the unsaturated allyl groups play an important role in lowering the viscosity. Not surprisingly the viscosity of an ionic liquid is related directly to the number of carbons and thus the length of the alkyl chain in the substituent arm, viz., the longer the chain the more viscous. With one n-octyl substituent, **6** is the most viscous liquid with a viscosity of 892 mPa s. The presence of an unsaturated allyl group does not seem to contribute to lowering the viscosity. Despite having the same number of constituent atoms, **7** has a lower viscosity than **6**. The di-n-butyl compound **1** is less viscous than **6** and **7**.

The heat of formation (ΔH_f) and heat of combustion (ΔH_c) are related to energetic performance of the fuel; the higher the values of these parameters the more efficient is the fuel. Their values were calculated using Gaussian 03 (Revision D.01) suite of programs and by taking the difference of the HOFs (ΔH_f°) between products and reactants on the basis of combustion equations, respectively (Table 1). Compounds **3**, **4** and **8** have negative heats of formation which arise from the presence of long alkyl chains. 1, 3-Diallylimidazolium borohydride [(AAIm)BH₄] (**5**) has the most positive heat of formation at 314.2 kJ mol⁻¹ and 1-allyl-3-n-butyl-imidazolium borohydride [ABIm(BH₄)] (**1**) also shows a positive heat of formation of 174.3 kJ mol⁻¹. All compounds exhibit higher heats of combustion than UDMH (- 1979 kJ mol⁻¹),^[7] indicating better mass/energy efficiency of the borohydride ionic liquids.

The specific impulse values (Isp) were calculated by using Explo5 v6.01 using densities and heats of formation. Specific impulse is an indication of fuel performance, which is of great importance in the design of the rocket engine. A desired Isp is greater than 300 s. These tetrahydroborate compounds have calculated Isp values ranging from 169 to 213 s, which are higher than that of UDMH (198 s). Compound **5** has highest specific impulse at 213 s.

Ignition-delay time is most important in determining whether the fuel itself is suitable for practical propellant application. A droplet test with white-fuming nitric acid (WFNA) as the oxidizer was employed to measure the IDs for the new ILs. A droplet of the IL (about 50 μL) was dropped into a 20 mL glass vial containing WFNA (2 mL). A high-speed camera operating at 1000 frames s^{-1} was used to record the ID time, which is measured as the time in milliseconds between the initial contact of the IL with the WFNA and the appearance of a flame. A series of high-speed camera photos (1000 fps) of the ignition tests for ILs **1** and **5** are shown in Figure 3.1. (AAIm) BH_4 (**5**) exhibited an ultrafast ignition-delay time of 3 ms. Owing to its low viscosity, high heat of formation, and high density, it meets nearly all of the desired criteria needed for new generation green propellant fuels. ABIm(BH_4) (**1**) also exhibits a short ignition delay time of 8

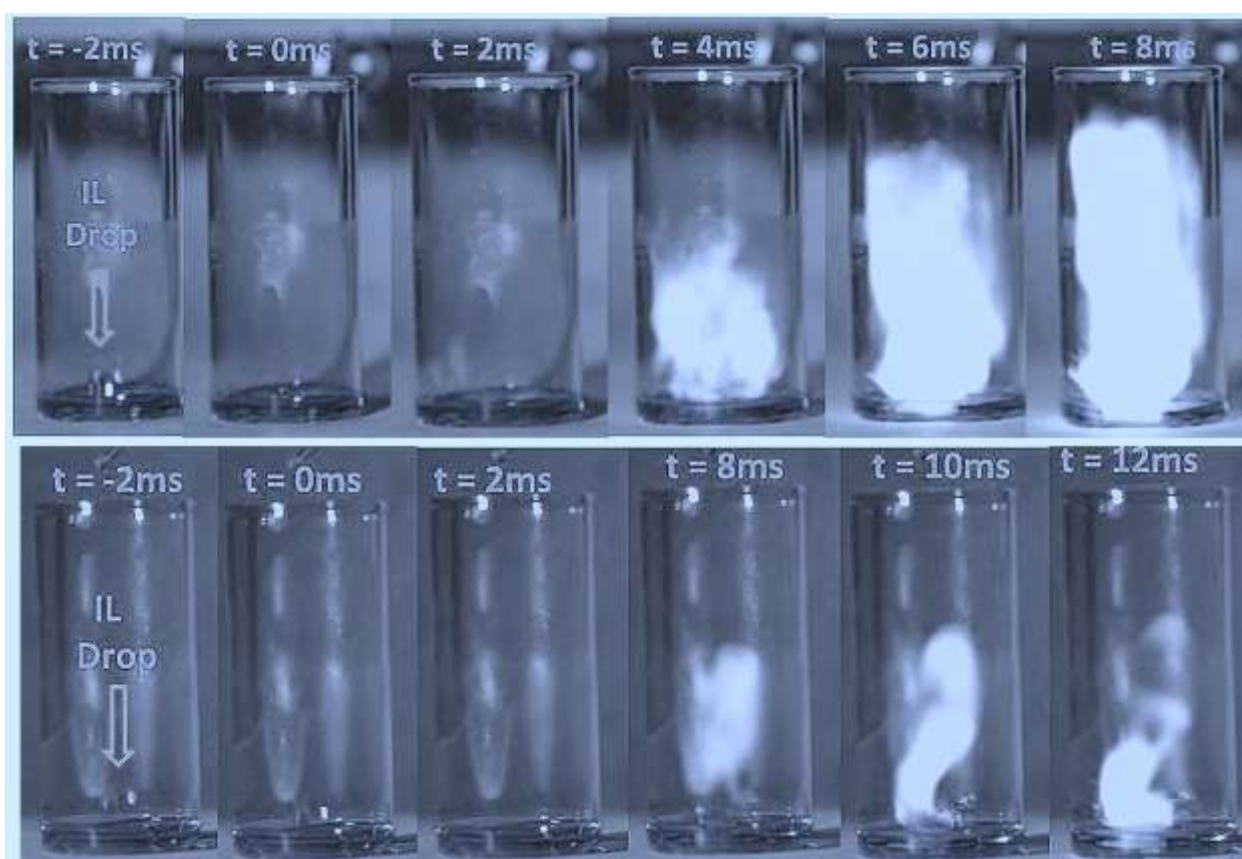


Figure 3.1 The ID test recorded using a high-speed camera photos (1000 frames/sec) of ionic liquids **5** [(AAIm)BH₄] (top) and **1** [ABIm(BH₄)] (bottom) with WFNA.

ms, it has other attractive features such as a high heat of formation, high density, etc. which makes it a good competitor as a green propellant fuel. It is noteworthy that the presence of one n-octyl group does not impact hydroborate compounds significantly, i.e., to give rise to a rather short ignition delay time as seen for **2**, **6** and **7**. However, long chain substituents bonded to both nitrogen atoms of the imidazole ring have an adverse effect on the value of the ignition delay time by increasing viscosity etc. as seen for **3** and **4**.

Borohydride-containing compounds are very often hydrolytically unstable and ionic liquids are no exception. One of our goals was to improve the hydrolytic stability of borohydride ionic liquids. By employing an n-octyl substituent bonded to each of the nitrogen atoms of the imidazole ring in **3**, it was found that the resulting ionic liquid is stable in and immiscible with water at 25 °C. Other salts, **1**, **2**, **4**, **5**, **6** with an n-butyl or an n-octyl substituent, react very slowly with water.

The new family of borohydride ionic liquids is important not only for space propulsion applications but they are also equally important in a role as mild reducing agents and as hydrogen storage materials^[9]. The efficient synthesis, availability of starting materials, better stability, and better performance should encourage the utilization of borohydride ionic liquids.

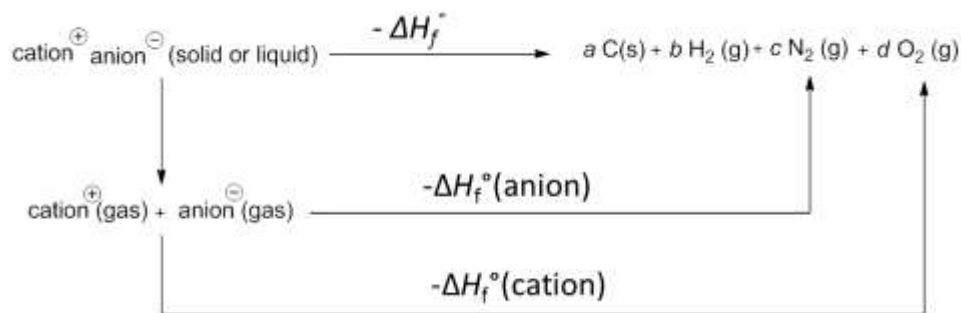
3.3 Computational Methods

Calculations were carried out with the Gaussian 03 (Revision D.01) suite of programs.^[10] The geometric optimization of the structures based on single-crystal structures, where available, and frequency analyses were carried out by using the B3LYP functional with the 6-31+G** basis set,^[11] and single energy points were calculated at the MP2/6-311+ +G** level. All of the optimized structures were characterized to be true local-energy minima on the potential energy surface without imaginary frequencies. Heats of formation (HOF) of the ILs are calculated based on a Born–Haber energy cycle (Scheme 2).

Calculation of the HOF of the ionic liquids is given by Equation (1):¹²

$$\Delta H_f^\circ (\text{salt}, 298 \text{ K}) = \Delta H_f^\circ (\text{cation}, 298\text{K}) + \Delta H_f^\circ (\text{anion}, 298\text{K}) - \Delta H_L \quad (1)$$

in which ΔH_L is the lattice energy of the salt. For 1:1 salts and considering the nonlinear nature of the cations and anion used, ΔH_L (kJmol⁻¹) can be predicted by Equation (2) suggested by Jenkins et al.¹³



Scheme 3.2 Born–Haber cycle for the formation of ILs

$$\Delta H_L = U_{\text{pot}} + [p(n_M/2 - 2) + q(n_X/2 - 2)]RT \quad (2)$$

in which n_M and n_X depend on the nature of the ions M_{p+} and X_{q-} , respectively, and have a value of 6 for nonlinear polyatomic ions. The equation for lattice potential energy U_{POT} has the form shown in Equation (3):

$$U_{\text{POT}} [\text{kJ mol}^{-1}] = \gamma (\rho_m/M_m)^{1/3} + \delta \quad (3)$$

where ρ_m is density (g cm^{-3}) and M_m is the chemical formula mass of the ionic material (g).

Heats of combustion were calculated as the difference in the HOFs between the products and reactants on the basis of combustion equations. The combustion equations are shown in the Supporting Information.

3.4 Conclusions

Eight tetrahydroborate compounds were synthesized using a straightforward, ammonia and halide-free, synthetic pathway. With the exception of **4** and **8**, all salts may be classified as ionic liquids. Based on its thermal behavior, **4** is a liquid crystal. Salts **1** and **3** exhibit very short ignition delay times of 8 and 3 ms, respectively. The short ignition delay times (IDs), high heats of formation, high densities and acceptable viscosities of these compounds make them good candidates as fuels for rocket propulsion systems. The hydrolytic stability was remarkably improved by carefully planned construction of the imidazolium cations such as 1, 3-di-(n-octyl)-imidazolium, etc. Tetrahydroborates are not usually water stable compounds; however, as was demonstrated for **3**, protection from water is possible by encapsulating the anion in a hydrophobic pocket of long chain alkyls. The new salts may also have potential applications as reducing agents and hydrogen storage materials.

3.5 Experimental section

Experimental procedures

IR spectra were recorded by using KBr plates on a Biorad Model 3000 FTS spectrometer. ^1H , and ^{13}C nmr spectra were obtained on a 300 MHz NMR spectrometer (Bruker AVANCE 300) operating at 300.13 and 75.48 MHz, respectively, using CDCl_3 as solvent and locking solvent unless otherwise stated. Chemical shifts in ^1H and ^{13}C NMR spectra are reported relative to Me_4Si . DSC measurements were performed on a TA DSC Q10 calorimeter equipped with an Auto cool accessory by heating from -80 to 400 $^\circ\text{C}$ by using a heating rate of 5 $^\circ\text{C min}^{-1}$. The densities of ionic liquids were measured at 25 $^\circ\text{C}$ on a Micrometrics Accupyc 1330 gas pycnometer. The viscosity measurements were performed on a microVISC viscometer (RheoSense, CA, USA) at 25 $^\circ\text{C}$.

Preparation of precursors

Allyl methanesulfonate, n-butyl methane sulfonate and n-octyl methanesulfonate were synthesized according to the literature.^[14] Imidazole methane sulfonate ionic liquids were synthesized based on a published route.^[15] One equivalent of imidazole and one equivalent of alkyl methanesulfonate were heated at 60 $^\circ\text{C}$ for 24 hrs to give the imidazolium methanesulfonate ionic liquids which were washed several times with boiling ethyl acetate and hexanes (5 times, 5 mL each). The purity of compounds was checked by using NMR.

General method for preparation of borohydride compounds:

One equivalent of imidazolium methane sulfonate was dissolved in dry acetonitrile (25 mL) and two and half equivalents of sodium borohydride were added. The mixture was stirred at room temperature for six hours under a nitrogen atmosphere. The white precipitate was removed by filtration and the filtrate was concentrated using a rotary evaporator. Dichloromethane was added to the filtrate and the mixture was filtered. The dichloromethane was removed by using a rotary evaporator to obtain the nonvolatile tetrahydroborate compound which was dried under vacuum. The yield is nearly quantitative.

1-Allyl-3-n-butyl-imidazolium borohydride (1).

^1H NMR: $\delta = 0.34\text{--}0.47$ (m, 4H; BH_4), 0.92 (m, 3H; CH_3), 1.31 (m, 2H; CH_2), 1.85 (m, 2H; CH_2), 4.25 (t, 2H; CH_2), 4.90 (d, 2H), 5.40 (m, 2H, $=\text{CH}_2$) 5.98 (m, 1H, CH), 7.3 (s, 1H)

7.4 (s, 1H), 9.8 ppm (s, 1H); ^{13}C NMR: $\delta = 13.54, 19.60, 32.27, 50.06, 52.14, 122.05, 122.44, 122.61, 130.17, 137.41$ ppm ; IR (KBr): $\tilde{\nu} 3133, 3087, 2961, 2872, 2288, 2228, 1562, 1460, 1340, 1165, 1084, 994, 945, 860, 761$ cm^{-1} . HRMS (ESI): m/z: calculated for cation $\text{C}_{10}\text{H}_{17}\text{N}_2$: 165.1392 $[\text{M}]^+$; found: 165.1396

1,3-Di-(n-butyl)-imidazolium borohydride (2).

^1H NMR: $\delta = 0.31\text{--}0.49$ (m, 4H; BH_4), 0.90 (t, 6H; CH_3), 1.31 (m, 6H; CH_2), 1.85 (m, 4H; CH_2), 4.26 (t, 2H; CH_2), 7.3 (m, 2H) 7.4 (m, 2H), 9.9 ppm (s, 1H); ^{13}C NMR: $\delta = 14.24, 20.29, 33.04, 50.64, 122.89, 138.18$ ppm ; IR (KBr): $\tilde{\nu} 3133, 3086, 2961, 2934, 2872, 2290, 2224, 2225, 1623, 1564, 1462, 1377, 1167, 1084, 864, 753$ cm^{-1} ; Elemental analysis: (%) calculated for $\text{C}_{11}\text{H}_{25}\text{BN}_2$ (196.14): C, 67.36; H, 12.85; N, 14.28 found C, 67.47; H, 13.28; N, 15.40.

1, 3-Di-(n-octyl)-imidazolium borohydride (3).

^1H NMR: $\delta = 0.30\text{--}0.51$ (m, 4H; BH_4), 0.84 (m, 6H; CH_3), 1.21 (m, 20; CH_2), 1.87 (b, 4H; CH_2), 4.27 (t, 4H; CH_2), 7.31 (s, 2H), 10.11 (s, 1H) ppm ; ^{13}C NMR: $\delta = 14.20, 22.75, 26.44, 29.12, 29.20, 30.50, 31.84, 50.36, 121.75, 138.20$ ppm ; IR (KBr): $\tilde{\nu} 3131, 3080, 2927, 2856, 2289, 2223, 1670, 1563, 1462, 1375, 1165, 1084, 872, 770, 645$ cm^{-1} ; Elemental analysis: (%) calculated for $\text{C}_{19}\text{H}_{41}\text{BN}_2$ (308.35): C, 74.01; H, 13.40; N, 9.08 found C, 73.06; H, 13.51; N, 9.68

1-n-Butyl-3-n-octyl-imidazolium borohydride (4).

^1H NMR: $\delta = 0.31\text{--}0.49$ (m, 4H; BH_4), 0.84 (m, 6H; CH_3), 1.26 (m, 12; CH_2), 1.85 (m, 4H; CH_2), 4.24 (q, 4H; CH_2), 7.35 (s, 1H), 7.38 (s, 2H), 9.97 (s, 1H) ppm ; ^{13}C NMR: $\delta = 13.54, 14.14, 19.58, 22.67, 26.35, 29.04, 29.13, 30.45, 31.77, 32.33, 49.95, 50.22, 122.06, 122.17, 137.57$ ppm ; IR (KBr): $\tilde{\nu} 3132, 3084, 2958, 2929, 2858, 2291, 2226, 1669, 1616, 1563, 1462, 1377, 1166, 1084, 868, 753, 644$ cm^{-1} ; HRMS (ESI): m/z: calculated for cation $\text{C}_{15}\text{H}_{29}\text{N}_2$: 237.2331 $[\text{M}]^+$; found: 237.2340

1, 3-Diallylimidazolium borohydride (5).

^1H NMR: $\delta = 0.35\text{--}0.46$ (m, 4H; BH_4), 4.91 (d, 4H; CH_2), 5.4 (m, 4H; $=\text{CH}_2$), 5.97 (m, 2H; CH), 4.24 (q, 4H; CH_2), 7.38 (s, 2H), 9.88 (s, 1H) ppm ; ^{13}C NMR: $\delta = 52.34, 122.18, 122.90,$

130.03, 137.53 ppm ; IR (KBr): $\tilde{\nu}$ 3132, 3088, 3037, 2984, 2855, 2226, 1643, 1561, 1424, 1337, 1293, 1163, 1084, 994, 944, 859, 763, 599 cm^{-1} ; HRMS (ESI): m/z: calculated for cation $\text{C}_9\text{H}_{13}\text{N}_2$: 149.1079 $[M]^+$; found: 149.1086

1-Allyl-3-n-octyl-imidazolium borohydride (6)

^1H NMR: δ = 0.37–0.39 (m, 4H; BH_4), 0.74 (t, 3H; CH_3), 1.22 (m, 10H; CH_2), 1.85 (b, 2H; CH_2), 4.20 (t, 2H; CH_2), 4.87 (d, 2H), 5.36 (m, 2H), 5.93 (m, 1H), 7.39 (s, 1H), 7.34 (s, 1H), 9.82 (s, 1H) ppm ; ^{13}C NMR: δ = 14.03, 22.56, 26.25, 28.93, 29.01, 30.31, 31.66, 50.21, 51.99, 122.11, 122.40, 122.44, 130.10, 137.10 ppm ; IR (KBr): $\tilde{\nu}$ 3131, 3084, 3025, 2927, 2857, 2288, 2225, 1645, 1562, 1458, 1375, 1343, 1164, 1084, 993, 942, 868, 763 cm^{-1} ; Elemental analysis: (%) calculated for $\text{C}_{14}\text{H}_{29}\text{BN}_2$ (236.20): C, 71.19; H, 12.37; N, 11.86 found C, 70.46; H, 12.71; N, 11.86

1-n-Octyl-3-allyl-imidazolium borohydride (7).

^1H NMR: δ = - 0.34–0.02 (m, 4H; BH_4), 0.80 (t, 3H; CH_3), 1.26 (m, 10H; CH_2), 1.86 (b, 2H; CH_2), 4.24 (t, 2H; CH_2), 4.91 (d, 2H), 5.38 (m, 2H), 5.96 (m, 1H), 7.37 (s, 1H), 7.39 (s, 1H), 9.92 (s, 1H) ppm ; ^{13}C NMR: δ = 14.14, 22.67, 26.37, 29.03, 29.12, 30.40, 31.77, 50.35, 52.15, 122.04, 122.40, 122.30, 122.61, 130.16, 137.46 ppm ; IR (KBr): $\tilde{\nu}$ 3130, 3084, 3024, 2927, 2856, 2289, 2225, 1739, 1643, 1561, 1458, 1375, 1164, 1083, 992, 941, 868, 764, 565 cm^{-1} ; HRMS (ESI): m/z: calcd for cation $\text{C}_{14}\text{H}_{25}\text{N}_2$: 221.2018 $[M]^+$; found: 221.2014

N,N-Methyl-n-butyl-pyrrolidinium borohydride (8).

^1H NMR: δ = - 0.56 – 0.25 (m, 4H; BH_4), 0.88 (t, 3H; CH_3), 1.36 (m, 2H; CH_2), 1.67 (m, 2H; CH_2), 2.18 (b, 4H; CH_2), 3.09 (s, 3H; CH_3), 3.45 (m, 2H, CH_2), 3.63 (b, 4H; CH_2), ppm ; ^{13}C NMR: δ = 13.70, 19.74, 21.67, 25.99, 48.61, 64.19, 64.47 ppm ; IR (KBr): $\tilde{\nu}$ 2962, 2934, 2385, 2292, 2225, 1630, 1466, 1381, 1126, 1076, 930 cm^{-1} ; Elemental analysis: (%) calculated for $\text{C}_9\text{H}_{24}\text{BN}$ (157.10): C, 68.81; H, 15.40; N, 8.92 found C, 68.39; H, 15.54; N, 9.31

3.6 References

- (1) a) C. A. V. Salvador, F. S. Costa, *J. Propul. Power* **2006**, 22, 1362–1372. b) S. G. Kulkarni, V. S. Bagalkote, S. S. Patil, U. P. Kumar, V. A. Kuma, *Propellants Explos. Pyrotech.* **2009**, 34, 520–525.
- (2) S. Schneider, T. Hawkins, M. Rosander, G. Vaghjiani, S. Chambreau, G. Drake, *Energy Fuels* **2008**, 22, 2871–2872.
- (3) a) S. Li, H. Gao, J. M. Shreeve, *Angew. Chem.* **2014**, 126, 3013–3016. *Angew. Chem. Int. Ed.* **2014**, 53, 2969–2972. b) Y. Zhang, J. M. Shreeve, *Angew. Chem.* **2011**, 123, 965–967; *Angew. Chem. Int. Ed.* 2011, 50, 935–937. c) Y. Zhang, H. Gao, Y-H. Joo, J. M. Shreeve; *Angew. Chem.* **2011**, 123, 9726–9734; *Angew. Chem. Int. Ed.* **2011**, 50, 9554–9562. d) H. Gao, S. Li, V. Thottempudi, J. P. Maciejewski, T. T. Vo, L. He, Q. Zhang, J. M. Shreeve, *Int. J. Energetic Materials Chem. Prop.* **2014**, 13 (3), 251–285. e) K. Wang, Y. Zhang, D. Chand, D. A. Parrish, J. M. Shreeve, *Chem. Eur. J.* **2012**, 18, 16931–16937.
- (4) Q. Zhang, J. M. Shreeve, *Chem. Rev.* **2014**, 114, 10527–10574.
- (5) M. Bürcner, A. M. T. Erle, H. Scherer, I. Krossing, *Chem. Eur. J.* **2012**, 18, 2254–2262
- (6) Wang, G. Song, Y. Peng, Y. Zhu, *Tetrahedron Lett.* **2008**, 49, 6518–6520.
- (7) K. Stappert, D. Ünal, B. Mallick, A. Mudring, *J. Mater. Chem. C*, **2014**, 2, 7976–7986.
- (8) V. N. Emel'yanenko, S. P. Verevkin, A. Heintz, *J. Am. Chem. Soc.* **2007**, 129, 3930–3937.
- (9) J. Wang, G. Song, Y. Peng, Y. Zhu, *Tetrahedron Lett.* **2008**, 49, 6518–6520.
- (10) M. J. Frisch, G. W. Trucks, H. B. Schlegel, G. E. Scuseria, M. A. Robb, J. R. Cheeseman, J. A. Montgomery, Jr., T. Vreven, K. N. Kudin, J. C. Burant, J. M. Millam, S. S. Iyengar, J. Tomasi, V. Barone, B. Mennucci, M. Cossi, G. Scalmani, N. Rega, G. A. Petersson, H. Nakatsuji, M. Hada, M. Ehara, K. Toyota, R. Fukuda, J. Hasegawa, M. Ishida, T. Nakajima, Y. Honda, O. Kitao, H. Nakai, M. Klene, X. Li, J. E. Knox, H. P. Hratchian, J. B. Cross, V. Bakken, C. Adamo, J. Jaramillo, R. Gomperts, R. E. Stratmann, O. Yazyev, A. J. Austin, R. Cammi, C. Pomelli, J. W. Ochterski, P. Y. Ayala, K. Morokuma, G. A. Voth, P. Salvador, J. J. Dannenberg, V. G. Zakrzewski, S. Dapprich, A. D. Daniels, M. C. Strain, O. Farkas, D. K. Malick, A. D. Rabuck, K.

Raghavachari, J. B. Foresman, J. V. Ortiz, Q. Cui, A. G. Baboul, S. Clifford, J. Cioslowski, B. B. Stefanov, G. Liu, A. Liashenko, P. Piskorz, I. Komaromi, R. L. Martin, D. J. Fox, T. Keith, M. A. Al-Laham, C. Y. Peng, A. Nanayakkara, M. Challacombe, P. M. W. Gill, B. Johnson, W. Chen, M. W. Wong, C. Gonzalez, J. A. Pople, Gaussian 03, Revision D.01; Gaussian, Inc.: Wallingford, CT, 2004.

- (11) R. G. Parr, W. Yang, *Density Functional Theory of Atoms and Molecules*, Oxford University Press: New York, 1989.
- (12) L. A. Curtiss, K. Raghavachari, G. W. Trucks, J. A. Pople, *J. Chem. Phys.* **1991**, 94, 7221–7230.
- (13) H. D. B. Jenkins, D. Tudela, L. Glasser, *Inorg. Chem.* **2002**, 41, 2364–2367.
- (14) a) S. Dykstra, H. S. Mosher, *J. Am. Chem. Soc.* **1976**, 79, 3474–3475 b) V. C. Sekera, C. S. Marvel, *J. Am. Chem. Soc.* **1933**, 55, 345–349.
- (15) M. Smiglak, J. M. Pringle, X. Lu, L. Han, S. Zhang, H. Gao, D. R. MacFarlane, R. D. Rogers, *Chem. Commun.* **2014**, 50, 9228–9250.

Chapter 4

Versatile Polyiodopyrazoles: Synthesis and Biocidal Promise

by

Deepak Chand and Jean'ne M. Shreeve

published in

Chemical Communications

(D. Chand, J. M. Shreeve, *Chem. Commun.* **2015**, 51, 3438–3441. Copyright © The Royal Society of Chemistry **2015**)

Abstract:

An efficient route to polyiodopyrazoles, 3, 4, 5-triiodopyrazole (**1**), 1-methyl-3, 4, 5-triiodopyrazole (**2**) and 1-diiodomethyl-3, 4, 5-triiodopyrazole (**3**), opens the door to a family of prospective biocides. A straightforward strategy for enhancing iodine concentration by the introduction of the N-diiodomethyl group is effective in expanding biocidal promise. Nitration of **1** and **2** leads to the formation of the previously inaccessible compounds, 3, 4-dinitro-5-iodopyrazole (**4**), and 3, 4-dinitro-5-iodo-1-methylpyrazole (**5**), respectively. All compounds were characterized by IR, ^1H and ^{13}C NMR, elemental analysis, and differential scanning calorimetry (DSC). The structure of **5** was determined by single crystal x-ray analysis. The iodine content ranges from 42.6% (**5**) to 89.2% (**3**). Detonation properties and detonation products are predicted by employing Cheetah 6.0. These compounds exhibit low detonation velocity and low detonation pressure. The calculated (Cheetah 6.0) gas phase detonation products, were I_2 and, in some cases, HI and I. These materials may find application as Agent Defeat Weapons (ADWs) and these synthetic pathways will open many fronts in pyrazole chemistry.

4.1 Introduction:

Modern warfare is no longer limited to the use of conventional weapons; there is believed to be a huge store of chemical and biological weapons distributed among various countries as well as illegitimate groups around the world. As a result interest in developing

Agent Defeat Weapons (ADWs) has grown significantly during the last few years.¹ ADWs are airborne warheads which contain anti bioagent materials which may be iodine-rich compounds that form large amounts of elemental iodine, and hydroiodic acid (HI) as detonation products – strong biocides against such agents as viruses, spores, bacteria, and parasites.^{2,3} ADWs demand easily containable, non sublimable, and thermally stable sources of iodine or iodine-containing species (Figure 4.1).

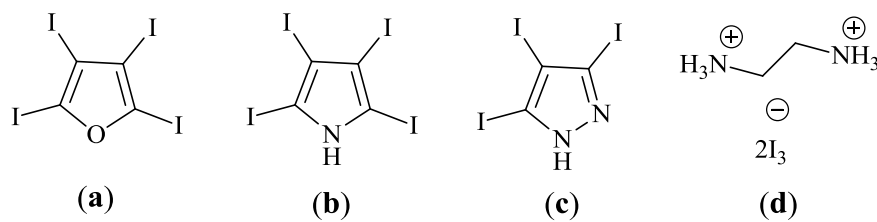


Figure 4.1 Possible ADWs - (a) Tetraiodofuran (TIF); (b) 2,3,4,5-Tetraiodo-1*H*-pyrrole; (c) 3,4,5-Triiodo-1*H*-pyrazole; (d) Ethane-1,2-diammonium-bis(triiodide).

Various periodo heterocyclicarenes including tetraiodofuran (TIF) and 3, 4, 5-triiodopyrazole have been synthesized in our lab and studied systematically.^{3a} They are being tested as effective antibioagent ingredients suitable for application as ADWs. Polyiodide salts which have low vapor pressure, high densities, and high iodine content also provide another opportunity to increase the iodine concentration in target compounds.^{3b}

Current methods for the iodination of pyrazoles suffer from a variety of difficulties. Pyrazoles with electron-donating substituents have been iodinated using iodine-iodide (I_2 -KI) or iodine monochloride (ICl); both routes often use large quantities of reactants.⁴ An iodine-aqueous ammonia combination gives a mixture of 3, 4-diiodo- and 3, 4, 5-triiodopyrazoles in very low yields.⁵ Only diiodo derivatives were obtained when an oxidative iodination methodology – I_2 - HIO_3 – was attempted.⁶ Likely because of the lack of good synthetic routes, the chemistry and properties of polyiodopyrazoles have not been studied widely.

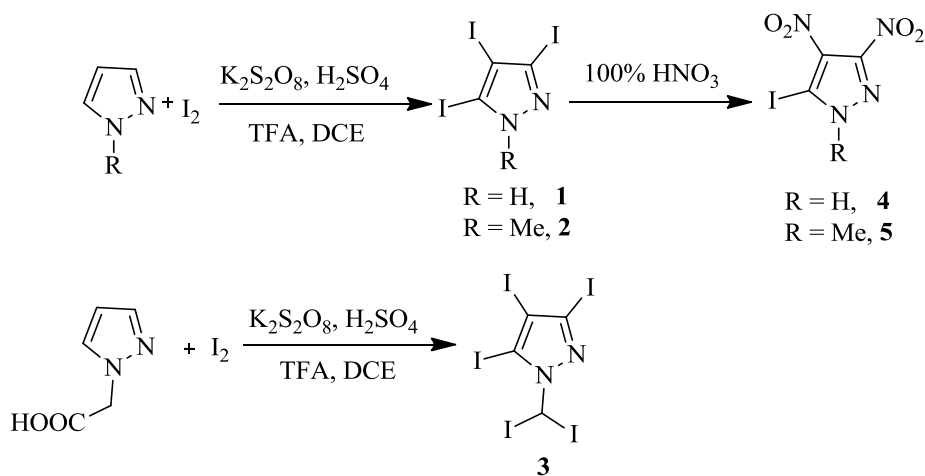
Now we report an efficient synthesis route for polyiodopyrazoles, viz., 3, 4, 5-triiodopyrazole (**1**), 1-methyl-3, 4, 5-triiodopyrazole (**2**) and 1-diiodomethyl-3, 4, 5-triiodopyrazole (**3**) in good to excellent yields. The introduction of the diiodomethyl group is an effective way to increase iodine concentration. Nitration of **1** and **2** leads to the formation

of the previously inaccessible 3, 4-dinitro-5-iodopyrazole (**4**) and 1-methyl-3, 4-dinitro-5-iodopyrazole (**5**), respectively, giving rise to more energetic iodopyrazoles.

4.2 Results and Discussion

Our continuing interest in ADWs, led us to seek alternative and more lucrative routes to the synthesis of polyiodopyrazoles. Thus a recent report where it was possible to synthesize various polyiodobenzenes by employing molecular iodine under electrophilic conditions, appeared to be useful,⁷ although the analytical purity of the products was not established using elemental analysis. Potassium persulfate was used as an oxidant in the presence of trifluoroacetic and sulfuric acids to generate the electrophilic species I^+ . It is likely that only highly stable substrates could survive under these harsh conditions thus suggesting pyrazoles known for their stability as excellent candidates for electrophilic substitution reactions.

Three equivalents of pyrazole or 1-methylpyrazole were treated with two equivalents of iodine in the presence of equal amounts of potassium persulfate in dichloroethane to obtain 3, 4, 5-triiodopyrazole (**1**) or 1-methyl-3,4,5-triiodopyrazole (**2**) in 63% and 82% yields, respectively. Compounds **1** and **2** were characterized by NMR, and IR spectra, elemental analysis, and DSC measurements (Scheme 4.1).

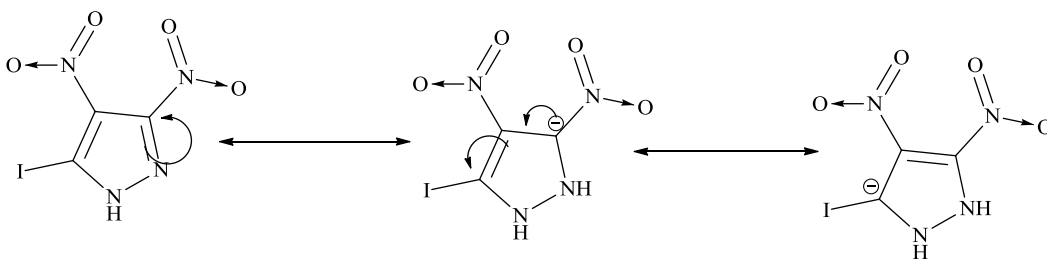


Scheme 4.1 Synthesis of **1-5**

The carbon-bonded methylene group in acetic acid is considered to be an active group for electrophilic nitration; it can be converted into the trinitromethyl group under nitrating

conditions.⁷ The 1-acetic acid substituent in pyrazole has such an active methylene group, and although it seemed likely that it should be possible to generate the triiodomethyl moiety using electrophilic iodination, only 1-diiodomethyl-3,4,5-triodopyrazole (**3**) was obtained in 30% yield (Scheme 4.1). It was fully characterized by using NMR, and IR spectra, elemental analysis, and DSC measurement techniques. Similar reactions with other heterocycles which contained the methylene group of acetic acid failed to react. However, apparently the nitrogen-linked acetic acid group has a sufficiently active methylene group for successful electrophilic iodination reactions under present conditions.

After discovering a reliable synthetic route to 3,4,5-triodopyrazole, attempts were made to introduce nitro groups onto the pyrazole ring. Although a variety of nitrating conditions were tried, it was not possible to obtain the 3,4,5-substituted trinitropyrazole. However, nitration of 3,4,5-triodopyrazole (**1**) or 1-methyl-3,4,5-triodopyrazole (**2**) with 100% nitric acid gave the new 3,4-dinitro-5-iodopyrazole (**4**) or 1-methyl-3,4-dinitro-5-iodopyrazole (**5**), respectively (Scheme 4.1), both of which previously had been inaccessible. Each was characterized by NMR, and IR spectra, elemental analysis and DSC measurement techniques. Single crystal structure analysis was carried out for **5**. Although **4** and **5** appeared to be susceptible to nucleophilic attack, e.g., to replace iodo at the 5-position, neither amination nor azidation of **4** and **5** under different conditions was successful. This may arise from significant localization of a negative charge at position 5 in the ring thus enhancing the strength of the carbon-iodine bond and precluding substitution (Scheme 4.2).



Scheme 4.2 Delocalization of electrons in **4**

Physical properties of all new polyiodo and iodo compounds are given in Table 4.1. Compound **5** has the lowest iodine content at 42.6% and **3** the highest at 89.2%. All compounds have high density; the density increasing with increase in the number of iodine

atoms. Compound **3** with five iodine atoms is the densest at 3.94 gcm^{-3} . All of the compounds decompose thermally above $250 \text{ }^\circ\text{C}$ which identifies them as thermally stable compounds. Compound **2** melts at $154 \text{ }^\circ\text{C}$ and does not decompose until $400 \text{ }^\circ\text{C}$ while **3** decomposes without melting at $371 \text{ }^\circ\text{C}$ which suggests that the presence of the diiodomethyl group is not detrimental to thermal stability.

Table 4.1 Physical properties of compounds **1–5**

Comp	$T_m^{[a]}$	$T_d^{[b]}$	$d^{[c]}$	$\Delta H_f^\circ [d]$	ΔH_f°	$D^{[e]}$	$P^{[f]}$	IS ^[g] [Iodine
1	224	272	3.38	461.1	1.03	2859	5.32	>40	85.4
2	154	-	3.35	307.2	0.66	2919	5.42	>40	82.8
3	-	371	3.94	453.1	0.63	2605	4.59	>40	89.2
4	150	292	2.46	621.6	2.19	5922	20.63	>40	44.7
5	81	363	2.30	644.8	2.16	6443	24.02	>40	42.6

[a] melting point; [b] decomposition temperature; [c] density - gas pycnometer $25 \text{ }^\circ\text{C}$); heat of formation - Gaussian 03; [e] calculated detonation velocity - Cheetah 6.0; [f] calculated detonation pressure - Cheetah 6.0; [g] impact sensitivities - BAM drop hammer.

Heats of formation of all compounds were calculated with the Gaussian 03 program suite using isodesmic reactions (Supporting Information Scheme S1). For these iodine-containing compounds, the (15s, 11p, 6d) basis of Stromberg et al.⁸ was augmented with other p shell and the five valence sp exponents optimized resulting in a [5211111111,411111111,3111] contraction scheme in conjunction with 6-31+G** for first row and second row elements. Single-point energy (SPE) refinement on the optimized geometries were performed with the use of MP2/6-311++G** level. Corresponding iodine sets were constructed in MP2 method by using all electron calculations and quasi relativistic energy-adjusted spin-orbit-averaged seven-valence-electron effective core potentials (ECPs). All compounds have positive heats of formation; as expected, **4** and **5** with nitro substituents have higher positive heats of formation. The calculated values for heats of formation and experimental densities were used to predict the detonation velocities (D) and detonation pressures (P) using the Cheetah 6.0 program. All the compounds have low detonation pressures which range from 4.59 to 24.02 GPa and the range of detonation velocities is 2605 to 6443 ms^{-1} .

The detonation products, I_2 , and in some cases, HI, and I, which are strong biocides, were predicted using Cheetah 6.0 calculations. Compound **1** with one hydrogen atom was

found to liberate HI while the other compounds do not liberate more than one percent HI or I. As shown in Figure 4.2, while compound **3** has the highest iodine concentration in its detonation

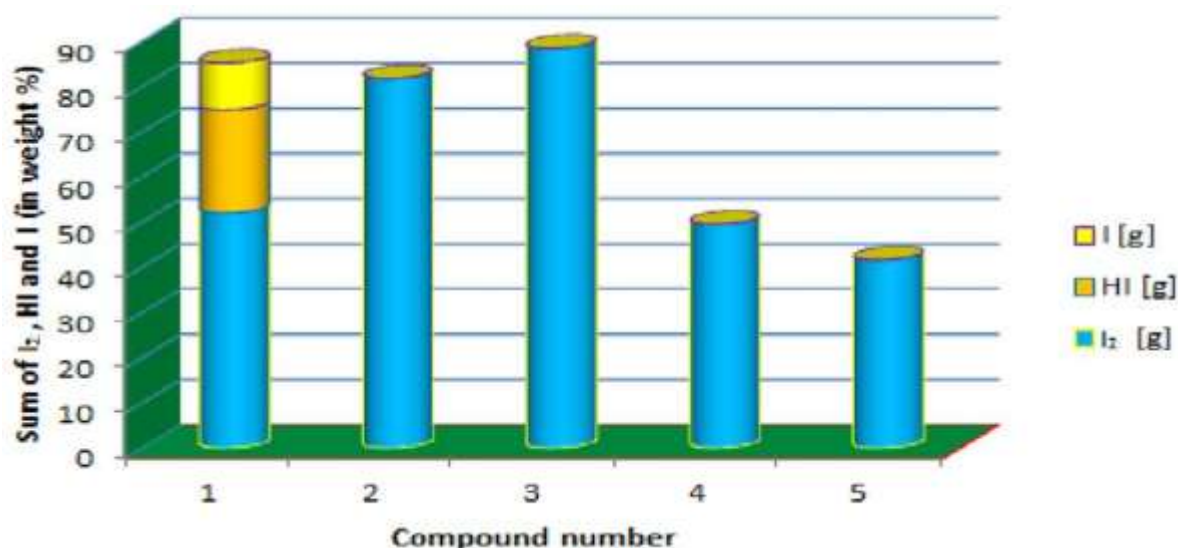


Figure 4.2 The sum of iodine-containing species in the detonation products of compounds **1**, **2**, **3**, **4** and **5** (weight percent).

products at ~89%, the detonation products of **1** - **3** each contains a high percentage of iodine that makes them good candidates as effective bio agent-defeat materials (Table 4.2).

4.3 X-ray crystallography:

The structure of **5** was obtained by X-ray single crystal crystallography. The crystallographic data are summarized in Table 4.3. Suitable crystals were obtained by the slow evaporation of a solution of **5** in benzene and diethyl ether. The crystals are triclinic falling in the $P2_1$ space group with two molecules per crystal lattice (Figure 4). The bond length between N1 and N2 is 1.364(6) Å falling in the typical range of N–N single bonds (1.363(11)–1.366(12) Å).^[9a] The bond length between the C(4) ring carbon and nitrogen of nitro group bonded to C(4) – N(8) is 1.419(8) Å. Similarly, the C(5) –N(11) bond length in 3, 4, 5-trinitropyrazole is 1.4538 (14) Å.^[9] Thus the effect of iodine substituents is clearly seen in shortening of the

C(4)-N(8) bond and lengthening in the C(5)-N(11) bond in comparison to similar bonds in 3, 4, 5-trinitropyrazole. The carbon-iodine bond length between C(3)-I(7) is 2.039(5) Å which is shorter than the normal carbon-iodine single bond length 2.13 Å.^[10] The shorter bond length may account for the failure of the amination or azidation reactions of **5**.

Table 4.2 Major detonation products shown by Cheetah 6.0 calculations [wt. % kg kg⁻¹]

Comp	N ₂ [g]	I ₂ [g]	HI [g]	I [g]	C [s]
1	6.22	52.1	22.87	10.34	8.00
2	6.09	81.9	-	-	8.51
3	3.93	88.6	-	-	6.34
4	22.2	49.6	-	-	8.36
5	18.8	41.7	-	-	5.07

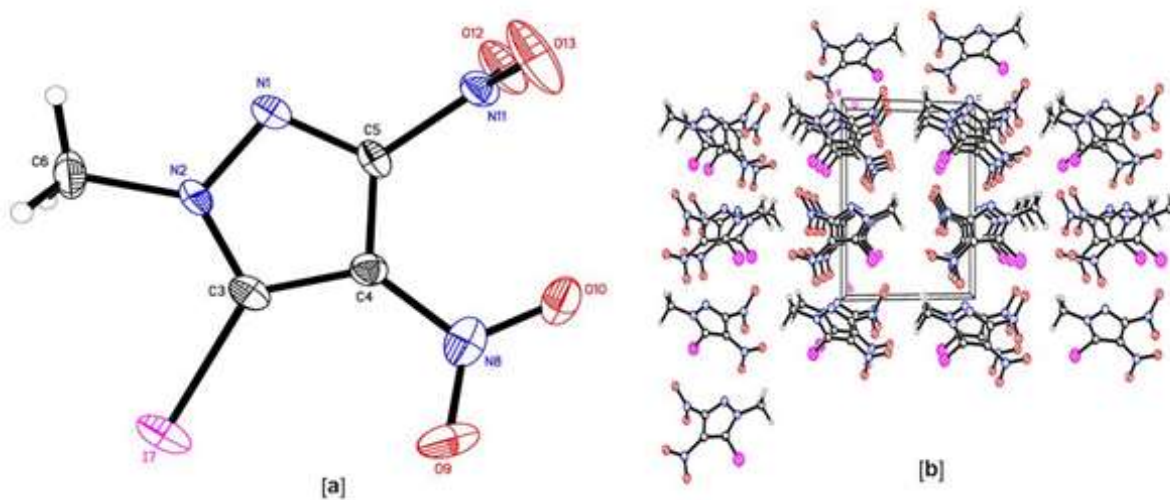


Figure 4.3 (a) Thermal ellipsoid plot (50%) of **5**. Hydrogen atoms are included but are unlabeled for clarity. (b) Ball and stick packing diagram of **5** viewed down the a-axis.

Table 4.3 Crystallographic data for compound **5**

Compound	5
Formula	C ₄ H ₃ IN ₄ O ₄
CCDC number	1031880
M_w	298.00
Crystal size [mm ³]	0.17 x 0.10 x 0.07
Crystal system	Monoclinic
Space group	P2 ₁
a [Å]	6.082(9)
b [Å]	8.835(14)
c [Å]	8.067(13)
α [°]	90
β [°]	107.606(19)
γ [°]	90
V [Å ³]	413.2(11)
Z	2
T [K]	150(2)
ρ_{calcd} [Mg m ⁻³]	2.395
μ [mm ⁻¹]	3.866
$F(000)$	280
θ [°]	2.65 to 28.21
Index ranges	-8<= h <=7
Reflections collected	1073
Independent reflections (R_{int})	1073 [$R_{\text{int}} = 0.0000$]
Data/restraints/parameters	1073 / 1 / 119
GOF on F^2	0.970
R_1 ($I > 2\delta(I)$) ^a	0.0229
wR_2 ($I > 2\delta(I)$) ^b	0.0394
R_1 (all data)	0.0252
wR_2 (all data)	0.0398
Largest diff. peak and hole [e. Å ⁻³]	1.030 and -0.782
^a $R_1 = \sum F_0 - F_c / \sum F_0 $ ^b $R_2 = [\sum w(F_0^2 - F_c^2)^2 / \sum w(F_0^2)^2]^{1/2}$	

4.4 Conclusions

Polyiodopyrazoles, 3, 4, 5-triodopyrazole (**1**), 1-methyl-3, 4, 5-triodopyrazole (**2**) and N-diiodomethyl-3, 4, 5-triodopyrazole (**3**), were synthesized in an efficient electrophilic reaction using molecular iodine in the presence of trifluoroacetic and sulfuric acid; the calculated detonation properties and products suggest that the compounds may be effective bio agent defeat agents. A synthetic method is an effective strategy for introducing an N-diiodomethyl group into pyrazole. Nitration of **1** and **2** with 100% HNO₃ resulted in the formation of the heretofore inaccessible iodo dinitropyrazoles, **4** and **5**. These polyiodopyrazoles may have application not only as ADWs but also to other areas such as medicinal chemistry, materials science, and synthetic organic chemistry.

4.5 Experimental

4.6 General methods

¹H and ¹³C spectra were recorded on 300 MHz (Bruker Avance 300) nuclear magnetic resonance spectrometer operating at 300.13 and 75.48 MHz by using [D₆]DMSO as solvent and locking solvent unless otherwise stated. The chemical shifts in ¹H and ¹³C spectra are reported relative to Me₄Si. The decomposition temperatures (onset) were obtained using a differential scanning calorimeter (TA Instruments Q 10) at a scanning rate of 5 °C per minute in closed aluminum containers with a small hole in the lids. IR spectra were recorded using KBR pellets for solids on a BIORAD model 3000 FTS spectrometer. Densities were determined at room temperature employing a Micromeritics AccuPyc 1330 gas pycnometer. Elemental analyses were carried out using an Exeter CE-440 elemental analyzer.

4.7 X-ray crystallography

An irregular yellow crystal of dimensions 0.17 x 0.10 x 0.07 mm³ was mounted on a MiteGen MicroMesh using a small amount of Cargille immersion oil. Data were collected on a Bruker three-circle platform diffractometer equipped with a SMART APEX II CCD detector. The crystals were irradiated using graphite monochromated MoK_α radiation (λ= 0.71073). An Oxford Cobra low temperature device was used to keep the crystals at a constant 150(2) °K during data collection.

Data collection was performed and the unit cell was initially refined using *APEX2* [v2010.3-0].^[11] The crystal was a non-merohedral twin. The data was refined and solved using the major component. Data reduction was performed using *SAINT* [v7.68A]^[12] and *XPREP* [v2008/2].^[13] Corrections were applied for Lorentz, polarization, and absorption effects using *TWINABS* v2008/2.^[14] The structure was solved and refined with the aid of the programs in the *SHELXTL-plus* [v2008/4] system of programs.^[15] The full-matrix least-squares refinement on F^2 included atomic coordinates and anisotropic thermal parameters for all non-H atoms. The H atoms were included using a riding model.

3, 4, 5-Triodopyrazole (1)

A mixture of pyrazole (2 g, 29.3 mmol), iodine (12.4 g, 48.8 mmol) and potassium persulfate (13.1 g, 48.8 mmol) in dichloroethane (DCE, 50 mL) in a 500 mL round-bottomed flask was stirred in an ice bath for five minutes. Trifluoroacetic acid (39 mL) was added drop wise followed by concentrated sulfuric acid (1.75 mL). The reaction mixture was stirred for half an hour in an ice bath. After stirring at room temperature for fifteen minutes, the reaction mixture was heated for eight to twelve hours at 70-80 °C. The mixture was cooled to room temperature and the solvent was evaporated by blowing air on the solution. The residue was washed with cold water and dissolved in ethanol with heating. The solution was filtered. Water (~ 15 mL) was added before evaporating the solution by blowing air to remove unreacted iodine. Finally the residue was again dissolved in ethanol and a little water was added. The solvent was removed using a rotary evaporator to give a white solid which was further washed with cold water to obtain a pure product (yield = 8.26g, 63.3%).

$T_{\text{melt}} = 224.0$ °C; $T_{\text{dec}} (\text{onset}) = 272.2$ °C; IR (KBr) ν 3398, 3075, 2953, 2875, 2733, 1647, 1516, 1417, 1314, 1242, 1130, 982, 961, 854, 449 cm^{-1} ; ^1H NMR δ 13.94 (broad, NH), 4.7; ^{13}C NMR δ 94.2, 85.1; elemental analysis: (%) calculated for $\text{C}_3\text{H}_3\text{I}_3\text{N}_2$ (445.77): C, 8.08; H, 0.23; N, 6.28; found C, 8.27; H, 0.22; N, 6.20.

1-Methyl-3, 4, 5-triodopyrazole (2)

A procedure similar to above was followed. 1-Methylpyrazole (3 g, 36.5 mmol), iodine (15.24 g, 60.0 mmol), potassium persulfate (16.2 g, 60.0 mmol), trifluoroacetic acid (48 mL),

sulfuric acid (2.16 mL), and DCE (50 mL) were reacted in 500 mL round-bottomed flask to obtain a white solid (yield, 13.8 g, 82.7 %).

$T_{\text{melt}} = 153.9\text{ }^{\circ}\text{C}$; $T_{\text{dec}} (\text{onset}) = 400^{\circ}\text{C}$; IR (KBr) ν 2929, 1645, 1359, 1325, 1258, 1161, 1076, 972, 947, 829, 714, 637, 447 cm^{-1} ; $^1\text{H NMR } \delta$ 3.95 (CH_3); $^{13}\text{C NMR } \delta$ 107.1, 98.6; elemental analysis: (%) calculated for $\text{C}_4\text{H}_3\text{I}_3\text{N}_2$ (459.79): C, 10.45; H, 0.66; N, 6.09; found C, 10.61; H, 0.65; N, 5.84.

1-Diiodomethyl-3, 4, 5-triodopyrazole (3)

Pyrazole-1-acetic acid was prepared according to the literature.^[16] Pyrazole (12.5 g, 183.6 mmol) was added to sodium hydroxide (16.2 g, 405 mmol) dissolved in water (185 mL) in a one liter round-bottomed flask. Then bromoacetic acid (28.1 g, 202.2 mmol) was added in portions with stirring and the resulting mixture heated at reflux for 2 hours. After cooling, the mixture was carefully acidified (2 M HCl) to \sim pH 3 with vigorous stirring whereupon the product precipitated from the solution (Note: product does not precipitate if HCl is added too fast) (yield, 15.26 g, 67 %).

Pyrazole acetic acid (0.2 g, 1.6 mmol), and iodine (1.27 g, 5 mmol) were stirred for five minutes in 100 mL round-bottomed flask and then trifluoroacetic acid (4 mL) was added drop wise followed by sulfuric acid (0.18 mL). The reaction mixture was stirred in an ice bath for ten minutes and at room temperature for half an hour. Then stirring continued at 70 $^{\circ}\text{C}$ to 80 $^{\circ}\text{C}$ for thirty six hours and allowed to cool to room temperature before pouring in ice-water. The residue was filtered and washed with cold water; dissolved in ethanol and about 5 mL water was added. Ethanol was removed by blowing air and residue was filtered and washed with cold water (yield: 0.21 g, 30%).

$T_{\text{dec}} (\text{onset}) = 372\text{ }^{\circ}\text{C}$; IR (KBr) ν 3448, 2922, 1637, 1401, 1344, 1296, 1273, 1107, 983, 439 cm^{-1} ; $^1\text{H NMR } \delta$ 13.61 (CHI_2); $^{13}\text{C NMR } \delta$ 109.8, 107.4, 85.1, 83.9; elemental analysis: (%) calculated for $\text{C}_4\text{H}_5\text{I}_5\text{N}_2$ (711.59): C, 6.75; H, 0.14; N, 3.94; found C, 6.75; H, 0.19; N, 4.89

3, 4-Dinitro-5-iodopyrazole (4)

3, 4, 5-Triiodopyrazole (5g, 11.2 mmol) was added portion wise to 100% nitric acid (50 mL) in 100 mL round-bottomed flask and the reaction mixture was stirred overnight at 100 $^{\circ}\text{C}$. After cooling to room temperature the mixture was poured into crushed ice; the resulting

solution was neutralized with solid sodium bicarbonate. The solution was acidified to pH 1 with concentrated hydrochloric acid and extracted with diethyl ether (3 x 20 mL). The combined extracts were washed with water and dried over anhydrous magnesium sulfate. A slightly yellow compound was obtained after evaporating the solvent using a rotary evaporator (yield, 2.3 g, 73.6%).

$T_{\text{melt}} = 150.0\text{ }^{\circ}\text{C}$; $T_{\text{dec}} (\text{onset}) = 291.9\text{ }^{\circ}\text{C}$; IR (KBr) ν 3219, 1618, 1550, 1468, 1421, 1362, 1326, 1109, 790, 848, 814, 511 cm^{-1} ; ^{13}C NMR δ 148.8, 129.6, 91.7; elemental analysis: (%) calculated for $\text{C}_3\text{HIN}_4\text{O}_4$ (283.97): C, 12.69; H, 0.35; N, 19.73; found C, 13.08; H, 0.17; N, 19.59.

3, 4-Dinitro-5-iodo-1-methylpyrazole (5)

1-Methyl-3, 4, 5-triiodopyrazole (5 g, 10.8 mmol) was added portion wise to 100% nitric acid (50 mL) and the reaction mixture was stirred overnight at 100 $^{\circ}\text{C}$. After cooling to room temperature the mixture was poured into crushed ice to obtain a white precipitate. The mixture was filtered and the residue washed with cold water to leave a white solid (yield, 2.3 g, 74%).

$T_{\text{melt}} = 81.0\text{ }^{\circ}\text{C}$; $T_{\text{dec}} (\text{onset}) = 363.0\text{ }^{\circ}\text{C}$; IR (KBr) ν 2924, 1554, 1531, 1491, 1454, 1413, 1355, 1325, 1229, 1124, 1080, 1020, 879, 808, 760, 732, 623 cm^{-1} ; ^1H NMR δ 4.0 (CH_3); ^{13}C NMR δ 147.9, 130.5, 96.7; elemental analysis: (%) calculated for $\text{C}_4\text{H}_3\text{IN}_4\text{O}_4$ (298.00): C, 16.12; H, 1.01; N, 18.80; found C, 16.15; H, 0.91; N, 18.54.

Acknowledgements

The authors gratefully acknowledge Dr. Joseph P. Hooper, Naval Postgraduate School, Monterey, CA 93943 for Cheetah 6.0 calculations. This work was supported by the Defense Threat Reduction Agency (HDTRA1-11-1-0034) and ONR (N00014-12-1-0536).

4.8 References

- (1) J. J. Baker, C. Gotzmer, R. Gill, S. L. Kim, M. Blachek, US Patent 7.568.432, **2009**.
- (2) D. Fischer, T. M. Klapötke, J. Stierstorfer, *Z. Anorg. Allg. Chem.* **2011**, 637, 660–665.
- (3) a) C. He, J. Zhang, J. M. Shreeve, *Chem. Eur. J.* **2013**, 19, 7503-7509. b) C. He, D. A. Parrish, J. M. Shreeve, *Chem. Eur. J.* **2014**, 20, 6699 – 6706.

- (4) a) R. Hüttel, O. Schäfer, P. Jochum, *Liebigs Ann. Chem.* **1955**, 593, 200–207. b) J. F. Hansen, Y. I. Kim, L. J. Griswold, G. W. Hoelle, D. L. Taylor, D. E. Vietti, *J. Org. Chem.* **1980**, 45, 76–80. (c) W. Holzer, H. Gruber, *J. Heterocycl. Chem.* **1995**, 32, 1351–1354.
- (5) a) D. Giles, E. W. Parnell, J. D. Renwick, *J. Chem. Soc. C* **1966**, 1179–1184. (b) M. M. Kim, R. T. Ruck, D. Zhao; M. A. Huffman, *Tetrahedron Lett.* **2008**, 4026–4028.
- (6) E. V. Tretyakov, S. F. Vasilevsky, *Mendeleev Commun.* **1995**, 233–234.
- (7) M. A. Rahman, F. Shito, T. Kitamura, *Synthesis* **2010**, 27–29.
- (8) M. J. Frisch, G. W. Trucks, H. B. Schlegel, G. E. Scuseria, M. A. Robb, J. R. Cheeseman, J. A. Montgomery, Jr., T. Vreven, K. N. Kudin, J. C. Burant, J. M. Millam, S. S. Iyengar, J. Tomasi, V. Barone, B. Mennucci, M. Cossi, G. Scalmani, N. Rega, G. A. Petersson, H. Nakatsuji, M. Hada, M. Ehara, K. Toyota, R. Fukuda, J. Hasegawa, M. Ishida, T. Nakajima, Y. Honda, O. Kitao, H. Nakai, M. Klene, X. Li, J. E. Knox, H. P. Hratchian, J. B. Cross, V. Bakken, C. Adamo, J. Jaramillo, R. Gomperts, R. E. Stratmann, O. Yazyev, A. J. Austin, R. Cammi, C. Pomelli, J. W. Ochterski, P. Y. Ayala, K. Morokuma, G. A. Voth, P. Salvador, J. J. Dannenberg, V. G. Zakrzewski, S. Dapprich, A. D. Daniels, M. C. Strain, O. Farkas, D. K. Malick, A. D. Rabuck, K. Raghavachari, J. B. Foresman, J. V. Ortiz, Q. Cui, A. G. Baboul, S. Clifford, J. Cioslowski, B. B. Stefanov, G. Liu, A. Liashenko, P. Piskorz, I. Komaromi, R. L. Martin, D. J. Fox, T. Keith, M. A. Al-Laham, C. Y. Peng, A. Nanayakkara, M. Challacombe, P. M. W. Gill, B. Johnson, W. Chen, M. W. Wong, C. Gonzalez, J. A. Pople, *Gaussian 03 (Revision D.01)*, Gaussian, Inc., Wallingford CT, **2004**.
- (9) a) Q. Zhang, J. Zhang, D. A. Parrish, J. M. Shreeve, *Chem. Eur. J.* **2013**, 19, 11000–11006. b) G. Hervé, C. Roussel, H. Grainger, *Angew. Chem. Int. Ed.* **2010**, 49, 3177–3181.
- (10) <http://cccbdb.nist.gov/>
- (11) Bruker, APEX2 v2010.3-0. Bruker AXS Inc., Madison, Wisconsin, USA, **2010**.
- (12) Bruker, SAINT v7.68A. Bruker AXS Inc., Madison, Wisconsin, USA, **2009**.
- (13) Bruker, XPREP v2008/2. Bruker AXS Inc., Madison, Wisconsin, USA, **2008**.
- (14) Bruker, TWINABS v2008/2, Bruker AXS Inc., Madison, Wisconsin, USA, **2008**.
- (15) Bruker, SHELXTL v2008/4. Bruker AXS Inc., Madison, Wisconsin, USA, **2008**.

- (16) A. N. Boa, J. D. Crane, R. M. Kowa, N. H. Sultana, *Eur. J. Inorg. Chem.* **2005**, 872–878.

Chapter 5

Electrophilic Iodination: A Gateway to Potential Biocides and Energetic Materials

by

Deepak Chand, Chunlin He, Lauren A. Mitchell, Damon A. Parrish, and Jean'ne M. Shreeve

submitted for publication in

Chemistry – A European Journal

Abstract

Up to nine iodine atoms were introduced into a single molecule 1,3,5-tris(3,4,5-triiodo-1*H*-pyrazol-1-yl)benzene (**9**) in a one-pot reaction using trifluoroacetic acid-mediated electrophilic iodination. The scope of this reaction was investigated extensively using diverse pyrazole substrates. Eleven polyiodo compounds with iodine content as high as 80% were synthesized and fully characterized. These polyiodo compounds are potential biocides when used with appropriate oxidizing agents. This synthetic methodology was also utilized successfully for iodination of benzimidazoles. Tetraiodobenzimidazole was nitrated with 100% nitric acid to give a high yield of 4,5,6,7-tetranitro-1*H*-benzimidazol-2(3*H*)-one (**14**) which was fully characterized and confirmed by single crystal X-ray analysis. High density, positive oxygen balance, and very good impact sensitivity values characterize **14**. For the first time, two 1,2,5-oxadiazole-*N*-oxide rings were introduced into a benzimidazole ring (**11**) which remarkably improves the stability of oxadiazole-*N*-oxide compounds.

5.1 Introduction

Biological agents like anthrax pose considerable potential public threat.¹ There is an estimate that deaths in millions could occur following the release of only 100 kg of anthrax.² As a result, interest in developing Agent Defeat Weapons (ADW) has grown remarkably during the last few years.³ These anti-bioagent materials could be iodine-rich compounds that form large amounts of elemental iodine, when detonated along with some suitable explosives.^{4,5} Earlier we synthesized various polyiodopyrazoles and established their biocidal potential through theoretical calculations.⁶ Electrophilic iodination employing trifluoroacetic acid proved to be an efficient methodology for the preparation of

polyiodopyrazoles. It is worthwhile to extend the scope of this methodology by testing it with diversely substituted pyrazoles. 4-Chloropyrazole, 4-bromopyrazole, ethylene-bridged pyrazole and ethylene-bridged 4-chloro pyrazoles were iodinated successfully. However, when the ethylene-bridged bromo derivatives are used, a mixture of products was obtained.

The scope of the reaction was extended to pyrazole bonded to benzene where it was found that only the pyrazole ring positions were iodinated in case of both bis and tris-substituted benzenes. With the successful iodination of benzimidazoles, a new avenue to trifluoroperacetic acid mediated electrophilic iodination was found which led the way to the efficient synthesis of new N-O materials. N-oxides are highly promising compounds which could possibly replace widely used secondary explosives. 1,2,5-Oxadiazole has proved to be beneficial for obtaining high performance explosives with good oxygen balance.^{7,8,9} For the first time we were able to introduce two furazan rings onto an benzimidazole ring. N-nitration of the resulting compound enhanced the density, improved oxygen balance but unfortunately the impact sensitivity was increased.

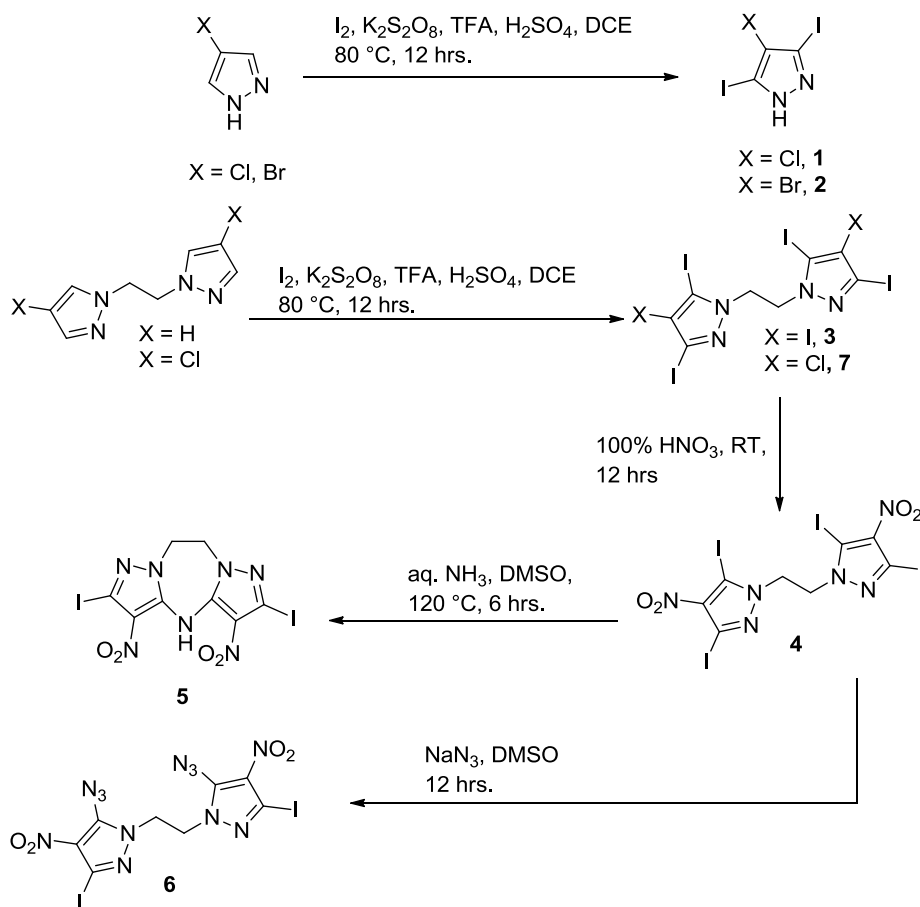
Secondary explosives with lower oxygen balance have restricted energy release due to incomplete oxidation. Polynitro compounds are attractive since they contain oxygen in the form of a nitro group which also contributes towards enhancement of density. Nitration of 4,5,6,7-tetraiodo-1*H*-benzimidazole gave a polynitro compound with a positive oxygen balance, 4,5,6,7 tetranitro-1*H*-benzimidazol-2(3*H*)-one (**14**).

5.2 Results and Discussion

5.3 Synthesis

Iodination of 4-chloro- and 4-bromopyrazole led to 4-chloro-3,5-diiodopyrazole (**1**) and 4-bromo-3,5- diiodopyrazole (**2**) in good yields (Scheme 5.1). These compounds were confirmed by NMR, IR, DSC and elemental analysis. 1,2-Bis(1*H*-pyrazol-1-yl)ethane, when iodinated, gave 1,2-bis(3,4,5-triiodo-1*H*-pyrazol-1-yl)ethane (**3**) in high yield and in very good purity. In an attempt to attain good oxygen balance in this iodine rich compound, room temperature nitration with 100% nitric acid gave the dinitro compound **4** which on treatment with sodium azide formed the diazido compound **6**. Amination of **4** resulted in the formation of the polycyclic compound **5** which was confirmed by single crystal X-ray structure analysis. Iodination of 1, 2-bis(4-chloro-1*H*-pyrazol-1-yl)ethane led to the dichloro compound, **7**.

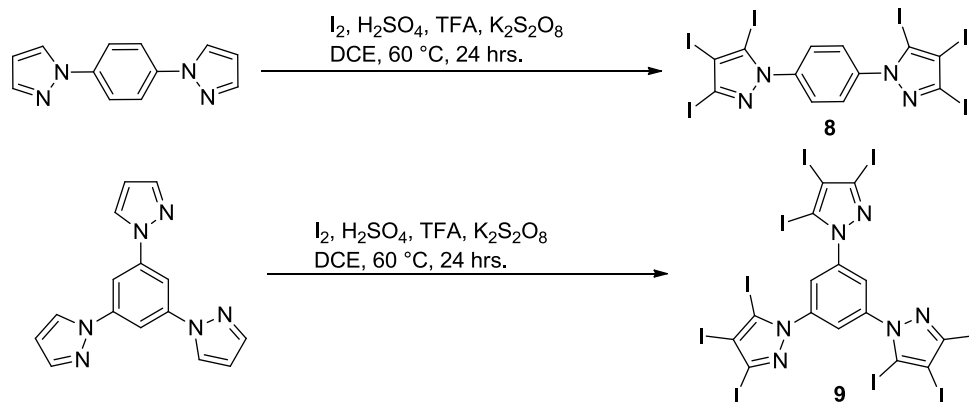
Additionally, iodination of 1,4-di(*1H*-pyrazol-1-yl)benzene resulted in the formation of **8** (Scheme 5.2), and of 1,3,5-tri(*1H*-pyrazol-1-yl)benzene **9**. A mixture of compounds which was difficult to purify because of poor solubility was obtained upon the iodination of benzimidazole; therefore direct nitration was carried out using this impure mixture. After aqueous workup, a yellow compound was isolated which upon recrystallization was confirmed to be **10**. (Scheme 5.3). It was fully characterized and further confirmed by single crystal X-ray structure analysis. Two oxadiazole-N-oxide (furoxan) rings and an imidazole ring were introduced into the benzimidazole ring to form **11** by cyclization of the diazido compound formed from the azidation of **10**.



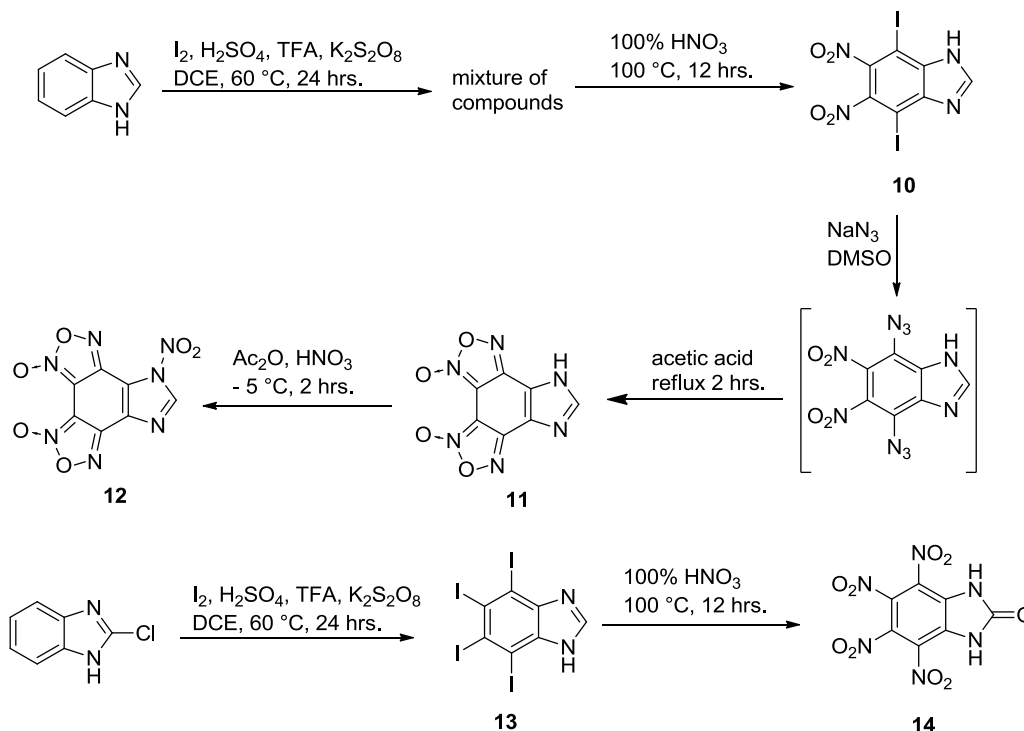
Scheme 5.1 Synthesis of compounds **1 - 7**

Due to safety concerns, the diazido compound was not characterized. Low temperature nitration of **11** resulted in the introduction of the N-nitro group to form **12** and was

characterized fully with NMR, IR, DSC and elemental analysis. Additionally, iodination of 2-chlorobenzimidazole resulted in the formation of pure tetraiodobenzimidazole (**13**). Nitration of this compound using 100% nitric acid at 100 °C gave 4,5,6,7- tetranitro-1*H*-benzimidazol-2(3*H*)-one (**14**) in 92% yield. Compound **14** was fully characterized and further confirmed by using single crystal X-ray analysis.



Scheme 5.2 Synthesis of **8** and **9**



Scheme 5.3 Synthesis of compounds **10** – **14**

5.4 Properties of compounds

The phase-transition and thermal stabilities of all compounds were determined by differential scanning calorimetry (DSC) (Table 5.1). The polyiodo compounds are found to be very stable thermally. Density was measured at room temperature using a gas pycnometer. For all polyiodo compounds; the presence of just two iodine atoms appears to increase the density above 2 g cm^{-3} .

Table 5.1: Properties of polyiodo compounds

Compound	Density ^a (g cm^{-3})	T_d ^b ($^{\circ}\text{C}$)	Iodine %	Oxygen balance ^c (%)
1	3.09	288	71.63	-
2	3.29	270	63.65	-
3	3.43	362	82.98	-
4	2.90	369	67.17	-12.7
5	2.29	306	49.09	-20.1
6	2.41	171	43.31	-16.4
7	2.90	361	69.09	-
8	3.09	372	78.85	-
9	2.87	374	81.04	-
10	3.05	>400	55.18	-13.9
13	3.18	300	81.65	-

^aMeasured by gas pycnometer. ^bOnset temperature DSC. ^cOxygen balance (based on CO) for $\text{C}_a\text{H}_b\text{O}_c\text{N}_d$, $1600(c - a - b/2)/\text{MW}$, MW = molecular weight.

Iodine content is the most important parameter for judging biocides; compounds with higher iodine concentration will be able to release larger amounts of iodine and/or HI, making them efficient biocides. Compounds **3**, **9**, and **13** contain more than 80% iodine. Although compounds **4**, **5**, **6** and **10** have lower iodine concentration, they would be good biocides since they also contain oxygen which contributes to improved oxygen balance.

Thermal stability is also very important in judging any energetic molecule (Table 5.2). In general, 1, 2, 5-oxadiazole-N-oxides do not have good thermal stability; however, in the case of **11** very good thermal stability was observed at $199 \text{ }^{\circ}\text{C}$ ($T_d \text{ RDX} = 204 \text{ }^{\circ}\text{C}$).¹⁰ With the

introduction of an N-nitro group in **12**, the thermal stability decreases to 148 °C (Table 2). The thermal stability of **14** is far better than either RDX or HMX.

Table 5.2 Properties of compounds **11**, **12** and **14**

Compound	T_d [°C] ^a	d [g cm ⁻³] ^b	ΔH_f [kJmol ⁻¹] /kJ g ⁻¹ ^c	P [GPa] ^d	v_D [ms ⁻¹] ^e	IS [J] ^f	FS [N] ^g	OB [%] ^h
11	199	1.75	515.5/2.2	24.85	7843	10	> 360	-27.3
12	148	1.80	525.2/1.9	29.78	8402	1	240	-8.6
14	299	1.87	-132.3/-0.4 -114.6/-0.36 ⁱ	30.19 30.52	8368 8388	35	> 360	5.1
TNT ^j	295	1.65	-67.0/-0.30	19.5	6881	15	353	-24.7
TATB ^j	324	1.94	-154.2/-0.54	31.15	8114	50	353	-18.6

^a Decomposition temperature (onset). ^b Density measured by gas pycnometer (25 °C). ^c Heat of formation – Gaussian 03 (See SI). ^d Detonation pressure (calculated with *EXPLO5* v6.01). ^e Detonation velocity (calculated with *EXPLO5* v6.01). ^f Impact sensitivity. ^g Friction sensitivity. ^h Oxygen balance (based on CO) for C_aH_bO_cN_d, 1600(c - a - b/2)/MW, MW = molecular weight. ⁱ Gamess software (See SI). ^j Reference 10.

High density is one of the most desired properties for energetic compounds. The presence of the N-oxide functionality in any compound is helpful in increasing density as it can participate in intramolecular as well as intermolecular hydrogen bonding. Compound **11** has a density of 1.75 g cm⁻³. The introduction of an N-nitro group proves to be a good strategy to enhance density and with it, the density of **12** is increased to 1.80 g cm⁻³ compared to **11**. The nitro functionality is known to contribute to formation of hydrogen bonds and therefore it can be helpful in increasing density. With four nitro groups and one carbonyl oxygen, **14** has a density of 1.87 g cm⁻³.

With two N-oxide moieties, **11** has a negative oxygen balance of -27.3%. With additional oxygen atoms from one more nitro group in **12**, the oxygen balance improves to -8.6%. Compound **14** has sufficient oxygen atoms to oxidize the carbon backbone completely to carbon monoxide, i.e., it has a positive oxygen balance of 5.1%.

Gas phase enthalpies were calculated based on isodesmic reactions (see SI). Geometric optimization and frequency analyses of the compounds in the isodesmic reactions

were performed using the B3LYP functional with the 6-31+G** basis set. All of the optimized structures were characterized to be true local energy minima on the potential energy surface without imaginary frequencies. The enthalpy of reaction is obtained by combining the MP2/6-311++G** energy difference for the reactions, the scaled zero point energies (ZPE), values of thermal correction (HT), and other thermal factors.^[11] 1, 2, 5-Oxadiazole compounds **11** and **12** show positive heats of formation at 2.2 and 1.9 kJ g⁻¹. Based on calculated heats of formation and experimental densities, detonation properties were calculated by using Explo5 v6.01.¹² Detonation pressure of **11** is 24.85 GPa with a detonation velocity of 7843 ms⁻¹. With higher density and better oxygen balance, **12** shows improved detonation performance with pressure of 29.78 GPa and detonation velocity of 8402 ms⁻¹. With a detonation pressure of 30.19 GPa and detonation velocity of 8368 ms⁻¹, **14** is superior to TNT and competitive with TATB.

Impact sensitivity and friction sensitivity were determined using a BAM Fallhammer apparatus and BAM friction tester, respectively. Compound **11** has an impact sensitivity of 10 J. However, likely due to the presence of the N-nitro group, **12** is a highly sensitive compound with an impact sensitivity of 1 J. In spite of having four nitro groups, **14** was found to have very good impact sensitivity at 35 J. Both **11** and **14** are friction insensitive compounds at > 360 N.

5.5 Single-crystal X-ray structure analysis

Suitable crystals for X-ray single crystal analysis of compound **5** were obtained by crystallizing from a DMSO/water solvent mixture. The compound was dissolved in DMSO by heating slowly. Then water was added dropwise while the solution was still warm until a precipitate was obtained. The mixture was refluxed to obtain a clear solution which was slowly cooled in an oil bath to obtain crystals of **5**. Crystallographic data are summarized in Table 5.3. The compound crystallizes with four unit cells in a monoclinic crystal system in a P2₁/c space group (Figure 5.1). The carbon-iodine bond [C(9)-I(10)] 2.070(6) Å is significantly longer than the carbon-nitrogen bond (from nitro group) [C(11)-N(12)] 1.412(7) Å. The bond angle [N(3)-N(4)-C(5)] 120.0(4) Å is slightly distorted in comparison to the bond angle [N(8)-N(7)-C(6)] 117.1(5) Å giving a distorted geometry to the two pyrazole nuclei.

Table 5.3 Crystallographic data for **5**, **10** and **14**

Compound	5	10•C₂H₆OS	14•C₄H₈O₂
Formula	C ₈ H ₅ I ₂ N ₇ O ₄	C ₉ H ₈ I ₂ N ₄ O ₅ S	C ₁₁ H ₁₀ N ₆ O ₁₁
CCDC number	1424001	1424002	1424003
M_w	516.99	538.05	402.25
Crystal size [mm ³]	0.209 x 0.034 x	0.123 x 0.057 x	0.310 x 0.175 x
Crystal system	Monoclinic	Monoclinic	Triclinic
Space group	P2 ₁ /c	P2 ₁ /c	P-1
a [Å]	16.6797(6)	5.34160(10)	7.8304(7)
b [Å]	98.956(2)	25.7684(6)	9.3182(8)
c [Å]	9.1213(3)	11.3694(3)	12.2176(11)
α [°]	90	90	102.459(3)
β [°]	107.606(19)	97.2720(10)	104.030(3)
γ [°]	90	90	100.776(3)
V [Å ³]	1339.59(8)	1552.35(6)	817.12(13)
Z	4	4	2
T [K]	150(2)	273(2)	296(2)
ρ_{calcd} [Mg m ⁻³]	2.498	2.302	1.635
μ [mm ⁻¹]	37.190	4.211	0.149
$F(000)$	960	1008	412
θ [°]	2.682 to 68.705	3.613 to 26.381	2.506 to 26.422
Index ranges	-17<= h <=20	-6<= h <=6	-8<= h <=9
Reflections collected	7543	14724	7885
Independent reflections (R_{int})	2389 [R_{int} =	3168 [R_{int} =	3321 [R_{int} =
Data/restraints/parameters	2389 / 1 / 193	3168 / 0 / 196	3321 / 0 / 275
GOF on F^2	1.024	0.827	1.069
R_1 ($I > 2\delta(I)$) ^a	0.0322	0.0275	0.0381
wR_2 ($I > 2\delta(I)$) ^b	0.0718	0.0758	0.1067
R_1 (all data)	$R_1 = 0.0536$	0.0410	0.0536
wR_2 (all data)	0.0797	0.0853	0.1197
Largest diff. peak and hole [e. Å ⁻³	0.830 and -0.874	0.855 and -0.449	0.257 and -0.203

^a $R_1 = \sum ||F_0| - |F_c|| / \sum |F_0|$ ^b $R_2 = [\sum w(F_0^2 - F_c^2)^2 / \sum w(F_0^2)^2]^{1/2}$

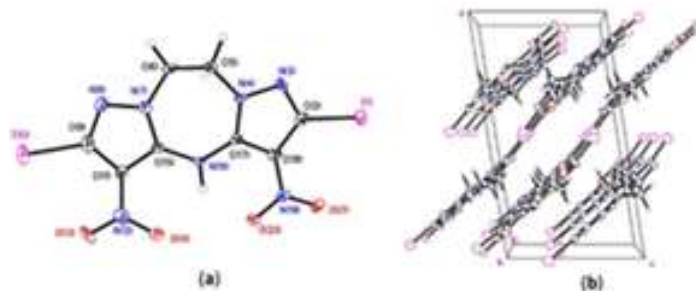


Figure 5.1 Thermal ellipsoid plot (50%) and labelling scheme for **5**. (b) Packing diagram of **5** along a-axis.

Crystals of compound **10** were obtained using DMSO/water solvent mixture following a procedure similar to that used for **5**. There is a molecule of DMSO associated with the crystal (Figure 5.2). There are four molecules per unit cell in the monoclinic crystal lattice. The crystals fall into the $P2_1/c$ space group. The carbon – iodine bond length [C(4)-I(5)] 2.099(4) Å and carbon-nitrogen (nitrogen from nitro group) [C(6)-N(7)] 1.480(6) Å are similar to bonds in **5**. There is strong π - π interactions between the benzimidazole ring giving high stability and high density to the compound.

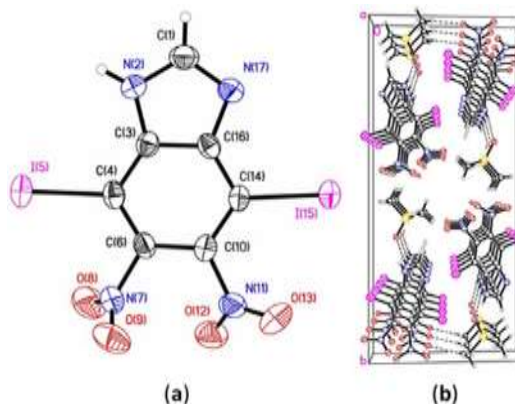


Figure 5.2 Thermal ellipsoid plot (50%) and labelling scheme for **10**. (b) Packing diagram of **10** along a-axis.

Crystals of **14** were obtained by slow evaporation of a saturated solution in benzene and ethyl acetate. The compound crystallizes with molecules per unit cell and they fall into the P-1 space group and triclinic crystal system. There is one ethyl acetate molecule associated with the crystal. As seen in Figure 5.3, there is very strong interaction between the rings which probably is responsible for the high thermal stability and higher density of the compound. The carbon-nitrogen (from the nitro group) bond falls between 1.464(2) – 1.481(2) Å.

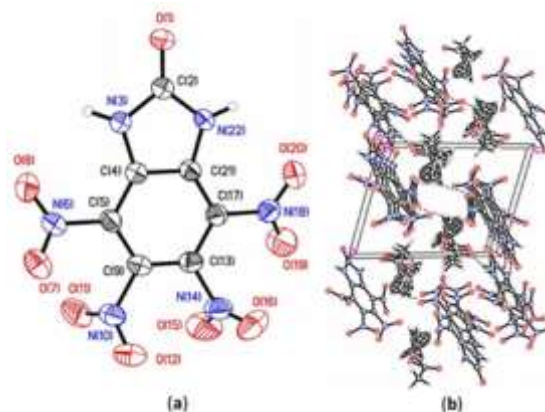


Figure 5.3 (a) Thermal ellipsoid plot (50%) and labeling scheme for **14**. (b) Packing diagram of **14** along a-axis.

Single crystal analysis was also carried out for **9** but publishable data were not obtained due to a much distorted channel of solvent trapped in the crystals; however, the structure of the compound was confirmed as shown in Figure 5.4.

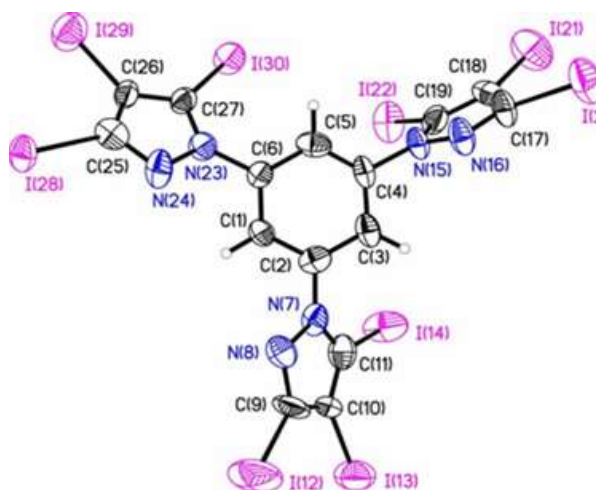


Figure 5.4 Thermal ellipsoid plot (50%) and labeling scheme for **9**.

5.6 Conclusions

Trifluoroacetic acid-mediated electrophilic iodination was explored extensively using diverse pyrazole substrates. Eleven polyiodo compounds were prepared with iodine content as high as 80%. These compounds are possible biocides. This methodology provides a very facile way of introducing iodine into a pyrazole moiety. Additionally, it was possible in reaction with benzimidazole to form tetraiodobenzimidazole which after the nitration reaction forms 4,5,6,7-tetranitro-1*H*-benzimidazol-2(3*H*)-one (**14**), a polynitro compound with high

density, positive oxygen balance, and good impact sensitivity. Two 1,2,5-oxadiazole-N-oxide rings were introduced onto the benzene ring concomitantly with the imidazole ring. Electrophilic iodination proves to be an attractive gateway to biocides and energetic materials.

5.7 Experimental Section

5.8 General Methods:

All reagents were purchased from Alfa Aesar and AK Scientific in analytical grade and were used as received. ^1H and ^{13}C NMR spectra were recorded on a Bruker 300 MHz nuclear magnetic resonance spectrometer operating at 300 and 75 MHz, respectively. Chemical shifts for ^1H and ^{13}C NMR spectra are reported relative to $(\text{CH}_3)_4\text{Si}$. D6-DMSO was used as a locking solvent unless otherwise stated. Elemental analyses (C, H, N) were performed on a CE-440 Elemental Analyzer. Melting and decomposition (onset) temperatures were recorded on a differential scanning calorimeter (TA Instruments Q10) at a scan rate of $5\text{ }^\circ\text{C min}^{-1}$. Impact sensitivity and friction sensitivity measurements were made using a standard BAM Fallhammer and BAM friction tester, respectively. IR spectra were recorded using KBr pellets with a Biorad model 3000 FTS spectrometer. Densities were determined at room temperature by employing a Micromeritics AccuPyc 1330 gas pycnometer.

5.9 X-ray crystal analysis:

A yellow needle of **5** of dimensions $0.209 \times 0.034 \times 0.005\text{ mm}^3$ was mounted on a MiteGen MicroMesh using a small amount of Cargille immersion oil. Data were collected on a Bruker three-circle platform diffractometer equipped with a SMART Platinum 135 CCD detector. The crystals were irradiated using a rotating anode CuK_α source ($\lambda = 1.54178$) with Helios optics. An Oxford Cobra low temperature device was used to keep the crystals at a constant $150(2)\text{ K}$ during data collection.

Similarly for **10** and **14**, a yellow needle of dimensions $0.123 \times 0.057 \times 0.032\text{ mm}^3$ and a colorless plate of dimensions $0.310 \times 0.175 \times 0.058\text{ mm}^3$, respectively, were mounted on a MiteGen MicroMesh using a small amount of Cargille Immersion Oil. Data were collected on a Bruker three-circle platform diffractometer equipped with a SMART APEX II CCD detector. The crystals were irradiated using graphite monochromated MoK_α radiation ($\lambda = 0.71073$). An Oxford Cobra low temperature device was used to maintain the crystals at a constant $296(2)\text{ K}$ during data collection.

Data collection was performed and the unit cell was initially refined using *APEX2* [v2014.3-0].¹³ Data reduction was performed using *SAINTE* [v7.68A]¹⁴ and *XPREF* [v2014/2].¹⁵ Corrections were applied for Lorentz, polarization, and absorption effects using *SADABS* [v2008/1].¹⁶ The structure was solved and refined with the aid of the programs *SHELXL-2014/7* within *WingX*.^{17,18} The full-matrix least-squares refinement on F^2 included atomic coordinates and anisotropic thermal parameters for all non-H atoms. The H atoms were included using a riding model. The ethyl acetate solvent molecule is disordered over two positions with a relative ratio of 79:21.

4-Chloro-3, 5-diiodopyrazole (1)

A mixture of 4-chloropyrazole¹⁹ (5 mmol, 0.5g), iodine (1.27 g, 5 mmol) and potassium persulfate (1.35 g, 5 mmol) in 10 mL dichloroethane (DCE) was stirred at 0 °C for 5 minutes. Trifluoroacetic acid (4 mL) was added drop wise followed by 0.18 mL concentrated sulfuric acid and the reaction mixture was stirred for half an hour at 0 °C. After stirring at room temperature for fifteen minutes, the mixture was heated at reflux overnight. Then it was cooled to room temperature and the solvent was evaporated by blowing air on it. The residue was washed with cold water. The residue was dissolved in ethanol with heating. The solution was filtered, a little water (5 mL) was added before evaporating the solvent by blowing air to remove unreacted iodine. Finally, the residue was again dissolved in ethanol and a little water was added. The solvent was removed using a rotary evaporator to leave a white solid which again was washed with cold water to give pure product. Yield, 63.3%

$T_{\text{melt}} = 172.9$ °C; $T_{\text{dec}} (\text{onset}) = 288.6$ °C; IR (KBr) ν 3091, 2995, 2919, 2847, 2756, 1633, 1519, 1345, 1248, 1123, 1026, 958, 821, 482 cm^{-1} ; $^1\text{H NMR } \delta$ 13.96 (broad, NH), 4.7; $^{13}\text{C NMR } \delta$ 121.3, 98.9; elemental analysis: (%) calculated for $\text{C}_3\text{HClI}_2\text{N}_2$ (354.32): C, 10.17; H, 0.28; N, 7.91; found C, 10.48; H, 0.27; N, 7.45.

4-Bromo-3,5-diiodopyrazole (2)

This compound was synthesized using a procedure similar to that for **1** with 4 mmol 4-bromopyrazole. Yield, 60%.

$T_{\text{melt}} = 189.3$ °C; $T_{\text{dec}} (\text{onset}) = 270.2$ °C; IR (KBr) ν 3092, 2978, 2903, 2837, 2746, 1629, 1516, 1333, 1116, 999, 956, 809, 462 cm^{-1} ; $^1\text{H NMR } \delta$ 14.00 (broad, NH), 4.7; $^{13}\text{C NMR } \delta$

129.8, 111.6; elemental analysis: (%) calculated for $C_3HBrI_2N_2$ (398.77): C, 9.04; H, 0.25; N, 7.03; found C, 9.50; H, 0.25; N, 6.88.

1,2-Bis(3,4,5-triiodo-1*H*-pyrazol-1-yl)ethane (3)

1,2-Di(1*H*-pyrazol-1-yl) was synthesized according to the literature.²⁰ Compound **3** was synthesized analogously to **1** using 1,2-di(1*H*-pyrazol-1-yl) (1 mmol, 0.16g), iodine (1.27 g, 5 mmol), potassium persulfate (1.35 g, 5 mmol), 10 mL dichloroethane (DCE), and trifluoroacetic acid (4 mL) was added drop wise followed by 0.18 mL concentrated sulfuric acid. Yield: 92.1 %

$T_{\text{melt}} = 332.7$ °C; $T_{\text{dec}} (\text{onset}) = 362.9$ °C; IR (KBr) ν 1627, 1442, 1429, 1317, 1288, 1022, 972, 734, 418 cm^{-1} ; $^1\text{H NMR } \delta$ 4.57 (-CH₂); $^{13}\text{C NMR } \delta$ 108.8, 99.2, 87.1, 53.5; elemental analysis: (%) calculated for $C_8H_4I_6N_4$ (917.57): C, 10.47; H, 0.44; N, 6.11; found C, 10.85; H, 0.42; N, 5.71.

1,2-Bis(3,5-diiodo-4-nitro-1*H*-pyrazol-1-yl)ethane (4)

Compound **3** (1g, 1.1 mmol) was added portion wise to 10 mL of 100% nitric acid and stirred at room temperature for 12 hrs. The reaction mixture was dropped onto crushed ice and the precipitate was filtered. The compound was washed with water and dried under vacuum to obtain an off-white solid. Yield 61%.

$T_{\text{dec}} (\text{onset}) 370.0$ °C; IR (KBr) ν 1513, 1442, 1429, 1391, 1313, 1064, 1010, 829, 749, 592, 468 cm^{-1} ; $^1\text{H NMR } \delta$ 4.70 (-CH₂); $^{13}\text{C NMR } \delta$ 139.6, 98.2, 95.0, 52.6; elemental analysis: (%) calculated for $C_8H_4I_6N_6O_4$ (755.77): C, 12.71; H, 0.53; N, 11.12; found C, 13.15; H, 0.47; N, 11.16.

3,5-Diiodo-2,6-dinitro-9,10-dihydro-4*H*-dipyrazolo[1,5,5',1']-[1,3,5]triazepine (5)

Compound **4** (1g, 1.3 mmol) was dissolved in DMSO and 10 mL aqueous ammonia was added slowly. The mixture was heated at 120 °C in a capped thick-walled pressure tube until a clear solution was obtained (~6 hrs.). The mixture was cooled to room temperature and air was blown over the surface. After some time a yellow precipitate formed. It was filtered, washed with water and dried under vacuum. Yield 65 %.

T_{dec} (onset) 306.0 °C; IR (KBr) ν 3437, 3013, 2922, 1615, 1549, 1486, 1404, 1317, 1230, 1111, 1047, 864, 799, 757, 702, 601 cm^{-1} ; ^1H NMR δ 11.38(NH), 4.71 (-CH₂); ^{13}C NMR δ 138.1, 121.7, 96.1, 50.7; elemental analysis: (%) calculated for C₈H₅I₂N₇O₄ (516.98): C, 18.59; H, 0.97; N, 18.97; found C, 18.67; H, 1.04; N, 18.53.

1,2-Bis(5-azido-3-iodo-4-nitro-1*H*-pyrazol-1-yl)ethane(6)

Compound **4** (0.54g, 0.59 mmol) was dissolved in DMSO and six equivalents of sodium azide (3.57 mmol, 0.23g) was added. The mixture was stirred at room temperature for 12 hrs and poured into ice water to obtain an off-white solid which was filtered, washed with water (3 x 20 mL), and dried in air. Yield 60%.

T_{dec} (onset) = 171.0. °C; IR (KBr) ν 2157, 1638, 1538, 1472, 1406, 1338, 1264, 1095, 1028, 867, 823, 758, 687, 599 cm^{-1} ; ^1H NMR δ 4.39 (-CH₂); ^{13}C NMR δ 137.7, 127.1, 96.7, 47.3; elemental analysis: (%) calculated for C₈H₄I₂N₁₂O₄ (586.00): C, 16.40; H, 0.69; N, 28.68; found C, 16.82; H, 0.63; N, 26.52

1,2-Bis(4-chloro-3,5-diiodo-1*H*-pyrazol-1-yl)ethane (7)

1,2-Bis(4-chloro-1*H*-pyrazol-1-yl)ethane was synthesized based on the literature.^[21] Compound **7** was synthesized analogously to **3** using 1,2-bis(4-chloro-1*H*-pyrazol-1-yl)ethane (0.46 g, 2 mmol). Yield 65 %.

T_{melt} = 294.0 °C; T_{dec} (onset) = 361.2 °C; IR (KBr) ν 1731, 1462, 1445, 1419, 1350, 1325, 1290, 1257, 1142, 1058, 1002, 756, 477, 418 cm^{-1} ; ^1H NMR δ 4.51 (-CH₂); ^{13}C NMR δ 122.7, 99.7, 90.2, 52.9; elemental analysis: (%) calculated for C₈H₄Cl₂I₄N₄ (734.67): C, 13.08; H, 0.55; N, 7.63; found C, 12.77; H, 0.60; N, 7.15.

1,4-Bis(3,4,5-triiodo-1*H*-pyrazol-1-yl)benzene (8)

1,4-Di(1*H*-pyrazol-1-yl)benzene was synthesized according to the literature.^[22] Compound **8** was synthesized analogously to **3** using 1,4-di(1*H*-pyrazol-1-yl)benzene (0.5 mmol, 0.1g), iodine (1.27 g, 5 mmol), potassium persulfate (1.35 g, 5 mmol), dichloroethane (10 mL) (DCE), trifluoroacetic acid (4 mL) and 0.18 mL concentrated sulfuric acid. The reaction mixture was heated at 60 °C for twenty four hours. An analytical sample was prepared by crystallizing the compound using a DMSO/water solvent mixture. Yield, 70%

T_{dec} (onset) = 372.4 °C; IR (KBr) ν 2924, 2855, 1629, 1512, 1431, 1365, 1313, 1105, 958, 841, 583 cm^{-1} . ^1H NMR δ 7.70 (-CH); ^{13}C NMR δ 140.3, 126.7, 111.3, 99.4, 90.29; elemental analysis: (%) calculated for $\text{C}_{12}\text{H}_4\text{I}_6\text{N}_4$ (965.61): C, 14.93; H, 0.42; N, 5.80; found C, 15.30; H, 0.38; N, 5.72

1,3,5-Tris(3,4,5-triiodo-1H-pyrazol-1-yl)benzene (9)

Compound **9** was synthesized using a procedure analogous to **8**. 1, 3, 5-Tri(1H-pyrazol-1-yl)benzene was synthesized according to the literature.^[23] Analytical samples were prepared by recrystallization using DMSO/water solvent mixture. Yield 71 %.

T_{dec} (onset) = 374.0 °C; IR (KBr) ν 3086, 2922, 1602, 1472, 1431, 1350, 1308, 1021, 966, 874, 790, 688, 642, 476 cm^{-1} ; ^1H NMR δ 7.92 (-CH); ^{13}C NMR δ 140.4, 124.5, 112.0, 99.8, 90.7; elemental analysis: (%) calculated for $\text{C}_{17}\text{H}_9\text{I}_9\text{N}_6\text{O}_8$ (1487.50): C, 13.73; H, 0.61; N, 5.65; found C, 13.61; H, 0.48; N, 5.72

4,7-Diiodo-5,6-dinitro-1H-benzimidazole (10)

A mixture of benzimidazole (5 mmol, 0.59 g), iodine (6.35 g, 25 mmol) and potassium persulfate (6.75 g, 25 mmol) in 50 mL dichloroethane (DCE) was stirred at 0 °C for 5 minutes. Trifluoroacetic acid (20 mL) was added drop wise followed by 0.9 mL concentrated sulfuric acid and the mixture was stirred for half an hour at 0 °C. After stirring at room temperature for fifteen minutes, the mixture was heated at 60 °C for twenty four hours. The mixture was cooled to room temperature and poured into ice water. The precipitate was filtered, washed with water and hexane (20 mL) to remove unreacted iodine. An off-white compound was obtained. Because of poor solubility, the compound was difficult to purify and therefore subjected directly to nitration. The impure mixture (~7 g) was added to 50 mL of 100 % nitric acid and refluxed at 100 °C for 12 hrs. After cooling to room temperature, the reaction mixture was dumped into crushed ice to obtain a yellow compound. The product was further purified by recrystallization using DMSO/water solvent mixture following the procedure similar to that used for **5** to give pure **10**.

T_{melt} = 106.0 °C; (T_{d} = > 400 °C). IR (KBr) ν 3407, 3172, 3106, 1545, 1467, 1385, 1332, 1215, 1145, 1020, 905, 868, 799, 766, 721, 700, 615, 567, 450 cm^{-1} ; ^1H NMR δ 14.00 (-NH), 8.66 (-CH-imidazole); ^{13}C NMR δ 154.3, 148.9, 148.5, 147.9; elemental analysis: (%)

calculated for $C_7H_2I_2N_4O_4$ (459.92): C, 18.28; H, 0.44; N, 12.18 ; found C, 18.55; H, 0.42; N, 12.05.

7*H*-imidazo[4',5':5,6]benzo[1,2,3,4]bis([1,2,5]oxadiazole) 3,4-dioxide (11)

4,7-Diiodo-5,6-dinitro-1*H*-benzimidazole (0.46 g, 1 mmol) was dissolved in DMSO and 5 equivalents of sodium azide (0.32 g, 5 mmol) was added. The mixture was stirred at room temperature for 12 hrs. The mixture was dropped into ice water and air was blown through it to obtain a yellow precipitate. After filtration, the compound was dried in air. Due to safety concerns no characterization was performed on this compound. It was used directly in the next step.

The yellow solid (0.5 g) was added slowly to 10 mL of acetic acid and refluxed for two hours. After cooling to room temperature the mixture was dropped into ice and filtered to obtain a slightly brown solid which was identified as **11**. Yield 60 %.

$T_{\text{melt}} = 148.3$ °C, $T_{\text{dec}} = 199.3$ °C ; IR (KBr) ν 3136, 3009, 2798, 2584, 1654, 1608, 1561, 1531, 1496, 1414, 1256, 1213, 1091, 1064, 995, 964, 928, 882, 812, 772, 741, 636, 538, 449 cm^{-1} ; ^1H NMR δ 14.00 (-NH), 8.48 (-CH-imidazole); ^{13}C NMR δ 143.7, 141.5, 105.2, 103.8; elemental analysis: (%) calculated for $C_7H_2N_6O_4$ (234.13): C, 35.91; H, 0.86; N, 35.89; found C, 35.86; H, 1.00; N, 34.67

7-Nitro-7*H*-imidazo[4',5,5,6]benzo[1,2,3,4]bis([1,2,5]oxadiazole)-3,4-dioxide (12)

Acetic anhydride (1.5 mL) was cooled to -5 °C and 0.84 mL of 100 % nitric acid was added dropwise. The resulting mixture was stirred for half an hour at -5 °C and **11** (1 mmol, 0.24 g) was added portion wise. After addition was complete, the mixture was stirred for two h and poured in crushed ice to obtain a brown precipitate which was filtered and washed with cold water and air dried. Yield 67 %.

$T_{\text{dec}} = 147.5$; IR (KBr) ν 3139, 1655, 1558, 1417, 1384, 1280, 1184, 1138, 1062, 1008, 967, 950, 817, 740, 623, 588 cm^{-1} ; ^1H NMR δ 9.50 (-CH-imidazole); ^{13}C NMR δ 142.9, 141.5, 140.9, 128.8, 114.3, 104.7, 104.5; elemental analysis: (%) calculated for $C_7HN_7O_6$ (279.13): C, 30.12; H, 0.36; N, 35.13; found C, 30.34; H, 0.57; N, 34.29.

4,5,6,7-Tetraiodo-1*H*-benzimidazole (13)

A mixture of 2-chlorobenzimidazole (10 mmol, 1.5 g), iodine (8.46 g, 33.3 mmol) and potassium persulfate (9 g, 33.3 mmol) in 50 mL dichloroethane (DCE) was stirred at 0 °C for 5 minutes. Trifluoroacetic acid (26.6 mL) was added drop wise followed by 1.2 mL concentrated sulfuric acid and the mixture was stirred for half an hour at 0 °C. After stirring at room temperature for fifteen minutes, the mixture was heated for twenty four hours at 60 °C. The mixture was cooled to room temperature and poured into ice water. The precipitate was filtered, washed with water, and then hexane to remove unreacted iodine. An off-white compound was obtained. Yield 89 %.

Compound **13** can be synthesized alternatively by using the method developed by A. Gianoncelli, et al.^[24]

$T_{\text{dec}} = 300^{\circ}\text{C}$; IR (KBr) ν 3398, 1629, 1466, 1404, 1367, 1331, 1258, 1219, 1174, 977, 922, 659, 576, 478 cm^{-1} ; ^1H NMR δ 8.02 (-CH-imidazole); ^{13}C NMR δ 141.1, 140.4, 139.5, 114.6 ; elemental analysis: (%) calculated for $\text{C}_7\text{H}_4\text{I}_4\text{N}_2$ (621.72): C, 13.52; H, 0.32; N, 4.51; found C, 13.79; H, 0.25; N, 4.48.

4, 5, 6, 7-Tetranitro-1*H*-benzimidazol-2(3*H*)-one (14)

4, 5, 6, 7-Tetraiodo-1*H*-benzimidazole (5 g) was added portion wise to 50 mL of 100% nitric acid and the mixture was refluxed overnight at 100 °C. After cooling at room temperature the mixture was poured into crushed ice to obtain a yellow precipitate which was filtered, and washed with cold water (10 mL x 3) to obtain **14**. Yield 92 %.

$T_{\text{dec}} = 299^{\circ}\text{C}$; IR (KBr) ν 3392, 3290, 1757, 1618, 1563, 1502, 1455, 1366, 1199, 1153, 983, 910, 761, 692, 444 cm^{-1} ; ^1H NMR δ 12.5(brd,-NH); ^{13}C NMR δ 155.3, 133.4, 130.7, 122.1 ; elemental analysis: (%) calculated for $\text{C}_7\text{H}_2\text{N}_6\text{O}_9$ (314.13): C, 26.76; H, 0.64; N, 26.75; found C, 26.31; H, 0.68; N, 25.46

Acknowledgements

The authors are grateful for the support of ONR (N00014-12-1-0536), and the Defense Threat Reduction Agency (HDTRA1-11-1-0034). We deeply appreciate the help of Dr. Jerry Boatz, Air Force Research Laboratory, Edwards Airforce Base, CA with the calculation of the heat of formation for **14**.

5.10 References

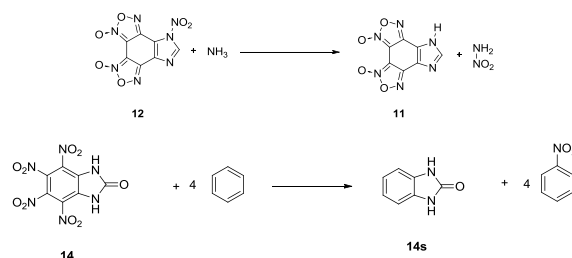
- (1) a) B. R. Clark, M. L. Pantoya, *Phys. Chem. Chem. Phys.* **2010**, *12*, 12653–12657. b) H. Wang, G. Jian, W. Zhou, J. B. DeLisio, V. T. Lee, M. R. Zachariah, *ACS Appl. Mater. Interfaces*, **2015**, *7*, 17363–17370.
- (2) a) T. V. Inglesby, D. A. Henderson, J. G. Bartlett, M. S. Ascher, E. Eitzen, A. M. Friedlander, J. Hauer; J. McDade, M. T. Osterholm, T. O'Toole, G. Parker, T. M. Perl, P. K. Russell, K. Tonat, *J. Am. Med. Assoc.* **1999**, *281*, 1735–1745. b) Office of Technology Assessment, US Congress, *Proliferation of Weapons of Mass Destruction*, Assesment, U.S. Government Printing Office, Washington, DC, **1993**.
- (3) a) K. O. Christe, R. Haiges, P. Vashista, Defense Threat Reduction Energy Report (DTRA-TR-13-23). April 2013. b) R. D. Chapman, US 8221566 B1 (July 17, 2012). c) J. M. Shreeve, Defence Threat Reduction Agency Report (HDTRA1-10-1-0116). July 2014. d) R. D. Chapman, R. A. Hollins, T. S. Jones, T. J. Groshens, G. T. Guck, D. Thompson, T. J. Schilling, D. Wooldridge, P. N. Cash, Defense Threat Reduction Energy Report (DTRA-TR-14-26). June 2014. e) J. J. Baker, C. Gotzmer, R. Gill, S. L. Kim, M. Blachek, US Pat., 7,568.432, 2009.
- (4) D. Fischer; T. M. Klapötke, J. Stierstorfer, *Z. Anorg. Allg. Chem.* **2011**, *637*, 660–665.
- (5) (a) C. He, J. Zhang, J. M. Shreeve, *Chem. Eur. J.* **2013**, *19*, 7503–7509. (b) C. He, D. A. Parrish, J. M. Shreeve, *Chem. Eur. J.* **2014**, *20*, 6699–6706.
- (6) a) D. Chand, J. M. Shreeve, *Chem. Commun.* **2015**, *51*, 3438 – 3441. b) M. A. Rahman, F. Shito, T. Kitamura, *Synthesis*, **2010**, 27–29.
- (7) a) H. Wei, J. Zhang, J. M. Shreeve, *Chem. Asian J.* **2015**, *10*, 1130. b) H. Wei, J. Zhang, C. He, J. M. Shreeve, *Chem. Eur. J.* **2015**, *21*, 8607. c) Y. Tang, H. Gao, D. A. Parrish, J. M. Shreeve, *Chem. Eur. J.* **2015**, *21*, 11401. d) J. Zhang, D. A. Parrish, J. M. Shreeve, *Chem. Asian J.* **2014**, *9*, 2953. e) V. Thottempudi, J. Zhang, C. He, J. M. Shreeve, *RSC Adv.* **2014**, *4*, 50361.
- (8) a) L. Liang, K. Wang, C. Bian, L. Liang, Z. Zhou, *Chem. Eur. J.* **2013**, *19*, 14902–14910. b) Z. Fu, R. Su, Y. Wang, W. Zeng, N. Xiao, Y. Wu, Z. Zhou, J. Chen, F. Chen, *Chem. Eur. J.* **2012**, *18*, 1886–1889.
- (9) a) J. Zhang, J. M. Shreeve, *J. Am. Chem. Soc.* **2014**, *136*, 4437–4445. b) P. Yin, Q. Zhang, J. Zhang, D. A. Parrish, J. M. Shreeve, *J. Mater. Chem. A* **2013**, *1*, 7500–7510.

- (10) Y. Zhang, D. A. Parrish, J. M. Shreeve, *Chem. Eur. J.* **2012**, 18, 987–994.
- (11) Gaussian 03 (Revision D.01): M. J. Frisch, G. W. Trucks, H. B. Schlegel, G. E. Scuseria, M. A. Robb, J. R. Cheeseman, J. A. Montgomery, Jr, T. Vreven, K. N. Kudin, J. C. Burant, J. M. Millam, S. S. Iyengar, J. Tomasi, V. Barone, B. Mennucci, M. Cossi, G. Scalmani, N. Rega, G. A. Petersson, H. Nakatsuji, M. Hada, M. Ehara, K. Toyota, R. Fukuda, J. Hasegawa, M. Ishida, T. Nakajima, Y. Honda, O. Kitao, H. Nakai, M. Klene, X. Li, J. E. Knox, H. P. Hratchian, J. B. Cross, V. Bakken, C. Adamo, J. Jaramillo, R. Gomperts, R. E. Stratmann, O. Yazyev, A. J. Austin, R. Cammi, C. Pomelli, J. W. Ochterski, P. Y. Ayala, K. Morokuma, G. A. Voth, P. Salvador, J. J. Rabuck, K. Raghavachari, J. B. Foresman, J. V. Ortiz, Q. Cui, A. G. Baboul, S. Clifford, J. Cioslowski, B. B. Stefanov, A. Li, G. Liu, P. Piskorz, I. Komaromi, R. L. Martin, D. J. Fox, T. Keith, M. A. Al-Laham, C. Peng, A. Nanayakkara, M. Challacombe, P. M. W. Gill, B. Johnson, W. Chen, M. Wong, C. Gonzalez, J. A. Pople, Gaussian 03, Revision D. 01, Gaussian, Inc, Wallingford CT, **2004**.
- (12) *EXPLO5*, version 6.01, M. Sucéska, **2013**.
- (13) *APEX2* v2010.3-0. Bruker AXS Inc., Madison, Wisconsin, USA, **2014**.
- (14) *SAINT* v7.68A. Bruker AXS Inc., Madison, Wisconsin, USA. **200**
- (15) *XPREP* v2008/2. Bruker AXS Inc., Madison, Wisconsin, USA. **2014**
- (16) *SADABS* v2008/1, Bruker AXS Inc., Madison, Wisconsin, USA. **2008**
- (17) G. M. Sheldrick, *SHELXL-2014/7*. University of Göttingen, Germany. **2014**
- (18) L. J. Farrugia, *J. Appl. Cryst.* **2012**, 45, 849 – 854.
- (19) P. Yin, J. Zhang, D. A. Parrish, J. M. Shreeve, *Chem. Eur. J.* **2014**, 20, 1 – 9.
- (20) N. J. Wheate, J. A. Broomhead, J. G. Collins, A. I. Day, *Aust. J. Chem.* **2001**, 54,141–144.
- (21) P. Yin, J. Zhang, D. A. Parrish, J. M. Shreeve, *Chem. Eur. J.* **2014**, 20, 1 – 9.
- (22) B. B. Yulia, E. Mostovich, V. Enkelmann, W. Bernd, T.C. Pham, U. Tutsch, M. Lang, M. Baumgarten, *J. Mater. Chem. C*, **2014**, 2, 6618–6629.
- (23) M. Shu, C. Tu, W. Xu, H. Jin, J. Sun, *Cryst. Growth Des.* **2006**, 6, 1890 –1896.
- (24) A. Gianoncelli, G. Cozza, A. Orzeszko, F. Meggio, Z. Kazimierczuk, L. A. Pinna, *Bioorg. Med. Chem.* **2009**, 17, 7281–7289.

5.11 Supporting Information (SI)

5.12 Gaussian Calculations

Geometric optimization and frequency analyses of the compounds in the isodesmic reactions were accomplished by using the B3LYP functional with the 6-31+G** basis set from Gaussian 03.^[1] All of the optimized structures were characterized to be true local energy minima on the potential energy surface without imaginary frequencies. The enthalpy of reaction is obtained by combining the MP2/6-311++G** energy difference for the reactions, the scaled zero point energies (ZPE), values of thermal correction (H_T), and other thermal factors. The gas phase heat of formation at 298.15K for compound **11** was calculated from the atomization energy at the G2 level, gas phase enthalpies of **12** and **14** were calculated based on isodesmic reactions in Scheme S1 at MP2/6-311++G(d,p)//B3LYP(6-31+G(d,p)) level. The gas phase enthalpies of formation of **11**, **12** and **14** were converted to the solid state enthalpies of formation by subtraction of sublimation enthalpy calculated according to Trouton's rule ($\Delta H_{\text{sub}} = 188T_m$) (Table S1).^[2]



Scheme S1: Isodesmic reactions for compounds **12** and **14**

Table S1. Calculated (MP2/6-311++G**//B3LYP/6-31+G**) total energy (E_0), corrected MP2 total energy (E_{corr}), zero-point energy (ZPE), thermal correction to enthalpy (H_T), heat of reaction for the isodesmic reaction (ΔH_R) and gas phase heats of formation ($\Delta_f H_m^\circ$) from Gaussian 03.¹

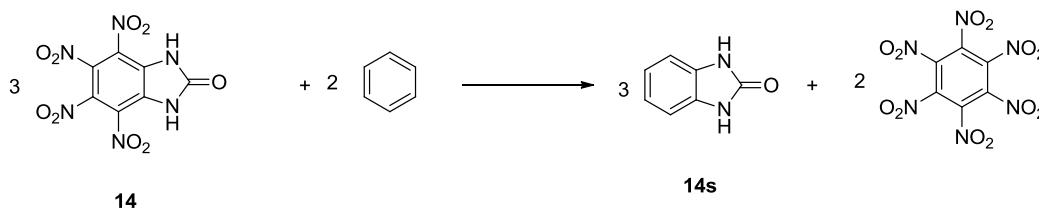
	ZPE [Hartree/Particle]	H_T [Hartree/Particle]	E_0 [Hartree/Particle]	ΔH_R (Hartree/Particle)	ΔH_{sub}^a (kJ mol ⁻¹)	$\Delta_f H_m^\circ$ (g) [kJ mol ⁻¹]	$\Delta_f H_m^\circ$ (s) [kJ mol ⁻¹]
Benzene	0.100441	0.105785	-231.5842377	-	-	+82.9 ^b	-
Nitrobenzene	0.103043	0.110809	-435.6906555	-	-	+68.5 ^b	-
11	0.109795	0.1223	-895.031117	-	88.7	+604.2 ^c	+515.5
12	0.110929	0.126049	-1099.084817	0.05495	79.1	+604.3	+525.2
14s	0.122904	0.131114	-453.9743248	-	-	-63.9 ^d	-
14	0.131244	0.149867	-1270.361893	-0.03684	107.5	-24.8	-132.3

^a Heat of sublimation calculated according to Trouton's rule ($\Delta H_{\text{sub}} = 0.188T_m$) ref: [2]. ^b Gas phase heat of formation NIST ref [3]; ^c Calculated from G2. ^d Experimental gas phase heat of formation ref [4]

Calculations – Dr. Jerry Boatz, Air Force Research Laboratory, Edwards Air Force Base, CA

5.13 GAMESS Calculations

The calculations for compound **14** were also performed by using GAMESS quantum chemistry program^[5,6] with a different isodesmic reaction shown in Scheme S2. The heat of reaction is obtained by combining corrected B3LYP/6-311++(d,p) energy difference of the products and reactants calculated at B3LYP /6-311++g(d,p)//B3LYP6-311++g(d,p)) level. The gas phase heats of formation for the related species were calculated from the atomization energy at the G3(MP2) level. The heat of sublimation was obtained using an approach developed by Rice and Byrd (Table S2).^{7,8}



Scheme S2: Isodesmic reaction for **14**

Table S2: Calculation of heat of formation of **14**

	B3LYP/6-311++(d,p)	B3LYP ZPE	B3LYP scaled ZPE	b3lyp elect+scaled ZPE	b3lyp thermal correction	ΔH_R (Hartree /Particle)	ΔH_f kcal /mol	ΔH_f kJ /mol	ΔH_{Sub} (kJ mol ⁻¹)	$\Delta_f H_m^\circ$ (s) [kJ mol ⁻¹]
14	-1272.842640	0.130986	0.128759	-1272.713881	0.018791	0.07378	1.5	6.3	120.9	-114.6
14s	-454.987584	0.122195	0.120118	-454.867467	0.008385			-62.9 ^a		
Hexanitrobenzene	-1458.901699	0.111421	0.109527	-1458.792172	0.021663			279.1 ^a		
Benzene	-232.157071	0.099939	0.098240	-232.058831	0.005412			78.2 ^a		

^a Calculated based on G3(MP2) using GAMESS.

5.14 References

- (1) Gaussian03, RevisionD.01, M. J. Frisch, G.W. Trucks, H.B. Schlegel, G.E. Scuseria, M.A. Robb, J.R. Cheeseman, J.A. Montgomery, Jr., T. Vreven, K.N. Kudin, J.C. Burant, J.M. Millam, S.S. Iyengar, J. Tomasi, V. Barone, B. Mennucci, M. Cossi, G. Scalmani, N. Rega, G.A. Petersson, H. Nakatsuji, M. Hada, M. Ehara, K. Toyota, R. Fukuda, J. Hasegawa, M. Ishida, T. Nakajima, Y. Honda, O. Kitao, H. Nakai, M. Klene, X. Li, J.E. Knox, H.P. Hratchian, J.B. Cross, V. Bakken, C. Adamo, J. Jaramillo, R. Gomperts,

- R.E. Stratmann, O. Yazyev, A.J. Austin, R. Cammi, C. Pomelli, J.W. Ochterski, P.Y. Ayala, K. Morokuma, G.A. Voth, P. Salvador, J.J. Dannenberg, V.G. Zakrzewski, S. Dapprich, A. D. Daniels, M.C. Strain, O. Farkas, D.K. Malick, A.D. Rabuck, K. Raghavachari, J. B. Foresman, J.V. Ortiz, Q. Cui, A.G. Baboul, S. Clifford, J. Cioslowski, B. B. Stefanov, G. Liu, A. Liashenko, P. Piskorz, I. Komaromi, R. L. Martin, D. J. Fox, T. Keith, M.A. Al-Laham, C.Y. Peng, A. Nanayakkara, M. Challacombe, P. M. W. Gill, B. Johnson, W. Chen, M. W. Wong, C. Gonzalez, J. A. Pople, Gaussian, Inc., Wallingford CT, 2004.
- (2) M. S. Westwell, M. S. Searle, D. J. Wales and D. H. Williams, *J. Am. Chem. Soc.* **1995**, *117*, 5013–5015.
- (3) <http://webbook.nist.gov/chemistry/>
- (4) V. M. F. Morais, M. S. Miranda, M. A. R. Matos, J. F Liebman, *Mol. Phys.* **2006**, *104*, 325–334.
- (5) M. W. Schmidt, K. K. Baldridge, J. A. Boatz, S. T. Elbert, M. S. Gordon, J. H. Jensen, S. Koseki, N. Matsunaga, K. A. Nguyen, S. Su, T. L. Windus, M. Dupuis, J.A. Montgomery. *J. Comput. Chem.* **1993**, *14*, 1347– 1363.
- (6) M. S. Gordon, M. W. Schmidt. Advances in Electronic Structure Theory, in Theory and Applications of Computational Chemistry: The First Forty Years; Dykstra, C.; Frenking, G.; Kim, K.; Scuseria, G., Eds.; Elsevier: Amsterdam, **2005**; pp 1167– 1190.
- (7) E.F.C. Byrd, B. M. Rice. *J. Phys. Chem. A* **2006**, *110* (3), 1005–1013; *ibid* **2009**, *113*, 5813.
- (8) E.F.C. Byrd, B. M Rice. *J. Phys. Chem. A* **2009**, *113* (1), 345–352.

Chapter 6

Biocidal Promise of Mono- and Diiodo-1, 2, 3-Triazoles

by

Deepak Chand, Chunlin He, James P. Hooper, Lauren A. Mitchell, Damon A. Parrish, and
Jean'ne M. Shreeve

submitted for publication in
Journal of Materials Chemistry A

Abstract:

4-Iodo-1*H*-1, 2, 3-triazole (**2**) and 4, 5-diiodo-1*H*-1, 2, 3-triazole (**3**) were synthesized using an efficient and viable synthetic route. These iodine- and nitrogen-rich compounds are attractive species to be explored based on their biocidal promise. The N-alkylation of **3** resulted in the formation of two tautomers. The N-alkyl-diiodo-triazoles were nitrated with 100% nitric acid to form monoiodo-mononitro-triazoles. The structures for 2-methyl-4, 5-diiodo-1, 2, 3-triazole (**5**), 1-ethyl-4, 5-diiodo-1, 2, 3-triazole (**6**), 1-methyl-4-nitro-5-iodo-1, 2, 3-triazole (**8**) and 1-ethyl-4-nitro-5-iodo-1, 2, 3-triazole (**10**) were confirmed by X-ray crystal analysis. All of the new triazoles were fully characterized via NMR, infrared, and elemental analyses as well as thermal and sensitivity properties. Decomposition products calculated using Cheetah 07 software show that these iodo-nitro triazoles liberate the biocidal species iodine. As a result, these compounds might be employed to neutralize chemical and biological agents.

6.1 Introduction

Chemical and biological agents pose a serious threat to public safety. Since these agents can become airborne moving over large areas very quickly, it is desirable to destroy them either before they escape from their storage or production facilities or, better, simultaneously with the entire facility. While the heat and shock waves originating from tailored explosives would destroy the storage and production facility, secondary chemical reagents are required to neutralize any remaining chemical and biological agents.¹ Therefore,

during the last few years considerable research has been going on in order to design and synthesize compounds that might play a biocidal role.

Hydrogen fluoride has long been recognized as an efficient antibacterial, and antimicrobial biocide with greater activity than HCl.² Therefore, energetic difluoroamines were investigated for this purpose.³ Iodine is also known for their biocidal properties; consequently we have synthesized a variety of polyiodo compounds as the source of biocidal agents. Additionally we have also described efficient syntheses of polyiodo pyrazoles including 3,4,5-triiodopyrazole and suggested their biocidal potential based on theoretical investigations.⁴ Various periodoheterocyclicarenes including tetraiodofuran (TIF) have been synthesized in our lab and studied systematically as a potential biocides.^{5a} They are being tested as effective antibioagent ingredients suitable for application as ADWs (Agent Defeat Weapons). Polyiodide salts which have low vapour pressure, high densities, and high iodine content also provide an alternate route to increase the iodine concentration in target compounds.^{5b}

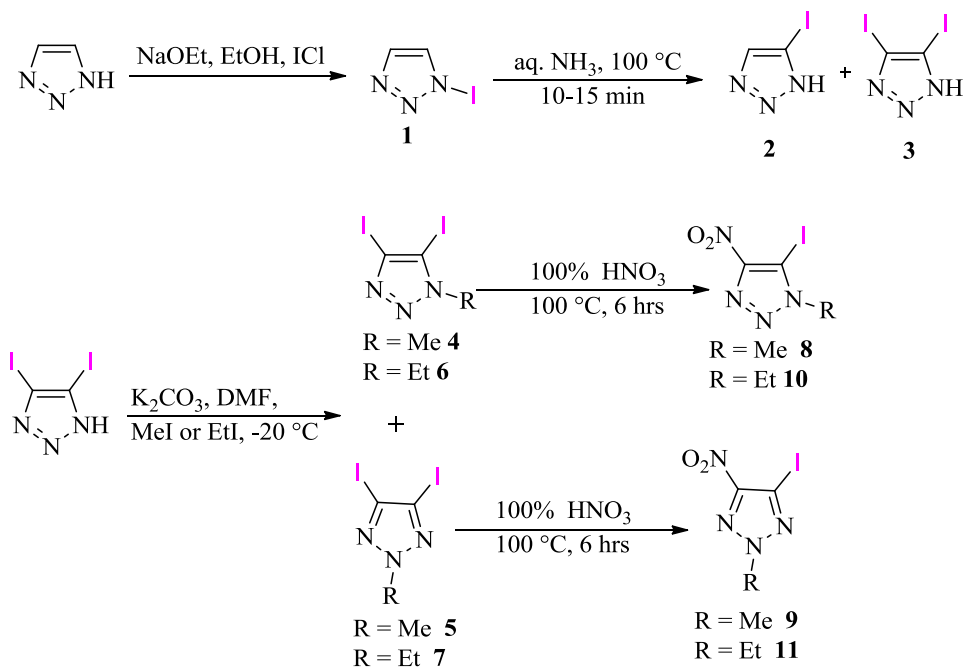
The 1,2,3-triazole ring is a moiety present in antiallergic, antibacterial, antifungal, antiviral, and analgesic drugs.⁶ Of the two constitutional triazole isomers, 1,2,3-triazole and 1,2,4-triazole, the latter one has been extensively investigated for energetic material applications.⁷ Because precursors are harder to synthesize, there are fewer reports dealing with the energetic material applications of 1,2,3-triazole.⁸

An efficient and practical synthesis for 4-iodo-1*H*-1,2,3-triazole (**2**) and 4,5-diiodo-1*H*-1,2,3-triazole (**3**) has been developed. A nitro functionality is helpful in enhancing the energy content as well as in attaining a better oxygen balance. However, due to the instability of these triazoles in strongly acidic solutions, direct nitration was not possible. Although iodo triazoles are less acidic than the parent 1,2,3-triazoles, alkylation reactions were realized successfully on these iodotriazoles. The new N-alkyl triazoles are tautomeric and can be nitrated employing 100% nitric acid. Gaussian 03 calculations were employed to predict the heat of formation values which were used as input parameters for Cheetah 7.0 calculations to obtain detonation properties and decomposition products. The calculated detonation properties and decomposition products suggest that the compounds may be effective bio agent defeat agents.

6.2 Results and discussion

6.3 Synthesis

Compounds **1** – **11** were synthesized as shown in Scheme 1. 1-Iodo-1,2,3-triazole (**1**) was synthesized based on literature procedures.⁹ 3,5-Dimethyl-1,2,4-triazole, an expensive and



Scheme 6.1 Synthesis of Compounds **1** – **11**

not readily available reagent, has been used in the literature to transform **1** into **2** and **3**.¹⁰ To our delight, we found that this transformation can be realized by using an inexpensive and readily available reagent – aqueous ammonia. When 1-iodo-1,2,3-triazole was heated in aqueous ammonia in a thick-walled-pressure tube at 100 °C for 10 – 15 min, ammonium salts of **2** and **3** were obtained. An aqueous solution of the resulting salts, when acidified with concentrated hydrochloric acid, formed a precipitate which was isolated by filtration and identified as 3,5-diiodo-1*H*-1,2,3-triazole (**3**). 4-Iodo-1*H*-1,2,3-triazole (**2**) was isolated from the filtrate by ether extraction. Because of the low stability of **2** and **3** in acidic solution, direct nitration was not possible. Low temperature alkylation of **3** was carried out using potassium carbonate as base and methyl and ethyl iodides as electrophiles. N1 and N2 alkylated products were isolated in each case in excellent yields. Column chromatography (ethyl acetate: hexane)

was employed to separate the resulting N-alkyl compounds. Nitration of **4**, **5**, **6** and **7** was successful by refluxing in 100% nitric acid and the 4-nitro products were isolated in good yields. Compounds **2** – **11** were fully characterized with NMR, and IR spectral analysis, DSC and elemental analysis. Single crystal structures were obtained for **5**, **6**, **8** and **10**.

6.4 Properties of compounds

Physical properties of **2** – **11** are summarized in Table 6.1. Heats of formation of all compounds were calculated with the Gaussian 03 program suite using isodesmic reactions¹¹

Table 6.1 Properties of compounds **2** - **11**

Comp	$T_m^{[a]}$ [°C]	$T_d^{[b]}$ [°C]	$d^{[c]}$ [gcm ⁻³]	$\Delta H_f^\circ^{[d]}$ [kJ mol ⁻¹]	ΔH_f° [kJ g ⁻¹]	$D^{[e]}$ [ms ⁻¹]	$P^{[f]}$ [GPa]	Iodine [%]
2	110.8	156.7	2.71	430.0	2.2	5112	15.33	65.1
3	-	189.9	3.32	474.4	1.5	4090	11.41	79.1
4	185.7	212.7	3.11	373.1	1.1	3985	10.07	75.8
5	129.7	-	2.90	358.6	1.1	3639	7.91	75.8
6	127.5	170.9	2.81	459.1	1.3	4066	9.96	72.7
7	108.1	-	2.73	443.7	1.3	3926	9.07	72.7
8	98.0	-	2.41	683.1	2.7	6028	21.24	50.0
9	156.0	235.0	2.13	671.1	2.6	5512	16.85	50.0
10	48.3	253.7	2.17	672.5	2.5	5710	20.03	47.4
11	111.2	-	2.11	658.7	2.5	5602	19.12	47.4

[a] melting point; [b] decomposition temperature; [c] density - gas pycnometer 25 °C ; [d] heat of formation - Gaussian 03; [e] detonation velocity - Cheetah 7.0; [f] detonation pressure - Cheetah 7.0.

(Supporting Information (SI) Scheme S1). For these iodine-containing compounds, the (15s, 11p, 6d) basis of Strömberg et al. was augmented with other p shell and the five valence sp exponents optimized resulting in a [5211111111, 4111111111, 3111] contraction scheme in conjunction with 6-31+G^{**} for first row and second row elements.¹² Single-point energy (SPE) refinement on the optimized geometries was performed with the use of MP2/6-311++G^{**} level. Corresponding iodine sets were constructed in MP2 method by using all electron calculations and quasi relativistic energy-adjusted spin-orbit-averaged seven-valence-electron effective core potentials (ECPs). All compounds have positive heats of formation; as expected, **8**, **9**, **10** and **11** with nitro substituents have higher values. The calculated values for heats of formation and experimental densities were used to predict the detonation velocities

(*D*) and detonation pressures (*P*) using the Cheetah 7.0 program. All the compounds have low detonation pressures which range from 7.91 to 21.24 GPa and the range of detonation velocities is 3639 to 6028 ms⁻¹.

The amount of decomposition product, I₂, which is a strong biocide, was predicted using Cheetah 7.0 calculations. As shown in Figure 6.1, while compound **3** has the highest iodine concentration in its decomposition products at ~79%, products of **2**, **4**, **6** and **8** are also comprised of iodine that makes them good candidates as effective bioagent defeat materials (Table 2). Each of the isomeric N-alkyl triazole pairs, i.e., **4**, **5** and **6**, **7** as well as **8**, **9** and **10**, **11** give the same decomposition products.

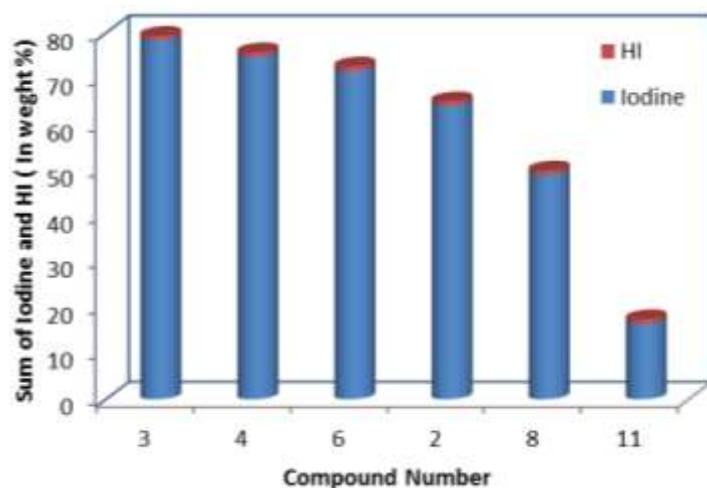


Figure 6.1 The iodine-containing species in the decomposition products of compounds **2**, **3**, **4**, **6**, **8** and **11** (weight percent).

Table 6.2 Major decomposition products - Cheetah 7.0 calculations [wt. % kg kg⁻¹]

comp	N ₂ [g]	I ₂ [g]	HI [g]	C [s]
2	21.6	64.1	1.0	9.3
3	12.0	78.4	1.0	6.6
4	12.6	74.8	1.0	8.1
6	12.0	71.6	1.1	10.0
8	22.1	49.0	1.0	5.9
11	21.0	16.4	1.1	7.9

Table 6.3 Crystallographic data for compounds **5**, **6**, **8** and **10**.

Compound	5	6	8	10
Formula	C ₃ H ₃ I ₂ N ₃	C ₄ H ₅ I ₂ N ₃	C ₃ H ₃ IN ₄ O ₂	C ₄ H ₅ IN ₄ O ₂
CCDC number	1446302	1446304	1446331	1446333
<i>M_w</i>	334.88	348.91	253.99	268.02
Crystal size [mm ³]	0.399 x 0.206	0.316 x 0.115	0.223 x 0.150	0.174 x 0.077
Crystal system	Orthorhombic	Triclinic	Triclinic	Triclinic
Space group	Pmn2 ₁	P-1	P-1	P-1
<i>a</i> [Å]	11.4559(8)	7.274(3)	7.0649(12)	6.9327(11)
<i>b</i> [Å]	4.1982(3)	7.508(3)	7.2001(12)	7.2485(11)
<i>c</i> [Å]	7.7048(5)	7.980(3)	70.362(5)	8.5638(12)
α [°]	90	84.239(4)	64.462(5)	77.511(5)
β [°]	90	83.370(5)	64.462(5)	67.263(4)°
γ [°]	90	68.174(4)	86.027(5)	83.499(5)°
<i>V</i> [Å ³]	370.56(4)	401.1(3)	339.95(10)	387.30(10)
<i>Z</i>	2	2	2	2
<i>T</i> [K]	150(2)	150(2)	150(2)	150(2)
ρ_{calcd} [Mg m ⁻³]	3.001	2.889	2.481	2.298
μ [mm ⁻¹]	8.396	7.763	4.654	4.091
<i>F</i> (000)	296	312	236	252
θ [°]	3.186 to	2.928 to	3.016 to	2.626 to
Index ranges	-14<= <i>h</i> <=14	-9<= <i>h</i> <=10	-8<= <i>h</i> <=8	-9<= <i>h</i> <=9
Reflections	3581	2117	2656	4209
Independent	838 [R _(int) =	2117	1247 [R _(int) =	2103 [R _(int) =
Data/restraints/para-	838 / 1 / 41	2117 / 0 / 84	1247 / 0 / 92	2103 / 0 / 101
GOF on <i>F</i> ²	1.088	1.165	1.065	1.049
<i>R</i> ₁ (<i>I</i> > 2 δ (<i>I</i>)) ^a	0.0186	0.0308	0.0312	0.0283
<i>wR</i> ₂ (<i>I</i> > 2 δ (<i>I</i>)) ^b	0.0452	0.0808	0.0762	0.0648
<i>R</i> ₁ (all data)	0.0187	0.0344	0.0341	0.0351
<i>wR</i> ₂ (all data)	0.0453	0.0831	0.0788	0.0675
Largest diff. peak	0.816 and -	1.489 and -	1.083 and -	1.243 and -

$$^a R_1 = \sum ||F_0| - |F_c|| / \sum |F_0| \quad ^b R_2 = [\sum w(F_0^2 - F_c^2)^2 / \sum w(F_0^2)^2]^{1/2}$$

6.5 X-ray Crystallography

Crystallographic data of compounds **5**, **6**, **8** and **10** are summarized in Table 6.3. Crystals of **5** were obtained by slow evaporation of a saturated solution of the compound in a mixture of ethyl acetate and hexane. The orthorhombic crystals are in the $Pmn2_1$ space group with two crystal units in a crystal lattice. The N2-methyl substituent does not seem to hinder strong $\pi - \pi$ stacking interactions between the rings as shown in Figure 6.2 (b). The carbon-iodine bond length I(1)-C(2) [2.070(5) Å] is comparable to similar bonds in **6** (Figure 6.3).

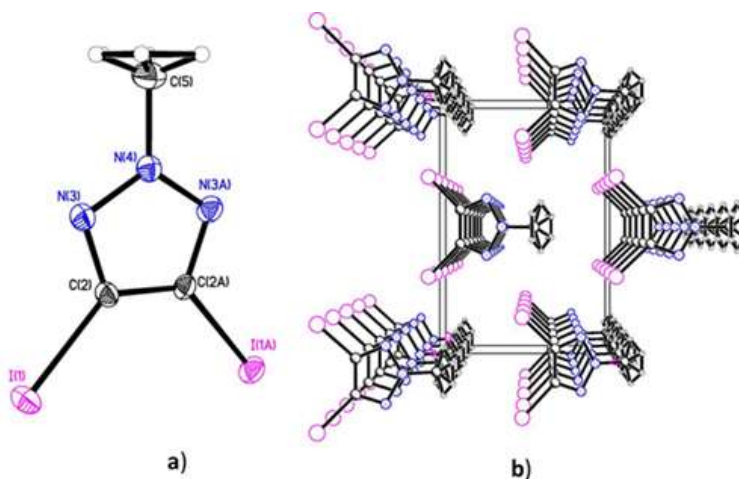


Figure 6.2 (a) Thermal ellipsoid plot (50%) and labeling scheme for **5**. (b) Packing diagram of **5** along a axis.

Slow evaporation of a saturated solution of **6** in a mixture of ethyl acetate and hexane gave suitable crystals for x-ray crystal structure analysis. There are two molecules per unit cell in the $P-1$ space group (Figure 6.3). Crystal units are packed so as to separate the bulky N-ethyl groups as seen in Fig. 6.3 (b). The C(8)-I(9) bond [2.069(6) Å] is slightly longer than the C(6)-I(7) bond [2.068(6) Å].

Triclinic crystals of **8** were obtained by slow evaporation of a saturated solution in benzene and diethyl ether at room temperature. There are molecules per unit cell which belong to the $P-1$ space group. As shown in Figure 6.4, there is strong intermolecular hydrogen bonding interaction between the hydrogen atoms of the methyl group and the oxygen atoms of the nitro group. A nitro group adjacent to a carbon-bearing iodine atom does not seem to influence the carbon iodine bond length C(5)-I(6) [2.072(5) Å].

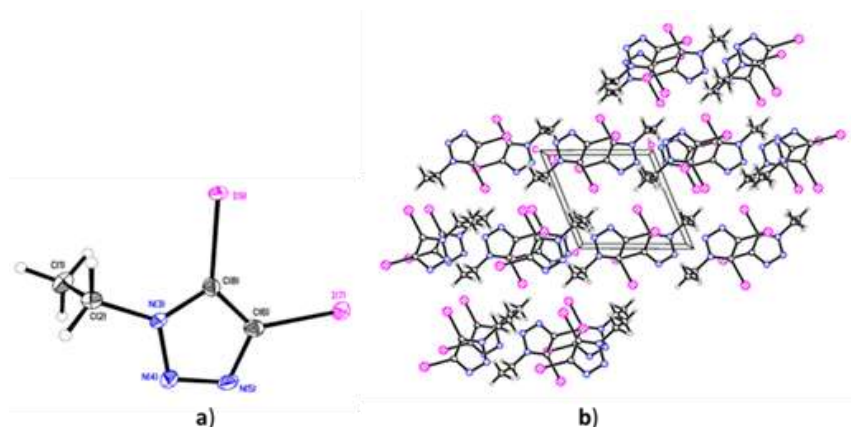


Figure 6.3 Thermal ellipsoid plot (50%) and labeling scheme for **6**. (b) Packing diagram of **6** along a axis.

Crystals of **10** suitable for x-ray crystallography were obtained by using a procedure similar to **8**. The triclinic crystals belong to the P-1 space group. There are two crystals per crystal lattice. The planarity of the ring is preserved even in the presence of the bulkier ethyl group. As a result there is strong π - π stacking interaction between the rings (Figure 6.5). Additionally, intermolecular van der Waals forces of attraction are operational between the iodine and the oxygen atoms of the nitro group. The carbon-iodine bond length is similar to that in the above compounds.

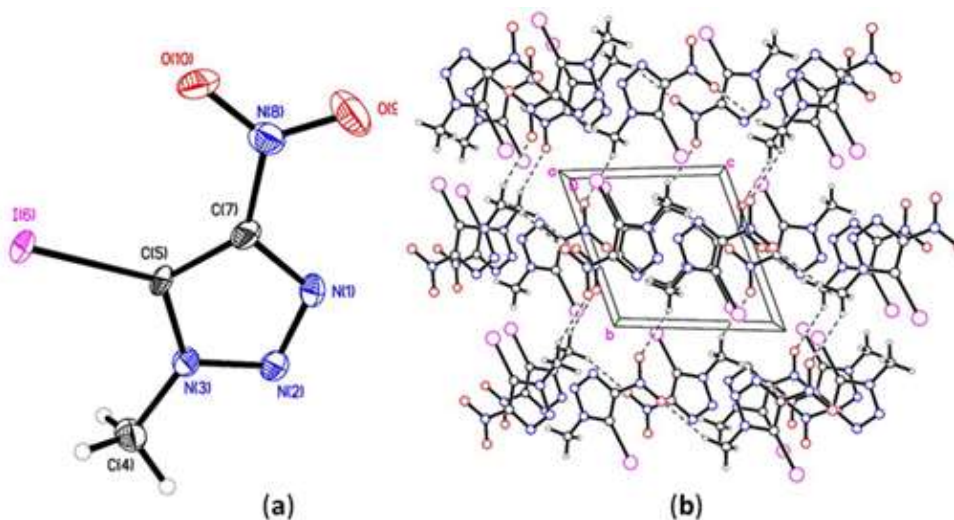


Figure 6.4 Thermal ellipsoid plot (50%) and labeling scheme for **8**. (b) Packing diagram of **8** along a axis.

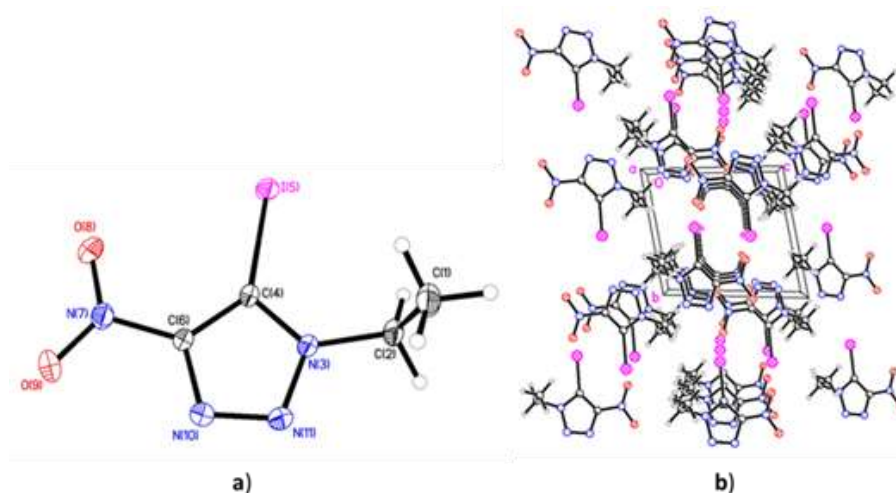


Figure 6.5 Thermal ellipsoid plot (50%) and labeling scheme for **10**. (b) Packing diagram of **10** along a- axis.

6.6 Conclusions

4-Iodo-[1*H*]-1, 2, 3-triazole and 4, 5-diiodo-[1*H*]-1, 2, 3-triazole were synthesized using an efficient synthetic route. N-alkylation of 4, 5-diiodo-[1*H*]-1, 2, 3-triazole was found to yield N1 and N2 alkylated isomers in each case. Nitration of these N-alkylated species results in the iodo triazoles with improved oxygen balance. The calculated detonation properties and products suggest that these compounds may be effective bio agent defeat agents. These iodotriazoles may increase the utility of 1*H*-1, 2, 3-triazoles in synthetic organic chemistry as well as in medicinal chemistry.

6.7 Experimental Section

6.8 General Methods

^1H and ^{13}C NMR spectra were recorded on a 300 MHz (Bruker Avance 300) nuclear magnetic resonance spectrometer operating at 300.13 and 75.48 MHz, respectively, by using [D₆]DMSO as solvent and locking solvent unless otherwise stated. The chemical shifts in ^1H and ^{13}C spectra are reported relative to Me₄Si. The decomposition temperatures (onset) were obtained using a differential scanning calorimeter (Model Q 10, TA Instruments Co.) at a scanning rate of 5 °C per minute in closed aluminum containers with small holes in the lids. IR spectra were recorded using KBr pellets for solids on a BIORAD model 3000 FTS spectrometer. Densities were determined at room temperature employing a Micromeritics

AccuPyc 1330 gas pycnometer. Elemental analyses were carried out using an Exeter CE-440 elemental analyzer.

6.9 X-ray crystallography

A colorless plate crystal of dimensions 0.399 x 0.206 x 0.018 mm³ for **5**, a colorless plate crystal of dimensions 0.316 x 0.115 x 0.104 mm³ for **6**, a colorless plate crystal of dimensions 0.223 x 0.150 x 0.037 mm³ for **8** or a colorless plate crystal of dimensions 0.174 x 0.077 x 0.014 mm³ for **10** was mounted on a MiteGen MicroMesh using a small amount of Cargille immersion oil. Data were collected on a Bruker three-circle platform diffractometer equipped with a SMART APEX II CCD detector. The crystals were irradiated using graphite monochromated MoK_α radiation ($\lambda = 0.71073$). An Oxford Cobra low temperature device was used to keep the crystals at a constant 150(2) K during data collection.

Data collection was performed and the unit cell was initially refined using *APEX3* [v2014.3-0].¹³ Data reduction was carried out using *SAINT* [v7.68A]¹⁴ and *XPREP* [v2014/2]¹⁵. Corrections were applied for Lorentz, polarization, and absorption effects using *SADABS* [v2008/1].¹⁶ The structure was solved and refined with the aid of the programs *SHELXL-2014/7* within *WingX*.^{17,18} The full-matrix least-squares refinement on F² included atomic coordinates and anisotropic thermal parameters for all non-H atoms. The H atoms were included using a riding model.

4-Iodo-[1H]-1, 2, 3-triazole (**2**) and 4, 5-diiodo-[1H]-1, 2, 3-triazole (**3**).

1-Iodo-1, 2, 3-triazole (0.06 mol, 11g) was suspended in 15 % aqueous ammonia (10 mL) and heated at 100 °C in a thick-walled pressure tube with occasional shaking. Heating was stopped after 10-15 minutes when a clear solution was obtained. The ammonia was evaporated by blowing air over the solution and the residue was taken up in water (100 mL). The solution was acidified with concentrated HCl to pH 3 to obtain an off-white precipitate which was filtered and washed with cold water. The compound was identified as 4, 5-diiodo-[1H]-1, 2, 3-triazole (**3**).

The filtrate was extracted with diethyl ether which was evaporated using a rotary evaporator and the residue was dried under vacuum. The compound was identified as 4-iodo-1,2,3-triazole (**2**).

2: Yield 33.3%. (3.9 g). $T_m = 110.8\text{ }^\circ\text{C}$, $T_{dec}(\text{onset}) = 156.6\text{ }^\circ\text{C}$; IR (KBr) ν 3429, 3115, 2962, 2916, 1633, 1504, 1445, 1300, 1224, 1178, 1136, 1074, 927, 864, 817, 636 cm^{-1} ; $^1\text{H NMR } \delta$ 15.4 (broad, NH), 8.0 (ring - CH); $^{13}\text{C NMR } \delta$ 135.9, 89.4; elemental analysis: (%) calculated for $\text{C}_2\text{H}_2\text{IN}_3$ (194.96): C, 12.32; H, 1.03; N, 21.55; found C, 12.15; H, 1.03; N, 21.15.

3: Yield 25%. $T_{dec}(\text{onset}) = 189.9\text{ }^\circ\text{C}$; IR (KBr) ν 3430, 3121, 2943, 2827, 1718, 1629, 1556, 1503, 1444, 1332, 1284, 1179, 1091, 1008, 979, 804, 458 cm^{-1} ; $^1\text{H NMR } \delta$ 15.6 (broad, NH); $^{13}\text{C NMR } \delta$ 104.2; elemental analysis: (%) calculated for $\text{C}_2\text{H}_2\text{I}_2\text{N}_3$ (320.86): C, 7.49; H, 0.31; N, 13.10; found C, 7.65; H, 0.24; N, 13.10.

1-Methyl-4, 5-diiodo-1, 2, 3-triazole (4) and 2-methyl-4, 5-diiodo-1, 2, 3-triazole (5).

4, 5-Diiodo-1, 2, 3-[1*H*]-triazole (14.6 mmol, 4.7 g) was dissolved in DMF (5 mL) and potassium carbonate (23.15 mmol, 3.2g) was added. The mixture was cooled to $-20\text{ }^\circ\text{C}$ in an ice-salt bath. Iodomethane (21.8 mmol, 1.36 mL) was added to the cooled mixture and stirred for two hours. An off-white precipitate was formed which was filtered and washed with water. TLC analysis showed the mixture consisted of two constituents which were separated using column chromatography [eluent - hexane: ethyl acetate (2:8)]. Yield = 82% (4.7 g).

4: Yield 48 %. $T_m = 185.7\text{ }^\circ\text{C}$, $T_{dec}(\text{onset}) = 212.7\text{ }^\circ\text{C}$; IR (KBr) ν 2924, 1421, 1383, 1265, 1195, 1084, 1028, 983, 709 cm^{-1} ; $^1\text{H NMR } \delta$ 4.1 (methyl, H), 8.0; $^{13}\text{C NMR } \delta$ 102.7, 95.3; elemental analysis: (%) calculated for $\text{C}_3\text{H}_3\text{I}_2\text{N}_3$ (334.88): C, 10.76; H, 0.90; N, 12.55; found C, 11.10; H, 0.91; N, 12.31.

5: Yield 52 %, $T_m = 129.7\text{ }^\circ\text{C}$; IR (KBr) ν 2925, 2854, 1638, 1438, 1413, 1365, 1292, 1018, 716, 644, 448 cm^{-1} ; $^1\text{H NMR } \delta$ 15.4 (broad, NH), 4.1 (methyl - H); $^{13}\text{C NMR } \delta$ 104.3, 42.3; elemental analysis: (%) calculated for $\text{C}_3\text{H}_3\text{I}_2\text{N}_3$ (334.88): C, 10.76; H, 0.90; N, 12.55; found C, 10.78; H, 0.88; N, 12.21.

1-Ethyl-4, 5-diiodo-1, 2, 3-triazole (6) and 2-ethyl-4, 5-diiodo-1, 2, 3-triazole (7)

N-ethylation of 4, 5-diiodo-1, 2, 3-triazole was carried out using the procedure for **4** and **5**. Yield 85%. The two isomers **6** and **7** were separated using silica gel column chromatography. [Eluent – hexane: ethyl acetate (1:9)]

6: Yield 47%. $T_m = 127.5\text{ }^\circ\text{C}$, $T_d = 170.9\text{ }^\circ\text{C}$; IR (KBr) ν 2992, 2975, 2955, 2932, 1631, 1531, 1418, 1438, 1431, 1404, 1376, 1340, 1296, 1238, 1097, 989, 1045, 989, 958, 785, 683 cm^{-1} ; $^1\text{H NMR } \delta$ 4.4 (CH_2), 1.4 (CH_3); $^{13}\text{C NMR } \delta$ 102.9, 93.9, 15.1; elemental analysis: (%) calculated for $\text{C}_4\text{H}_5\text{I}_2\text{N}_3$ (348.91): C, 13.77; H, 1.44; N, 12.04; found C, 13.67; H, 1.42; N, 11.52.

7: Yield 47%. $T_m = 108.1\text{ }^\circ\text{C}$; IR (KBr) ν 2981, 2926, 2852, 1443, 1386, 1361, 1330, 1084, 1016, 964, 795, 690, 657, 430 cm^{-1} ; $^1\text{H NMR } \delta$ 4.4 (CH_2), 1.4 (CH_3); $^{13}\text{C NMR } \delta$ 104.4, 50.7, 14.5; elemental analysis: (%) calculated for $\text{C}_4\text{H}_5\text{I}_2\text{N}_3$ (348.91): C, 13.77; H, 1.44; N, 12.04; found C, 13.98; H, 1.44; N, 12.04.

1-Methyl-4-nitro-5-iodo-1,2,3-triazole (8).

1-Methyl-4,5-diiodo-1,2,3-triazole (1 g, 3 mmol) was added portion wise to 10 mL of 100% nitric acid and the mixture was heated at reflux for six hours. After cooling to room temperature the mixture was poured onto crushed ice to give a pale yellow precipitate which was filtered, and washed with cold water (10 mL x 3) to obtain **8**. Yield 62 %.

$T_m = 98.0\text{ }^\circ\text{C}$; IR (KBr) ν 2924, 2853, 1539, 1435, 1377, 1300, 1267, 1219, 1097, 1045, 831, 717, 435 cm^{-1} ; $^1\text{H NMR } \delta$ 4.1 (CH_3); $^{13}\text{C NMR } \delta$ 155.3, 88.3, 38.6; elemental analysis: (%) calculated for $\text{C}_3\text{H}_3\text{IN}_4\text{O}_2$ (253.99): C, 14.19; H, 1.19; N, 22.06; found C, 14.49; H, 1.22; N, 21.63.

2-Methyl-4-nitro-5-iodo-1,2,3-triazole (9)

This material was prepared following a procedure similar to that for **8** by using 2-methyl-4, 5-diiodo-1, 2, 3-triazole(1 g, 3 mmol) .Yield 63.3 %.

$T_m = 156.0\text{ }^\circ\text{C}$, $T_d = 235.0\text{ }^\circ\text{C}$; IR (KBr) ν 2924, 2853, 1633, 1541, 1416, 1362, 1331, 1085, 831, 725, 644 cm^{-1} ; $^1\text{H NMR } \delta$ 4.2 (CH_3); $^{13}\text{C NMR } \delta$ 154.3, 91.4, 38.6; elemental analysis:

(%) calculated for $C_3H_3IN_4O_2$ (253.99): C, 14.19; H, 1.19; N, 22.06; found C, 14.63; H, 1.23; N, 20.91.

1-Ethyl-4-nitro-5-iodo-1, 2, 3-triazole (10)

This material was prepared following a procedure similar to that for **8** by using 1-ethyl-4, 5-diiodo-1, 2, 3-triazole (1 g, 2.9 mmol). Yield 63 %

$T_m = 111.2$ °C, $T_d =$ °C, $T_d = 235.0$ °C; IR (KBr) ν 1537, 1431, 1387, 1325, 1095, 1072, 968, 827, 650, 571, 474, 426 cm^{-1} ; 1H NMR δ 4.5(CH₃), 1.4 (CH₂); ^{13}C NMR δ 154.2, 91.4, 51.8, 13.8; elemental analysis: (%) calculated for $C_4H_5IN_4O_2$ (268.01): C, 17.93; H, 1.88; N, 20.90; found C, 18.14; H, 1.87; N, 20.66

2-Ethyl-4-nitro-5-iodo-1, 2, 3-triazole (11)

This material was prepared following a procedure similar to **8** by using 2-ethyl-4, 5-diiodo-1, 2, 3-triazole (1 g, 2.9 mmol).

Yield 64 %. $T_m = 111.2$ °C, $T_d =$ °C; IR (KBr) ν 2992, 2924, 1635, 1538, 1484, 1440, 1410, 1374, 1295, 1255, 1186, 1105, 1043, 958, 833, 692 cm^{-1} ; 1H NMR δ 4.5(CH₃), 1.4 (CH₂); ^{13}C NMR δ 155.3, 87.0, 47.2, 14.4; elemental analysis: (%) calculated for $C_4H_5IN_4O_2$ (268.01): C, 17.93; H, 1.88; N, 20.90; found C, 17.99; H, 1.84; N, 20.50.

Acknowledgements

The authors gratefully acknowledge the support of the Defense Threat Reduction Agency (HDTRA1-11-1-0034) and the ONR (N00014-12-1-0536).

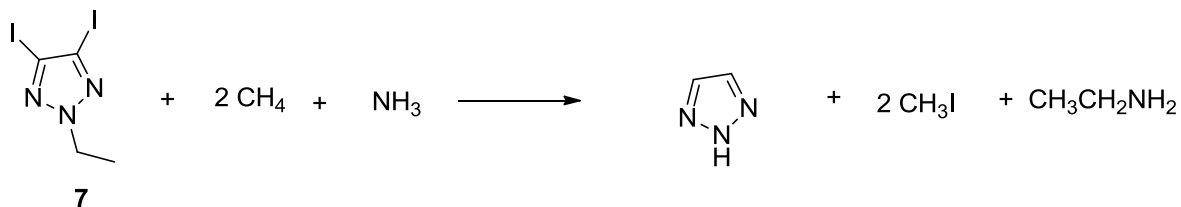
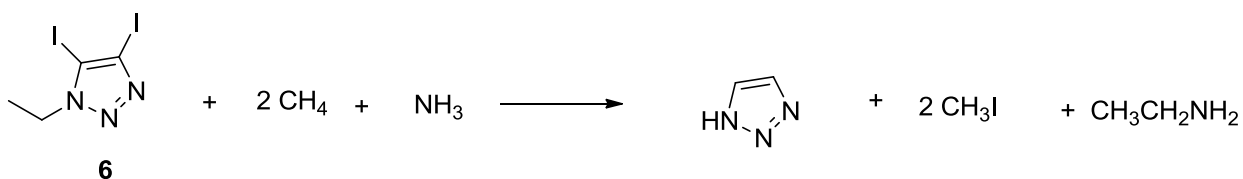
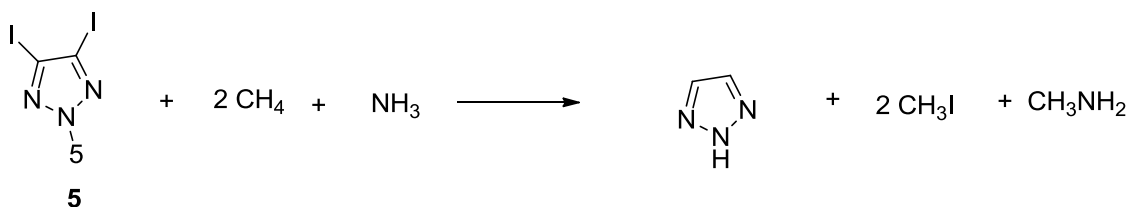
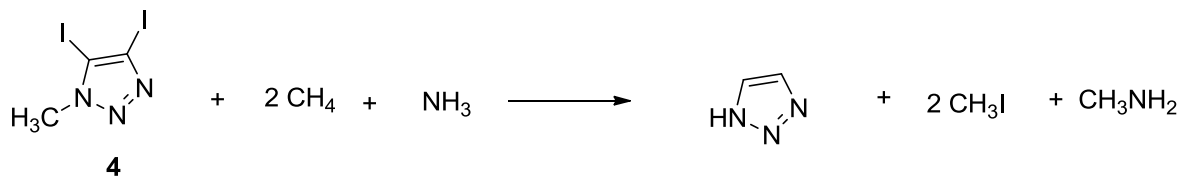
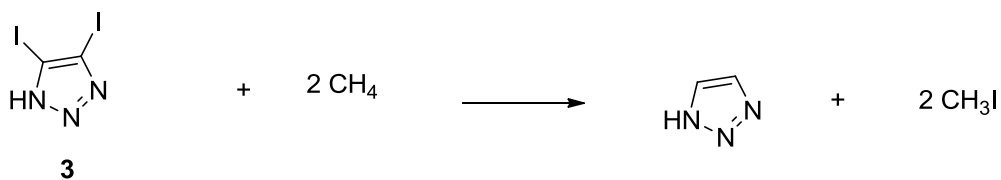
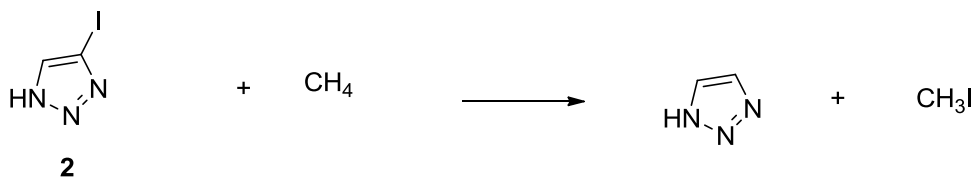
6.10 References:

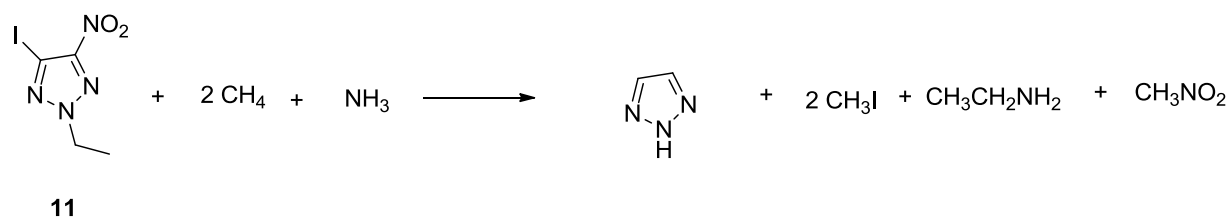
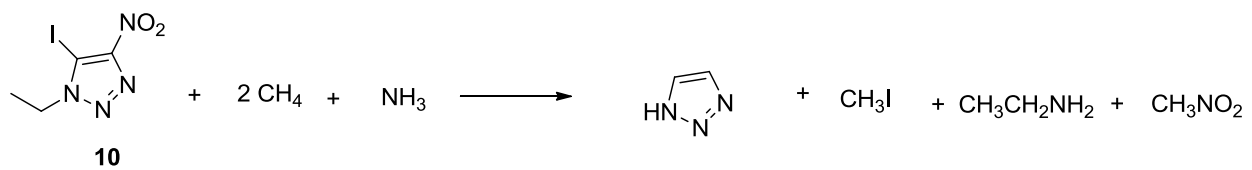
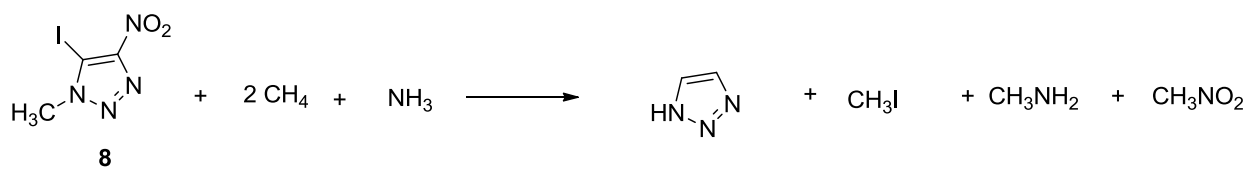
- (1) K. O. Christe, R. Haiges, P. Vashista, Defense Threat Reduction Energy Report (DTRA-TR-13-23).
- (2) R. D. Chapman, US 8221566 B1 (July 17, 2012).
- (3) R. D. Chapman, R. A. Hollins, T. S. Jones, T. J. Groshens, G. T. Guck, D. Thompson, T. J. Schilling, D. Wooldridge, P. N. Cash, Defense Threat Reduction Energy Report (DTRA-TR-14-26).
- (4) a) D. Chand, J. M. Shreeve, *Chem. Commun.* **2015**, 51, 3438 – 3441. b) J. J. Baker, C. Gotzmer, R. Gill, S. L. Kim, M. Blachek, US Patent 2009 7,568.432.

- (5) a) C. He, J. Zhang, J. M. Shreeve, *Chem. Eur. J.* **2013**, 19, 7503-7509. b) C. He, D. A. Parrish, J. M. Shreeve, *Chem. Eur. J.* **2014**, 20, 6699 – 6706.
- (6) W. P. Oziminska, J. C. Dobrowolska, A. P. Mazureka, *J. Mol. Struct.* **2003**, 651, 697–704.
- (7) a) P. Yin, J. M. Shreeve, *Angew. Chem. Int. Ed.* **2015**, 54, 14513 – 14517. b) R. Haiges, G. Belanger-Chabot, S. M. Kaplan, K. O. Christe, *Dalton Trans.* **2015**, 44, 2978 – 2988. c) P. Yin, D. A. Parrish, J. M. Shreeve, *Angew. Chem. Int. Ed.* **2014**, 53, 12889 –12892. d) D. E. Chavez, J. C. Bottaro, M. Petrie, D. A. Parrish, *Angew. Chem. Int. Ed.* **2015**, 54, 12973 – 12975. e) A. A. Dippold, T. M. Klapötke, *J. Am. Chem. Soc.* **2013**, 135, 9931–9938.
- (8) a) Y. Zhang, D. A. Parrish, J. M. Shreeve, *J. Mater. Chem. A* **2013**, 1, 585. b) A. T. Baryshnikov, B. I. Erashko, N. I. Zubanova, B. I. Ugrak, *Bull. Russ. Acad. Sci., Chem. Ser.* **1992**, 41, 751–757.
- (9) A. C. Tome, *Science of Synthesis* **2004**, 13, 415 – 601.
- (10) R. Miethchen, H. Albrecht, E. Rachow, *Z. Chem.*, 1970, **10**, 220 – 221
- (11) M. J. Frisch, G. W. Trucks, H. B. Schlegel, G. E. Scuseria, M. A. Robb, J. R. Cheeseman, J. A. Montgomery, Jr., T. Vreven, K. N. Kudin, J. C. Burant, J. M. Millam, S. S. Iyengar, J. Tomasi, V. Barone, B. Mennucci, M. Cossi, G. Scalmani, N. Rega, G. A. Petersson, H. Nakatsuji, M. Hada, M. Ehara, K. Toyota, R. Fukuda, J. Hasegawa, M. Ishida, T. Nakajima, Y. Honda, O. Kitao, H. Nakai, M. Klene, X. Li, J. E. Knox, H. P. Hratchian, J. B. Cross, V. Bakken, C. Adamo, J. Jaramillo, R. Gomperts, R. E. Stratmann, O. Yazyev, A. J. Austin, R. Cammi, C. Pomelli, J. W. Ochterski, P. Y. Ayala, K. Morokuma, G. A. Voth, P. Salvador, J. J. Dannenberg, V. G. Zakrzewski, S. Dapprich, A. D. Daniels, M. C. Strain, O. Farkas, D. K. Malick, A. D. Rabuck, K. Raghavachari, J. B. Foresman, J. V. Ortiz, Q. Cui, A. G. Baboul, S. Clifford, J. Cioslowski, B. B. Stefanov, G. Liu, A. Liashenko, P. Piskorz, I. Komaromi, R. L. Martin, D. J. Fox, T. Keith, M. A. Al-Laham, C. Y. Peng, A. Nanayakkara, M. Challacombe, P. M. W. Gill, B. Johnson, W. Chen, M. W. Wong, C. Gonzalez, J. A. Pople, Gaussian 03 (Revision D.01), Gaussian, Inc., Wallingford CT, 2004.
- (12) A. Strömberg, O. Gropen, U. Wahlgren, *J. Comput. Chem.*, 1983, **4**, 181 – 186.
- (13) Bruker (2014). APEX2 v2010.3-0. Bruker AXS Inc., Madison, Wisconsin, USA.

- (14) Bruker (2009). SAINT v7.68A. Bruker AXS Inc., Madison, Wisconsin, USA.
 (15) Bruker (2014). XPREP v2008/2. Bruker AXS Inc., Madison, Wisconsin, USA.
 (16) Bruker (2008). SADABS v2008/1, Bruker AXS Inc., Madison, Wisconsin, USA.
 (17) Sheldrick, G. M. (2014). SHELXL-2014/7. University of Göttingen, Germany.
 (18) L. J. Farrugia, *J. Appl. Cryst.*, 2012, **45**, 849 – 854.

6.11 Supporting Information





Scheme S1: Isodesmic reactions

Appendix 1: Proof of Approval

3032016

RightLink Private License

JOHN WILEY AND SONS LICENSE TERMS AND CONDITIONS

Mar 30, 2016

This Agreement between Deepak Chand ("You") and John Wiley and Sons ("John Wiley and Sons") consists of your license details and the terms and conditions provided by John Wiley and Sons and Copyright Clearance Center.

License Number:	3838871303392
License date:	Mar 30, 2016
Licensed Content Publisher:	John Wiley and Sons
Licensed Content Publication:	Chemistry - A European Journal
Licensed Content Title:	Borohydride Ionic Liquids as Hypergolic Fuels: A Quest for Improved Stability
Licensed Content Author:	Deepak Chand, Jiaheng Zhang, Jean/na M. Shraeve
Licensed Content Date:	Jul 29, 2015
Pages:	5
Type of use:	Dissertation/Thesis
Requestor type:	Author of this Wiley article
Format:	Print
Portion:	Full article
Will you be translating?:	No
Title of your thesis / dissertation:	Quest for green energetic materials, green rocket fuels and polyiodo biocides
Expected completion date:	May 2016
Expected size (number of pages):	100
Requestor Location:	Deepak Chand 209 W Taylor Ave Apt 17 MOSCOW, ID 83843 United States Attn: Deepak Chand
Billing Type:	Invoice
Billing Address:	Deepak Chand 209 W Taylor Ave Apt 17 MOSCOW, ID 83843 United States Attn: Deepak Chand
Total:	0.00 USD
Terms and Conditions:	

<https://www.copyright.com/AppDispatchServlet>

15